DISSERTATION

MULTIFUNCTIONAL NANOWIRE SCAFFOLDS FOR NEURAL TISSUE ENGINEERING APPLICATIONS

Submitted by

Samuel Leo Bechara

Graduate Degree Program in Bioengineering

In partial fulfillment of the requirements

For the Degree of Doctor of Philosophy

Colorado State University

Fort Collins, Colorado

Spring 2012

Doctoral Committee:

Advisor: Ketul Popat

John Sladek
Stuart Tobet
Bernard Rollin
Marie Legare

ABSTRACT

MULTIFUNCTIONAL NANOWIRE SCAFFOLDS FOR NEURAL TISSUE ENGINEERING APPLICATIONS

Unlike other regions of the body, the nervous system is extremely vulnerable to damage and injury because it has a limited ability to self-repair. Over 250,000 people in the United States have spinal cord injuries and due to the complicated pathophysiology of such injuries, there are few options available for functional regeneration of the spinal column. Furthermore, peripheral nerve damage is troublingly common in the United States, with an estimated 200,000 patients treated surgically each year. The current gold standard in treatment for peripheral nerve damage is a nerve autograft. This technique was pioneered over 45 years ago, but suffers from a major drawback. By transecting a nerve from another part of the body, function is regained at the expense of destroying a nerve connection elsewhere. Because of these issues, the investigation of different materials for regenerating nervous tissue is necessary. This work examines multi-functional nanowire scaffolds to provide physical and chemical guidance cues to neural stem cells to enhance cellular activity from a biomedical engineering perspective. These multi-functional scaffolds include a unique nanowire nano-topography to provide physical cues to guide cellular adhesion. The nanowires were then coated with an electrically conductive polymer to further enhance cellular activity. Finally, nerve growth factor was conjugated to the surface of the scaffolds to provide chemical cues for the

neural stem cells. The results in this work suggest that these multifunctional nanowire scaffolds could be used in vivo to repair nervous system tissue.

To my Mom and Pop

I could not have done this work without your support, love, and inspiration and for that I am eternally grateful.

TABLE OF CONTENTS

LIST OF TABLES

LIST OF FIGURES

Figure 7.8 A: Young's modulus and B: Harness measured using nanoindentation. (★, @ ➔ $p < 0.05$)

Chapter 1 Introduction and Specific Aims

1.1 Introduction

This research evaluates polycaprolactone (PCL) nanowire scaffolds and subsequent modifications on neural progenitor cell adhesion, proliferation, viability, and differentiation *in vitro*. Vertically aligned, high aspect ratio, substrate bound nanowires fabricated using a simple nanotemplating process were used in all studies presented in this work. This work has investigated neural stem cell response to modified multifunctional PCL nanowire scaffolds *in vitro.* This is a proof-of-concept work and should be used as a preliminary study proceeding animal studies.

The sequential nature of this work is arranged into 5 specific aims. The work presented here begins with a preliminary study of PCL nanowire scaffolds and their effect on PC12 cell functionality. The specific were then were directed towards varying nanowire diameter to investigate whether or not it had an effect on neural stem cell functionality and investigating the response of a more physiologically relevant cell line, C17.2 neural progenitor cells. The work then progressed by modifying the PCL nanowire scaffold by coating it with an electrically conductive polymer, polypyrrole. This was motivated by the nature of neurons and their communication through electrical signals and the fact that polypyrrole has been shown to be biocompatible. Next, the specific aims were directed towards modifying the scaffolds further by conjugating the biomolecule nerve growth factor (NGF) to the surface. This was motivated by the ability of NGF to

promote healing, survival, and differentiation in the nervous system. Finally, the work concludes with an investigation into micro-patterning the nanowire surfaces to direct neural stem cell adhesion and proliferation.

This thesis attempts to address the hypothesis that PCL nanowire scaffolds are reproducible, have an advantageous nano-architecture, and can easily be modified to enhance neural stem cell functionality. The findings indicate that these scaffolds were sequentially modified in a manner that enhances neural stem cell functionality and suggests that PCL nanowire scaffolds are a promising avenue to explore tissue-engineering therapies for repairing nervous system injuries and disorders.

1.2 Fundamental hypothesis

Polymeric nanowire scaffolds are reproducible, have an advantageous nano-architecture, and can easily be modified to enhance neural stem cell functionality.

1.3 Specific Aim 1

Hypothesis (1): If cell adhesion and proliferation is related to surface nano-topography, then PC12 cells will preferentially adhere and will experience enhanced proliferation on nanowire scaffolds

Specific Aim 1: PCL nanowire scaffolds will be created and provide a nanowire nanotopography that can encourage PC12 cell adhesion and proliferation at a greater rate than on surfaces lacking a nanotopography. *This research is presented in Chapter 3.*

A. Create highly reproducible PCL nanowire scaffolds consisted of substrate bound, high aspect ratio, nanowires.
B. Investigate PC12 cell response to nanowire scaffolds before differentiation
C. Investigate PC12 cell response to nanowire scaffolds after induced differentiation

1.4 Specific Aim 2

Hypothesis (2): If nanotopography plays a critical role in neural stem cell adhesion and proliferation, varying the nanowire diameter will affect C17.2 cellular functionality.

Specific Aim 2: PCL nanowire scaffolds will be fabricated with different nanowire diameters and subsequent C17.2 cell functionality will be evaluated. *This research is presented in Chapter 4.*

A. Create nanowire scaffolds with varying diameters

B. Investigate C17.2 cellular response to nanowire scaffolds of different diameter

1.5 Specific Aim 3

Hypothesis (3): If nervous system cells are known to propogate electrical signals, creating an electrically conductive surface will enhance neural stem cell activity

Specific Aim 3: Coat nanowire scaffolds with the electrically conductive polymer polypyrrole and investigate C17.2 neural stem cell response. *This research is presented in Chapter 5.*

A. Coat polypyrrole onto nanowire scaffolds in a repeatable and consistent manner

B. Evaluate the surface characteristics of the polypyrrole coating in terms of morphology and resistivity.

C. Ensure that the polypyrrole coating is robust by conducting a degradation study in physiological conditions

D. Investigate C17.2 cellular response to polypyrrole coated nanowire surfaces

1.6 Specific Aim 4

Hypothesis (4): If neural stem cells react to biochemical cues, by introducing the biomolecule NGF to the substrate surface, we can enhance the differentiation potential of neural progenitor cells

Specific Aim 4: Conjugate the biomolecule nerve growth factor onto the polypyrrole coated nanowire scaffolds and evaluate C17.2 cellular functionality. *This research is presented in Chapter 6.*

A. Create a chemical conjugation technique that can consistently conjugate NGF to the polypyrrole coated nanowire surface
B. Evaluate the surface characteristics of the NGF coated polypyrrole nanowire surfaces
C. Evaluate the elution of NGF from the NGF conjugated surfaces
D. Investigate C17.2 cellular functionality on NGF conjugated polypyrrole coated nanowire surfaces

1.7 Specific Aim 5

Hypothesis (5): If neural stem cells have been shown to adhere and proliferate with increased activity on nanowire surfaces, cellular growth can be directed by patterning surfaces with regions of nanowires bordered by regions lacking a nanotopography

Specific Aim 5: Micropattern nanowire surfaces with regions lacking a nanotopography bordered by nanowire regions to allow for preferential adherence and proliferation of C17.2 neural stem cells. *This research is presented in Chapter 7.*

A. Consistently and reproducibly micro-pattern nanowire surfaces
B. Evaluate micropatterned surface for surface properties
C. Investigate C17.2 cellular response to micro-patterned surfaces

Chapter 2 Literature Review

2.1 Myelopathic Injuries

2.1.1 Background

Tissue engineering therapies targeted at nerve regeneration could have broad social and economic benefits to the American population. Myelopathic injuries represent one area where tissue-engineering strategies can be applied. Although myelitis and vascular myelopathy can also cause damage to neurons in the central nervous system (Kirshblum, Groah, McKinley, Gittler, & Stiens, 2002), perhaps no other cause for damage is as troubling as trauma, more commonly referred to as spinal cord injuries (SCI). Over 250,000 people in the United States alone have SCI with approximately 11,000 new injuries occurring each year ("Spinal Cord Injury Facts & Statistics," n.d.). Unlike most injuries, which befall the elderly, SCI occur predominately in Americans between the ages of 16-30 where the leading cause of injury is vehicular accidents. Even with shocking statistics as these, there is still no clinically proven way to reverse spinal cord damage. Spinal cord regeneration after injury is inhibited by extensive scarring caused by several different reactions, such as, changes in blood flow (Olive, McCully, & Dudley, 2002), excessive neurotransmitter release (Xiaohai Wang, Arcuino, et al., 2004) and nerve cell death (Hulsebosch, 2002). Tissue engineering coupled with cell therapies offers a potential solution to rehabilitate patients with SCI to regain

function otherwise lost for a lifetime (Cao, 2002). There is not only a patient benefit in regaining function but also an economic incentive as well. A staggering 63% of patients suffering from SCI are unemployed eight years after their injury ("Spinal Cord Injury Facts & Statistics," n.d.). Tissue engineering coupled with cell therapies aimed at SCI have the potential to improve the quality of life by allowing injured patients to regain the lost tissue functions.

2.1.2 Current SCI therapies

Several tissue engineering as well as stem cell approaches have been investigated as potential routes for functional improvement in SCI. Acellular tissue scaffolds comprised of materials ranging from hydrogels to algae have been examined for their potential in spinal cord tissue repair (Bakshi et al., 2004; Harley et al., 2004; Kataoka et al., 2001; Maquet et al., 2001). Tissue scaffolds remain promising because of the ability of the scaffold to guide neuronal processes from one end of the injury to the other side allowing potential synapse reformation and functional regeneration. However, relying on cell migration may not work in a scarred spinal cord. Human embryonic stem cells have shown some promise but there is some debate as to whether or not patient-specific human embryonic stem cells could be produced (Armstrong, Lako, Dean, & Stojkovic, 2006). Further, neural stem cells have been investigated for use and have shown some functional improvement when derived from adult brains (Karimi-Abdolrezaee, Eftekharpour, Wang, Morshead, & Fehlings, 2006) and spinal cords (Hofstetter et al., 2005). However, it has

been shown that direct stem cell implantation into the spinal column can lead to severe side effects (Hofstetter et al., 2005). In the end, the complicated pathophysiology of SCI probably means that there will never be a "gold standard" for SCI repair and it is unarguable that investigating a wide variety of materials is valuable in this field.

2.2 Peripheral Nerve Damage

Peripheral nerve damage is troublingly common in the United States, with an estimated 200,000 patients treated surgically each year (Cohen, Die-gelmann, Lindblad, & Hugo, 1992). The most common cause of peripheral nerve damage is vehicular accidents, closely followed by tumor removal or other iatrogenic side effects from surgeries (Kretschmer, Antoniadis, Braun, Rath, & Richter, 2001). Despite the obvious disadvantages, the current gold standard in treatment for such injuries is a nerve autograft, a technique first pioneered over 45 years ago (Kline, 1990; Mackinnon, Doolabh, Novak, & Trulock, 2001; Millesi, 1967). Allografts are often not considered due to the fact that they incur immunological complications and require immunosuppressives to be effective (Mackinnon et al., 2001). Perhaps the most troubling aspect of autografts is the fact that by transecting a nerve from another part of the body, the patient is trading functionality by destroying a nerve connection elsewhere. Furthermore, motor nerves have been shown to work better in nerve autografts when compared to sensory nerves. This implies that for a patient to receive optimal treatment, the patient would lose some motor function in order to repair the damaged nerve

(Moradzadeh et al., 2008). Finally, due to the current limited ability of autografts, nerves can only be repaired if the damage does not exceed 3 cm in length (Ryu, Beimesch, & Lalli, 2011).

2.2.1 Nerve Conduits

Aside from allografts, several nerve conduits have been constructed and shown some promise. The ideal conduit would undergo 4 phases and take approximately 21 days to heal the damaged nerve tissue (Figure 2.1). Collagen conduits manufactured by NeuraGen from bovine flexor tendons have been shown effective in treating sciatic nerve defects in rats but are limited to 20mm defects (Yoshii et al., 2001). Another company, Polyganics, has developed a biodegradable tube from Neurolac which is a copolyester poly (DL-lactide-e-caprolactone) and have seen results similar to those from standard repair techniques. However, there were more complications in the Neurolac group when compared to controls (Bertleff, Meek, & Nicolai, 2005). There are currently five other similar devices approved for FDA use as nerve conduits, however, none can repair nerve damages over 6cm in length (Kehoe, Zhang, & Boyd, 2011).

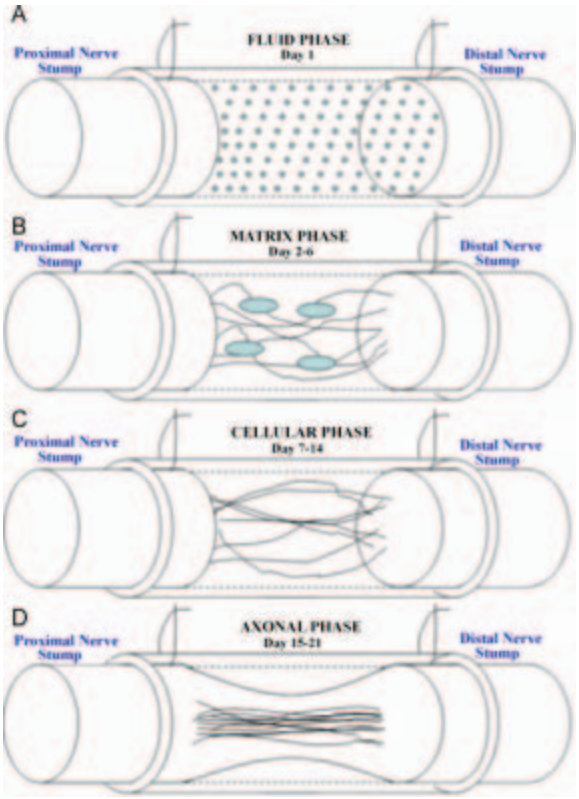

Figure 2.1: In the ideal conduit, this is the sequence of events leading to the growth of a new nerve cable: (A) chamber walls with a protein-rich fluid (containing neurotrophic factors); (B) generation of a fibrin-rich scaffold; (C) cell migration (perineural, endothelial and schwann cells); (D) axonal cables elongation. Adapted from (Kehoe et al., 2011)

2.2.2 Other Diseases

Diabetic neuropathy (DN) is damage of the peripheral nerves due to increased blood sugar levels. Currently there are approximately 23.6 million people with diabetes in the United States. Approximately 50% of people with diabetes contract some form of DN. The only treatment option available is palliative pain medication, which does not combat the disease in any way other than making it slightly more bearable for the patients

(“Diabetic Neuropathy Information Page: National Institute of Neurological Disorders and Stroke (NINDS),” n.d.). Even more troubling is giant axonal neuropathy (GAN). GAN is a rare, inherited genetic disorder that is characterized by a systematic degradation and destruction of neurons. This disease progresses slowly and starts in the peripheral nervous system, which controls movement and sensation in the arms, legs, and other parts of the body; followed by progression to the central nervous system where it can cause cognitive disabilities (“Giant Axonal Neuropathy Information Page: National Institute of Neurological Disorders and Stroke (NINDS),” n.d.). Currently there are no treatment options available for GAN. From the current limitations coupled with the seriousness of the diseases associated with them, it is apparent that other strategies for nerve repair need to be explored.

2.3 Nanotechnology

Nanotechnology offers interesting avenues to explore tissue engineering in the nervous system. Currently, nanotechnology is being considered in a variety of basic science and clinical neuroscience applications including functional regeneration of both the peripheral and central nervous system (Silva, 2006). On the basic science side, some studies have shown that by simply creating nanoporous surfaces, neurite formation among neural cells can be greatly enhanced while simultaneously limiting glial scarring (Moxon et al., 2004). This would be especially beneficial in SCI where glial scarring is a major hurdle in functional recovery. In addition, there is evidence that physical features,

specifically sub-micron scale surface patterning, can greatly enhance neuronal growth (Fan et al., 2002). On the clinical side, studies have shown that manipulating the nanotopography by creating nanofibers leads to differentiation of neural progenitor cells into neurons by incorporating a molecular design that is known to promote neurite growth (Kam, Shain, Turner, & Bizios, 2001; Koh, Yong, Chan, & Ramakrishna, 2008; Matsuzawa, Weight, Potember, & Liesi, 1996; Silva et al., 2004). It has also been shown that when mouse cerebellar progenitor cells were cultured on PLLA nanofibers, they differentiated into mature neurons to expressed extensive neurite networks (Yang et al., 2004).

2.3.1 Nanotopography

Advances in tissue engineering have lead to the development of approaches towards design of biomimetic scaffolds for neural tissue engineering applications (J. Lee et al., 2011; Ranieri et al., 1994). However, there are significant challenges in supporting growth and differentiation of neuronal cells for prolonged periods of time on scaffold surfaces. Several studies have reported enhanced neural stem cell (NSC) response on nanofiber polymer scaffolds (Christopherson, Song, & Mao, 2009; Ghasemi-Mobarakeh, Prabhakaran, Morshed, Nasr-Esfahani, & Ramakrishna, 2008; Yang, Murugan, Wang, & Ramakrishna, 2005; Yoo, Kim, & Park, 2009) and hydrogels (Crompton et al., 2007; Yu & Shoichet, 2005) both of which provide a unique nanotopography for the cells to adhere and differentiate. These studies and several other studies imply that scaffolds with

unique nanotopography have the potential to support neural cell growth and specifically to support NSC functionality. By manipulating the topography of the scaffold surface at the nanoscale, we can enhance neuronal cell functionality, which in turn will prove to be beneficial for tissue engineering applications fot the treatment of neurological diseases and disorders.

Several in vitro studies have reported enhanced functionality of neuronal cells on polymer nanofiber scaffolds (Christopherson et al., 2009; He et al., 2010; F. Yang et al., 2005), nanoporous scaffolds (Moxon et al., 2004) and nanowire scaffolds (S. L. Bechara, Judson, & Popat, 2010). In addition, there is evidence that neural stem cells (NSC) promote extensive axonal growth when implanted with nanofiber scaffolds into the site of a spinal cord injury and can also reduce the functional deficits in a sciatic nerve injury model in vivo (Y.-T. Kim, Haftel, Kumar, & Bellamkonda, 2008). Thus, it can easily be concluded that nanotopography on a scaffold surface plays a positive role in neuronal cell-surface interactions.

2.4 Electrical Conductivity

Most of the scaffolds presented thus far do not have physiologically relevant surface properties. NSCs are known to preferentially adhere and differentiate on electrically charged surfaces (Maroudas, 1975). Therefore, while nanotopography has been shown to enhance cellular response, it seems necessary to further functionalize the scaffolds and create an electrically charged surface for growth and maintenance of NSCs.

2.4.1 Polypyrrole

The electrically conductive polymer polypyrrole (PPy) has garnered substantial interest for applications in neural tissue engineering due its biocompatibility (George, Lyckman, LaVan, Hegde, Leung, Avasare, Testa, Alexander, Langer, & Sur, 2005a; Xioadong Wang, Gu, et al., 2004) (Figure 2.2), ease of synthesis (J. Y. Lee, Bashur, Goldstein, & Schmidt, 2009), and electrical properties (Y. Li, Neoh, Cen, & Kang, 2005). It has been commonly used in biosensors and polymer batteries for these reasons (Olea, Viratelle, & Faure, 2008). Polypyrrole is unique in that is simply an organic chain of alternating double and single bonded sp^2 hybridized atoms (Guimard, Gomez, & Schmidt, 2007). This gives polypyrrole electrically conductive properties akin to metal.

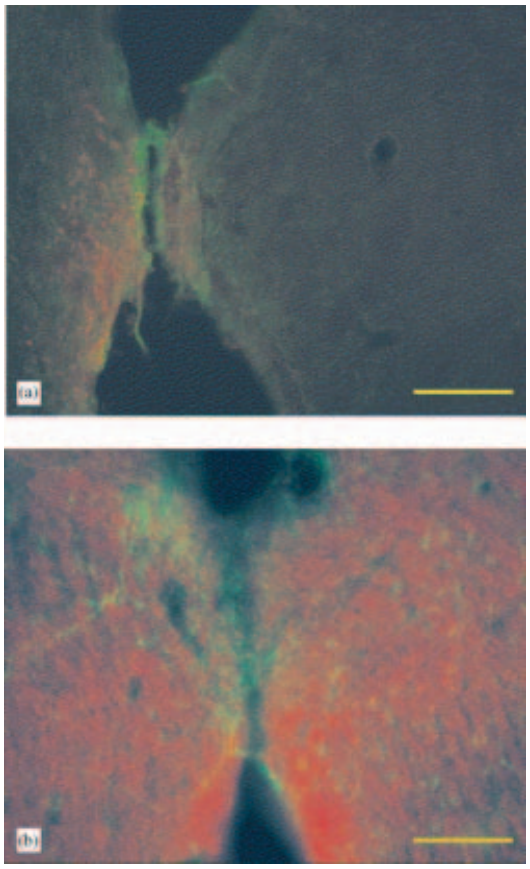

Figure 2.2: A fluorescence labeled section of neural tissue in an implant lumen highlighting PPy biocompatibility: (a) Neural tissue in the lumen of the Teflon implants, (b) neural tissue in the PPy lumen where the glia has reformed and neurons are present, scale bar: 100 μm, green: glia, red: neurons. This study showed that PPy is biocompatible. Adapted from (George, Lyckman, LaVan, Hegde, Leung, Avasare, Testa, Alexander, Langer, & Sur, 2005b)

2.4.2 Polypyrrole as a Biomaterial

Studies have shown that PPy has the ability to promote growth of endothelial cells (Garner, Hodgson, Wallace, & Underwood, 1999), primary neurons (Gomez, Lee, Nickels, & Schmidt, 2007), and even mesenchymal stem cells (Castano, O'Rear, McFetridge, & Sikavitsas, 2004). The need for an electrically conductive polymer for

neural tissue engineering applications arises from the fact that uncharged surfaces are less than optimal for promoting normal cellular phenotypic behaviors (Maroudas, 1975). Furthermore, the ability to deliver an electrical current to the cells via the scaffold surface may have several advantages. Current research has emerged showing that physiologically relevant electrical stimulation can enhance nerve regeneration (Kotwal, 2001) and help replenish NSCs in an injury site (Becker, Gary, Rosenzweig, Grill, & McDonald, 2010). Therefore it is advantageous to design scaffolds that not only have unique surface nanotopography, but also have the ability to provide physiological levels of electrical stimulation for the NSCs to modulate and enhance their cellular response.

2.5 Nerve Growth Factor

Due to the inability of the nervous system to promote functional repair, neural tissue engineering has focused on investigating potential materials that can encourage healing when implanted into an injury site. For this reason, nerve growth factor (NGF) has appealed to tissue engineers as it is produced naturally and plays a critical role in nervous system development and maintenance (Blesch, Lu, & Tuszynski, 2002). NGF was discovered over 60 years ago as a molecule that enhanced the survival of sensory and sympathetic neurons (Levi-Montalcini & Hamburger, 1951). NGF acts on the cell by binding to either the p75 or TrkA receptor (Bothwell, 1995; Kaplan & Miller, 1997). However, the diversity of actions that NGF can take on a cell is wide ranging and NGF

signaling is broad based, dynamically regulated, and depends on the context (Sofroniew, Howe, & Mobley, 2001).

2.5.1 Nerve growth factor Applications

In the nervous system, several studies have suggested that NGF has the potential to treat patients with Alzheimer's disease and brain injuries (Gage & Björklund, 1986; M H Tuszynski, Buzsaki, & Gage, 1990). Outside of the nervous system, NGF treatments have been shown to increase bone formation (L. Wang et al., 2010) and even promote the healing of neurotropic ulcers (Aloe, Tirassa, & Lambiase, 2008). Other groups have conjugated NGF onto various tissue engineering scaffolds and have shown that NGF can influence the differentiation potential of mesenchymal stem cells (Cho, Choi, Jeong, & Yoo, 2010) and that these types of scaffolds can enhance sciatic nerve regeneration (Chung et al., 2011; A. C. Lee et al., 2003). From this it is apparent that NGF plays a variety of different roles in the body and is highly dependent on the context in which it is used. Therefore it is possible that NGF has the potential to be beneficial in a neural tissue engineering application.

2.6 Micropatterning

In order for a scaffold to be considered a suitable neurosuture, it must be able to correctly guide regeneration of the nerve to traverse the damaged section. To this end, several groups have investigated different micro-patterns that can direct cellular growth and potentially reconnect the damaged nerve region (Morelli et al., 2010). One group has

shown that by patterning a cell attractant to an otherwise cell repulsive surface, they can direct neural progenitor cell (NPC) adhesion (A. Ruiz et al., 2008). Furthermore, astrocytes have also been shown to align to patterned ligand surfaces (Meng, Hlady, & Tresco, 2012). Although the application suggested in this work is not for nerve repair, regions of phosphorous doped diamond like carbon micro-patterns have been shown to promote neuronal adhesion over their non doped regions (Kelly et al., 2008). Other groups have shown that micro-patterning alone can influence NPC differentiation (Luo et al., 2011; Recknor, Sakaguchi, & Mallapragada, 2006; Tsuruma, Tanaka, Yamamoto, & Shimomura, 2008) From this it is apparent that micro-patterning scaffolds have great potential in developing a new therapy for nervous system applications by allowing scaffolds to transect damaged regions of nerve to reconnect the severed pathways.

2.7 References

Aloe, L., Tirassa, P., & Lambiase, A. (2008). The topical application of nerve growth factor as a pharmacological tool for human corneal and skin ulcers. *Pharmacological Research*, *57*(4), 253-258. Retrieved from http://www.sciencedirect.com/science/article/pii/S1043661808000200

Armstrong, L., Lako, M., Dean, W., & Stojkovic, M. (2006). Epigenetic modification is central to genome reprogramming in somatic cell nuclear transfer. *Stem cells (Dayton, Ohio)*, *24*(4), 805-14. doi:10.1634/stemcells.2005-0350

Bakshi, A., Fisher, O., Dagci, T., Himes, B. T., Fischer, I., & Lowman, A. (2004). Mechanically engineered hydrogel scaffolds for axonal growth and angiogenesis after transplantation in spinal cord injury. *Journal of neurosurgery. Spine*, *1*(3), 322-9. doi:10.3171/spi.2004.1.3.0322

Bechara, S. L., Judson, A., & Popat, K. C. (2010). Template synthesized poly([var epsilon]-caprolactone) nanowire surfaces for neural tissue engineering. *Biomaterials*, *31*(13), 3492-3501. Retrieved from http://www.sciencedirect.com/science/article/B6TWB-4YC39RW-5/2/b9a281830087f2631912339503ac195e

Becker, D., Gary, D. S., Rosenzweig, E. S., Grill, W. M., & McDonald, J. W. (2010). Functional electrical stimulation helps replenish progenitor cells in the injured spinal cord of adult rats. *Experimental neurology*, *222*(2), 211-8. doi:10.1016/j.expneurol.2009.12.029

Bertleff, M. J. O. E., Meek, M. F., & Nicolai, J.-P. A. (2005). A prospective clinical evaluation of biodegradable neurolac nerve guides for sensory nerve repair in the hand. *The Journal of hand surgery*, *30*(3), 513-8. doi:10.1016/j.jhsa.2004.12.009

Blesch, A., Lu, P., & Tuszynski, M. H. (2002). Neurotrophic factors, gene therapy, and neural stem cells for spinal cord repair. *Brain Research Bulletin*, *57*(6), 833-838. Retrieved from http://www.sciencedirect.com/science/article/pii/S0361923001007742

Bothwell, M. (1995). Functional interactions of neurotrophins and neurotrophin receptors. *Annual review of neuroscience*, *18*, 223-53. Annual Reviews 4139 El Camino Way, P.O. Box 10139, Palo Alto, CA 94303-0139, USA. doi:10.1146/annurev.ne.18.030195.001255

Cao, Q. (2002). Differentiation of Engrafted Neuronal-Restricted Precursor Cells Is Inhibited in the Traumatically Injured Spinal Cord. *Experimental Neurology*, *177*(2), 349-359. doi:10.1006/exnr.2002.7981

Castano, H., O'Rear, E. A., McFetridge, P. S., & Sikavitsas, V. I. (2004). Polypyrrole thin films formed by admicellar polymerization support the osteogenic differentiation of mesenchymal stem cells. *Macromolecular bioscience*, *4*(8), 785-94. doi:10.1002/mabi.200300123

Cho, Y. I., Choi, J. S., Jeong, S. Y., & Yoo, H. S. (2010). Nerve growth factor (NGF)-conjugated electrospun nanostructures with topographical cues for neuronal differentiation of mesenchymal stem cells. *Acta biomaterialia*, *6*(12), 4733-4725. doi:10.1016/j.actbio.2010.06.019

Christopherson, G. T., Song, H., & Mao, H.-Q. (2009). The influence of fiber diameter of electrospun substrates on neural stem cell differentiation and proliferation. *Biomaterials*, *30*(4), 556-64. doi:10.1016/j.biomaterials.2008.10.004

Chung, T.-W., Yang, M.-C., Tseng, C.-C., Sheu, S.-H., Wang, S.-S., Huang, Y.-Y., & Chen, S.-D. (2011). Promoting regeneration of peripheral nerves in-vivo using new PCL-NGF/Tirofiban nerve conduits. *Biomaterials*, *32*(3), 734-743. Retrieved from http://www.sciencedirect.com/science/article/pii/S0142961210011786

Cohen, I. K., Die-gelmann, R. F., Lindblad, W. J., & Hugo, N. E. (1992). Wound Healing: Biochemical and Clinical Aspects. *Plastic and Reconstructive Surgery*, *90*(5). Retrieved from http://journals.lww.com/plasreconsurg/Fulltext/1992/11000/Wound_Healing__Biochemical_and_Clinical_Aspects.34.aspx

Crompton, K. E., Goud, J. D., Bellamkonda, R. V., Gengenbach, T. R., Finkelstein, D. I., Horne, M. K., & Forsythe, J. S. (2007). Polylysine-functionalised thermoresponsive chitosan hydrogel for neural tissue engineering. *Biomaterials*, *28*(3), 441-9. doi:10.1016/j.biomaterials.2006.08.044

Diabetic Neuropathy Information Page: National Institute of Neurological Disorders and Stroke (NINDS). (n.d.). Retrieved March 6, 2012, from http://www.ninds.nih.gov/disorders/diabetic/diabetic.htm

Fan, Y. W., Cui, F. Z., Hou, S. P., Xu, Q. Y., Chen, L. N., & Lee, I.-S. (2002). Culture of neural cells on silicon wafers with nano-scale surface topograph. *Journal of*

neuroscience methods, *120*(1), 17-23. Retrieved from http://www.ncbi.nlm.nih.gov/pubmed/12351203

Gage, F. H., & Björklund, A. (1986). Enhanced graft survival in the hippocampus following selective denervation. *Neuroscience*, *17*(1), 89-98. Retrieved from http://www.sciencedirect.com/science/article/pii/0306452286902277

Garner, B., Hodgson, A. J., Wallace, G. G., & Underwood, P. A. (1999). Human endothelial cell attachment to and growth on polypyrrole-heparin is vitronectin dependent. *Journal of materials science. Materials in medicine*, *10*(1), 19-27. Retrieved from http://www.ncbi.nlm.nih.gov/pubmed/15347990

George, P. M., Lyckman, A. W., LaVan, D. A., Hegde, A., Leung, Y., Avasare, R., Testa, C., et al. (2005). Fabrication and biocompatibility of polypyrrole implants suitable for neural prosthetics. *Biomaterials*, *26*(17), 3511-9. doi:10.1016/j.biomaterials.2004.09.037

Ghasemi-Mobarakeh, L., Prabhakaran, M. P., Morshed, M., Nasr-Esfahani, M.-H., & Ramakrishna, S. (2008). Electrospun poly(epsilon-caprolactone)/gelatin nanofibrous scaffolds for nerve tissue engineering. *Biomaterials*, *29*(34), 4532-9. doi:10.1016/j.biomaterials.2008.08.007

Giant Axonal Neuropathy Information Page: National Institute of Neurological Disorders and Stroke (NINDS). (n.d.). Retrieved March 6, 2012, from http://www.ninds.nih.gov/disorders/gan/GiantAxonalNeuropathy.htm

Gomez, N., Lee, J. Y., Nickels, J. D., & Schmidt, C. E. (2007). Micropatterned Polypyrrole: A Combination of Electrical and Topographical Characteristics for the Stimulation of Cells. *Advanced functional materials*, *17*(10), 1645-1653. doi:10.1002/adfm.200600669

Guimard, N. K., Gomez, N., & Schmidt, C. E. (2007). Conducting polymers in biomedical engineering. *Progress in Polymer Science*, *32*(8-9), 876-921. doi:10.1016/j.progpolymsci.2007.05.012

Harley, B. A., Spilker, M. H., Wu, J. W., Asano, K., Hsu, H.-P., Spector, M., & Yannas, I. V. (2004). Optimal degradation rate for collagen chambers used for regeneration of peripheral nerves over long gaps. *Cells, tissues, organs*, *176*(1-3), 153-65. doi:10.1159/000075035

He, L., Liao, S., Quan, D., Ma, K., Chan, C., Ramakrishna, S., & Lu, J. (2010). Synergistic effects of electrospun PLLA fiber dimension and pattern on neonatal mouse cerebellum C17.2 stem cells. *Acta biomaterialia*, *6*(8), 2960-9. doi:10.1016/j.actbio.2010.02.039

Hofstetter, C. P., Holmström, N. A. V., Lilja, J. A., Schweinhardt, P., Hao, J., Spenger, C., Wiesenfeld-Hallin, Z., et al. (2005). Allodynia limits the usefulness of intraspinal neural stem cell grafts; directed differentiation improves outcome. *Nature neuroscience*, *8*(3), 346-53. doi:10.1038/nn1405

Hulsebosch, C. E. (2002). RECENT ADVANCES IN PATHOPHYSIOLOGY AND TREATMENT OF SPINAL CORD INJURY. *Advan Physiol Educ*, *26*(4), 238-255. Retrieved from http://advan.physiology.org/cgi/content/abstract/26/4/238

Kam, L., Shain, W., Turner, J. N., & Bizios, R. (2001). Axonal outgrowth of hippocampal neurons on micro-scale networks of polylysine-conjugated laminin. *Biomaterials*, *22*(10), 1049-54. Retrieved from http://www.ncbi.nlm.nih.gov/pubmed/11352086

Kaplan, D. R., & Miller, F. D. (1997). Signal transduction by the neutrophin receptors. *Current Opinion in Cell Biology*, *9*(2), 213-221. doi:10.1016/S0955-0674(97)80065-8

Karimi-Abdolrezaee, S., Eftekharpour, E., Wang, J., Morshead, C. M., & Fehlings, M. G. (2006). Delayed transplantation of adult neural precursor cells promotes remyelination and functional neurological recovery after spinal cord injury. *The Journal of neuroscience : the official journal of the Society for Neuroscience*, *26*(13), 3377-89. doi:10.1523/JNEUROSCI.4184-05.2006

Kataoka, K., Suzuki, Y., Kitada, M., Ohnishi, K., Suzuki, K., Tanihara, M., Ide, C., et al. (2001). Alginate, a bioresorbable material derived from brown seaweed, enhances elongation of amputated axons of spinal cord in infant rats. *Journal of biomedical materials research*, *54*(3), 373-84. Retrieved from http://www.ncbi.nlm.nih.gov/pubmed/11189043

Kehoe, S., Zhang, X. F., & Boyd, D. (2011). FDA approved guidance conduits and wraps for peripheral nerve injury: A review of materials and efficacy. *Injury*. doi:10.1016/j.injury.2010.12.030

Kelly, S., Regan, E. M., Uney, J. B., Dick, A. D., McGeehan, J. P., Mayer, E. J., & Claeyssens, F. (2008). Patterned growth of neuronal cells on modified diamond-like

carbon substrates. *Biomaterials*, *29*(17), 2573-80. doi:10.1016/j.biomaterials.2008.03.001

Kim, Y.-T., Haftel, V. K., Kumar, S., & Bellamkonda, R. V. (2008). The role of aligned polymer fiber-based constructs in the bridging of long peripheral nerve gaps. *Biomaterials*, *29*(21), 3117-27. doi:10.1016/j.biomaterials.2008.03.042

Kirshblum, S. C., Groah, S. L., McKinley, W. O., Gittler, M. S., & Stiens, S. A. (2002). Spinal cord injury medicine. 1. Etiology, classification, and acute medical management. *Archives of physical medicine and rehabilitation*, *83*(3 Suppl 1), S50-7, S90-8. Retrieved from http://www.ncbi.nlm.nih.gov/pubmed/11973697

Kline, D. G. (1990). Surgical repair of peripheral nerve injury. *Muscle & Nerve*, *13*(9), 843-852. Wiley Subscription Services, Inc., A Wiley Company. doi:10.1002/mus.880130911

Koh, H. S., Yong, T., Chan, C. K., & Ramakrishna, S. (2008). Enhancement of neurite outgrowth using nano-structured scaffolds coupled with laminin. *Biomaterials*, *29*(26), 3574-82. doi:10.1016/j.biomaterials.2008.05.014

Kotwal, A. (2001). Electrical stimulation alters protein adsorption and nerve cell interactions with electrically conducting biomaterials. *Biomaterials*, *22*(10), 1055-1064. doi:10.1016/S0142-9612(00)00344-6

Kretschmer, T., Antoniadis, G., Braun, V., Rath, S. A., & Richter, H.-P. (2001). Evaluation of iatrogenic lesions in 722 surgically treated cases of peripheral nerve trauma. *Journal of Neurosurgery*, *94*(6), 905-912. Journal of Neurosurgery Publishing Group. doi:10.3171/jns.2001.94.6.0905

Lee, A. C., Yu, V. M., Lowe, J. B., Brenner, M. J., Hunter, D. A., Mackinnon, S. E., & Sakiyama-Elbert, S. E. (2003). Controlled release of nerve growth factor enhances sciatic nerve regeneration. *Experimental Neurology*, *184*(1), 295-303. doi:10.1016/S0014-4886(03)00258-9

Lee, J. Y., Bashur, C. A., Goldstein, A. S., & Schmidt, C. E. (2009). Polypyrrole-coated electrospun PLGA nanofibers for neural tissue applications. *Biomaterials*, *30*(26), 4325-35. doi:10.1016/j.biomaterials.2009.04.042

Lee, J., Chu, B. H., Sen, S., Gupte, A., Chancellor, T. J., Chang, C.-Y., Ren, F., et al. (2011). Modulating malignant epithelial tumor cell adhesion, migration and

mechanics with nanorod surfaces. *Biomedical microdevices*, *13*(1), 89-95. doi:10.1007/s10544-010-9473-7

Levi-Montalcini, R., & Hamburger, V. (1951). Selective growth stimulating effects of mouse sarcoma on the sensory and sympathetic nervous system of the chick embryo. *Journal of Experimental Zoology*, *116*(2), 321-361. doi:10.1002/jez.1401160206

Li, Y., Neoh, K. G., Cen, L., & Kang, E. T. (2005). Porous and electrically conductive polypyrrole-poly(vinyl alcohol) composite and its applications as a biomaterial. *Langmuir : the ACS journal of surfaces and colloids*, *21*(23), 10702-9. doi:10.1021/la0514314

Luo, C., Liu, L., Ni, X., Wang, L., Nomura, S. M., Ouyang, Q., & Chen, Y. (2011). Differentiating stem cells on patterned substrates for neural network formation. *Microelectronic Engineering*, *88*(8), 1707-1710. doi:10.1016/j.mee.2010.12.062

Mackinnon, S. E., Doolabh, V. B., Novak, C. B., & Trulock, E. P. (2001). Clinical Outcome following Nerve Allograft Transplantation. *Plastic and Reconstructive Surgery*, *107*(6). Retrieved from http://journals.lww.com/plasreconsurg/Fulltext/2001/05000/Clinical_Outcome_following_Nerve_Allograft.16.aspx

Maquet, V., Martin, D., Scholtes, F., Franzen, R., Schoenen, J., Moonen, G., & Jér me, R. (2001). Poly(D,L-lactide) foams modified by poly(ethylene oxide)-block-poly(D,L-lactide) copolymers and a-FGF: in vitro and in vivo evaluation for spinal cord regeneration. *Biomaterials*, *22*(10), 1137-46. Retrieved from http://www.ncbi.nlm.nih.gov/pubmed/11352093

Maroudas, N. G. (1975). Adhesion and spreading of cells on charged surfaces. *Journal of Theoretical Biology*, *49*(1), 417-424. doi:10.1016/S0022-5193(75)80044-0

Matsuzawa, M., Weight, F. F., Potember, R. S., & Liesi, P. (1996). Directional neurite outgrowth and axonal differentiation of embryonic hippocampal neurons are promoted by a neurite outgrowth domain of the B2-chain of laminin. *International journal of developmental neuroscience : the official journal of the International Society for Developmental Neuroscience*, *14*(3), 283-95. Retrieved from http://www.ncbi.nlm.nih.gov/pubmed/8842805

Meng, F., Hlady, V., & Tresco, P. A. (2012). Inducing alignment in astrocyte tissue constructs by surface ligands patterned on biomaterials. *Biomaterials*, *33*(5), 1323-35. doi:10.1016/j.biomaterials.2011.10.034

Millesi, H. (1967). [Nerve transplantation for reconstruction of peripheral nerves injured by the use of the microsurgical technic]. *Minerva chirurgica*, *22*(17), 950-1. Retrieved from http://www.ncbi.nlm.nih.gov/pubmed/6055379

Moradzadeh, A., Borschel, G. H., Luciano, J. P., Whitlock, E. L., Hayashi, A., Hunter, D. A., & Mackinnon, S. E. (2008). The impact of motor and sensory nerve architecture on nerve regeneration. *Experimental neurology*, *212*(2), 370-6. doi:10.1016/j.expneurol.2008.04.012

Morelli, S., Salerno, S., Piscioneri, A., Papenburg, B. J., Di Vito, A., Giusi, G., Canonaco, M., et al. (2010). Influence of micro-patterned PLLA membranes on outgrowth and orientation of hippocampal neurites. *Biomaterials*, *31*(27), 7000-11. doi:10.1016/j.biomaterials.2010.05.079

Moxon, K. A., Kalkhoran, N. M., Markert, M., Sambito, M. A., McKenzie, J. L., & Webster, J. T. (2004). Nanostructured surface modification of ceramic-based microelectrodes to enhance biocompatibility for a direct brain-machine interface. *IEEE transactions on bio-medical engineering*, *51*(6), 881-9. doi:10.1109/TBME.2004.827465

Olea, D., Viratelle, O., & Faure, C. (2008). Polypyrrole-glucose oxidase biosensor. Effect of enzyme encapsulation in multilamellar vesicles on analytical properties. *Biosensors & bioelectronics*, *23*(6), 788-94. doi:10.1016/j.bios.2007.08.018

Olive, J. L., McCully, K. K., & Dudley, G. A. (2002). Blood flow response in individuals with incomplete spinal cord injuries. *Spinal cord*, *40*(12), 639-45. Nature Publishing Group. doi:10.1038/sj.sc.3101379

Ranieri, J. P., Bellamkonda, R., Bekos, E. J., Gardella, J. A., Mathieu, H. J., Ruiz, L., & Aebischer, P. (1994). Spatial control of neuronal cell attachment and differentiation on covalently patterned laminin oligopeptide substrates. *International Journal of Developmental Neuroscience*, *12*(8), 725-735. doi:10.1016/0736-5748(94)90052-3

Recknor, J. B., Sakaguchi, D. S., & Mallapragada, S. K. (2006). Directed growth and selective differentiation of neural progenitor cells on micropatterned polymer substrates. *Biomaterials*, *27*(22), 4098-4108. Retrieved from http://www.sciencedirect.com/science/article/pii/S0142961206002626

Ruiz, A., Buzanska, L., Gilliland, D., Rauscher, H., Sirghi, L., Sobanski, T., Zychowicz, M., et al. (2008). Micro-stamped surfaces for the patterned growth of neural stem cells. *Biomaterials*, *29*(36), 4766-74. doi:10.1016/j.biomaterials.2008.08.017

Ryu, J., Beimesch, C. F., & Lalli, T. J. (2011). (iii) Peripheral nerve repair. *Orthopaedics and Trauma*, *25*(3), 174-180. doi:10.1016/j.mporth.2011.03.003

Silva, G. A. (2006). Neuroscience nanotechnology: progress, opportunities and challenges. *Nature reviews. Neuroscience*, *7*(1), 65-74. doi:10.1038/nrn1827

Silva, G. A., Czeisler, C., Niece, K. L., Beniash, E., Harrington, D. A., Kessler, J. A., & Stupp, S. I. (2004). Selective differentiation of neural progenitor cells by high-epitope density nanofibers. *Science (New York, N.Y.)*, *303*(5662), 1352-5. doi:10.1126/science.1093783

Sofroniew, M. V., Howe, C. L., & Mobley, W. C. (2001). Nerve growth factor signaling, neuroprotection, and neural repair. *Annual review of neuroscience*, *24*, 1217-81. doi:10.1146/annurev.neuro.24.1.1217

Spinal Cord Injury Facts & Statistics. (n.d.). Retrieved March 6, 2012, from http://www.sci-info-pages.com/facts.html

Tsuruma, A., Tanaka, M., Yamamoto, S., & Shimomura, M. (2008). Control of neural stem cell differentiation on honeycomb films. *Colloids and Surfaces A: Physicochemical and Engineering Aspects*, *313-314*, 536-540. doi:10.1016/j.colsurfa.2007.05.079

Tuszynski, M H, Buzsaki, G., & Gage, F. H. (1990). Nerve growth factor infusions combined with fetal hippocampal grafts enhance reconstruction of the lesioned septohippocampal projection. *Neuroscience*, *36*(1), 33-44. Retrieved from http://www.sciencedirect.com/science/article/pii/0306452290903499

Wang, L, Cao, J., Lei, D. L., Cheng, X. B., Zhou, H. Z., Hou, R., Zhao, Y. H., et al. (2010). Application of nerve growth factor by gel increases formation of bone in mandibular distraction osteogenesis in rabbits. *British Journal of Oral and Maxillofacial Surgery*, *48*(7), 515-519. Retrieved from http://www.sciencedirect.com/science/article/pii/S0266435610000628

Wang, Xiaohai, Arcuino, G., Takano, T., Lin, J., Peng, W. G., Wan, P., Li, P., et al. (2004). P2X7 receptor inhibition improves recovery after spinal cord injury. *Nature medicine*, *10*(8), 821-7. doi:10.1038/nm1082

Wang, Xioadong, Gu, X., Yuan, C., Chen, S., Zhang, P., Zhang, T., Yao, J., et al. (2004). Evaluation of biocompatibility of polypyrrole in vitro and in vivo. *Journal of biomedical materials research. Part A*, *68*(3), 411-22. doi:10.1002/jbm.a.20065

Yang, F., Murugan, R., Ramakrishna, S., Wang, X., Ma, Y.-X., & Wang, S. (2004). Fabrication of nano-structured porous PLLA scaffold intended for nerve tissue engineering. *Biomaterials*, *25*(10), 1891-900. Retrieved from http://www.ncbi.nlm.nih.gov/pubmed/14738853

Yang, F., Murugan, R., Wang, S., & Ramakrishna, S. (2005). Electrospinning of nano/micro scale poly(L-lactic acid) aligned fibers and their potential in neural tissue engineering. *Biomaterials*, *26*(15), 2603-10. doi:10.1016/j.biomaterials.2004.06.051

Yoo, H. S., Kim, T. G., & Park, T. G. (2009). Surface-functionalized electrospun nanofibers for tissue engineering and drug delivery. *Advanced drug delivery reviews*, *61*(12), 1033-42. doi:10.1016/j.addr.2009.07.007

Yoshii, S., Oka, M., Ikeda, N., Akagi, M., Matsusue, Y., & Nakamura, T. (2001). Bridging a peripheral nerve defect using collagen filaments. *The Journal of hand surgery*, *26*(1), 52-9. Retrieved from http://www.ncbi.nlm.nih.gov/pubmed/11172368

Yu, T. T., & Shoichet, M. S. (2005). Guided cell adhesion and outgrowth in peptide-modified channels for neural tissue engineering. *Biomaterials*, *26*(13), 1507-14. doi:10.1016/j.biomaterials.2004.05.012

Chapter 3 Template Synthesized Poly(ε-caprolactone) Nanowire Surfaces enhance PC12 cellular adhesion and proliferation

3.1 Introduction

In this study, a novel solvent-free nanotemplating technique for fabricating poly(ε-caprolactone) (PCL) scaffolds with controlled arrays of high aspect ratio substrate-bound nanowires for the growth and maintenance of differentiated states of neuronal cells was developed to address specific aim 1. PCL is a biodegradable and biocompatible polymer, and as such, has been used in tissue engineering applications ranging from bone regeneration (Oh, Park, Kim, & Lee, 2007; J. R. Porter, Henson, & Popat, 2009; Tiaw et al., 2005; Williamson & Coombes, 2004; Yoshimoto, Shin, Terai, & Vacanti, 2003) to nerve tissue regeneration and differentiation (Chew, Mi, Hoke, & Leong, 2008; Flynn, Dalton, & Shoichet, 2003; Ghasemi-Mobarakeh et al., 2008; Nisbet, Rodda, Horne, Forsythe, & Finkelstein, 2009; Schnell et al., 2007; Xie et al., 2009). The PCL nanowire templating technique is especially advantageous because it is solvent free and has the potential for incorporating active biomolecules or drugs into the scaffold without compromising their bioactivity (Mooney, Baldwin, Suh, Vacanti, & Langer, 1996). Further, research on polymer-based tissue engineering scaffolds has also revealed that the use of organic solvents during fabrication or bioactive molecule encapsulation may have cytotoxic effects (Hile & Pishko, n.d.; Jameela, Suma, & Jayakrishnan, 1997; W. J. Lin & Yu, n.d.; Miyai et al., 2008; Mooney et al., 1996). Therefore, the solvent free

nanotemplating technique for fabrication of PCL scaffolds is ideal. PC12 cells were used as model cells to study viability, adhesion, proliferation and differentiation on PCL nanowire surfaces. This cell line has been extensively used as a model system for neural tissue engineering research (Foley, Grunwald, Nealey, & Murphy, 2005; J. Y. Lee et al., 2009; Miyoshi, Date, Ohmoto, & Iwata, 1996; Ohnuma, Toyota, Ariizumi, Sugawara, & Asashima, 2009; K.-H. Park & Yun, 2004; Vallbacka, Nobrega, & Sefton, 2001). It is derived from a transplantable rat pheochromocytoma that responds to nerve growth factor by differentiating into neurosecretory cells which can release significant amounts of neurotransmitters (Greene & Tischler, 1976). We hypothesized that if cell adhesion and proliferation is related to surface nano-topography, then PC12 cells will preferentially adhere and will experience enhanced proliferation on nanowire scaffolds. Our results indicate that PCL nanowire surfaces enhance neuronal functionality of PC12 cells and may be a suitable template for neural tissue engineering applications.

3.2 Materials and Methods

3.2.1 Fabrication of PCL Nanowire Surfaces

PCL nanowire surfaces were fabricated according to a protocol previously developed in our lab (J. R. Porter, Henson, et al., 2009) and illustrated in Figure 3.1. Briefly, nanowire surfaces were fabricated via template synthesis from PCL using commercially available nanoporous aluminum oxide membranes (ANOPORE^{TM}, Whatman). Polymer discs were placed on the surface of the membrane (Figure 3.1 a),

and the nanowires were extruded through the membranes in an oven at 115^{o}C for 3 to 5 minutes (Figure 3.1 b and c). The aluminum oxide membranes were dissolved in 1M NaOH for 75 min to remove the membrane thus releasing the extruded nanowires (Figure 3.1 d). Nanowire surfaces were then soaked and rinsed in DI water, dried, and stored in a desiccator until further use. Scanning electron microscopy was used to characterize the surface nanoarchitecture. Throughout this chapter, the following notations will be used for all substrates: **NW** – PCL nanowire surfaces; **SPCL**– smooth PCL surfaces without nanowires; **PS** – smooth polystyrene surfaces.

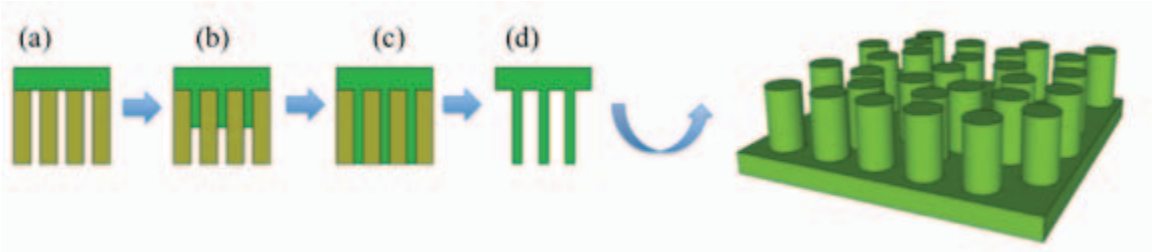

Figure 3.1: Schematic of PCL nanowire fabrication - (a) PCL is placed on top of the alumina nanoporous membrane; (b, c) PCL is extruded through the nanoporous membrane in an vacuum oven; (d) Alumina nanoporous membrane is dissolved in NaOH to release the nanowires.

3.2.2 PC-12 Cell Culture

The PC-12 (ATCC) cell line was used for the proposed studies. This cell line is derived from a rate pheochromocytoma of adrenal medullary origin (Greene & Tischler, 1976). PC12 cells stop dividing and terminally differentiate when treated with nerve growth factor (NGF, Sigma)(Greene & Tischler, 1976). This makes PC12 cells useful as a model system for neuronal differentiation. The cells exhibit a normal neuronal

phenotype after differentiation. Cells below passage 10 were used in all experiments. The medium used for growing the PC12 cells consisted of RPMI-1640 (Invitrogen) media supplemented with 10% Horse Serum (Sigma) and 5% Fetal Bovine Serum (Sigma). Since, PC12 cells do not adhere well on tissue culture polystyrene, the flasks were coated with 50 μg/mL rat tail type I collagen (Sigma) for 30 min to ensure appropriate level of cell adhesion. The medium was changed every 2-3 days, and the subculture was done at a ratio of 1:4. The cells were maintained in an incubator at 37^{o}C and 5% CO_2 for the entire duration of culture. NW, SPCL and PS were sterilized in 24-well plates by incubating them with 70% ethanol for 30 minutes followed by exposure to UV light for 30 mins in a biosafety cabinet. Prior to cell seeding, all the substrates were washed three times with sterile PBS. PC12 cells were seeded at a density of 200,000 cells/well. After 4 days of culture, the media was supplemented with 5ng/ml of NGF to induce neuronal differentiation. Cell response was investigated in two phases:

1. Cell adhesion, proliferation and viability for up to 4 days of culture (pre-differentiation)
2. Cell differentiation and phenotypic behavior for up to 11 days of culture, i.e. 7 days after providing NGF (post-differentiation)

All test and control substrates were cultured and assayed in triplicate at each time point specified. Note: The test and control substrates were <u>not</u> coated with collagen prior to PC12 cell seeding.

3.2.3 Pre-differentiation response of PC-12 cell on PCL nanowire surfaces

After 1 and 4 days of culture, cell response to NW was evaluated using cell adhesion, viability and morphology. The results were compared with that from SPCL and PS.

PC12 adhesion was investigated using calcein-AM (Invitrogen) staining. Calcein-AM is a cell-permeant and non-fluorescent compound that is widely used for determining cell viability. In live cells the non-fluorescent calcein-AM is hydrolyzed by intracellular esterases into the strongly green fluorescent anion calcein-AM. The fluorescent calcein-AM is well retained in the cytoplasm of the live cells. The substrates were removed from culture media; rinsed with PBS and incubated in calcein-AM (2 μM in PBS) solution for 45 min at 37^{o}C. The substrates were rinsed in PBS and then viewed using FITC MF101 green filter with a Zeiss Axioplan 2 fluorescence microscope (Carl Zeiss).

Cell viability was measured after 1 and 4 days of culture (log phase growth) using a commercially available MTT assay kit (Sigma). The MTT assay is a colorimetric assay system that measures the reduction of a tetrazolium component (MTT) into an insoluble formazan product by the mitochondria of viable cells. Substrates with adhered cells were removed from the culture media, rinsed with PBS and incubated in MTT solution (3-[4,5-dimethylthiazol-2-yl]-2,5-diphenyl tetrazolium bromide) for 3 hrs at 37^{o}C. The formazan crystals formed on the substrate surface were then dissolved in the MTT solvent. Optical density was measured at 570nm using a plate reader (FLUOstar Omega, BMG Labtech). Background absorbance at 690 nm was subtracted from the measured absorbance. The

optical density of the dissolved crystals is proportional to the mitochondrial activity of the cells on the surface.

To view the morphology of adhered PC12 cells on different control and test substrates, the cells were fixed, dehydrated, and viewed using scanning electron microscopy (SEM). The cells were fixed in a solution of 3% glutaraldehyde (Sigma), 0.1 M sodium cacodylate (Polysciences), and 0.1 M sucrose (Sigma) for 45 min. The substrates were then soaked in a buffer containing 0.1 M sodium cacodylate and 0.1 M surcrose. The cells were dehydrated by soaking the substrates in increasing concentrations of ethanol (35%, 50%, 70%, 95%, and 100%) for 10 minutes each. Cells were dehydrated further by soaking the substrates in hexamethyldisilazane (HMDS, Sigma) for 10 min. The substrates were then dried under vacuum and stored in a desiccator until examined with SEM. They were sputter coated with 10nm of gold and imaged using a JEOL JSM 6500F at voltages ranging from 10-15kV.

3.2.4 Post-differentiation response of PC-12 cell on PCL nanowire surfaces

After 4 days of culture, the media was supplemented with 5ng/ml of NGF. PC12 cell response to test and control substrates was investigated after 1, 4 and 7 days of differentiation (i.e. after 5, 8 and 11 days of initial culture). The cell response was evaluated using cell viability, cell morphology and immunofluorescence.

The cells were stained with CMFDA (5-chloromethylfluorescein diacetate) to evaluate their viability and neuronal network formation. CMFDA is a fluorescent

chloromethyl derivative that freely diffuses through the membranes of live cells. Once inside the cell, it reacts with intracellular components to produce fluorescence that can be detected using fluorescence microscopy. The substrates were removed from the culture media, washed with PBS and incubated with CMFDA solution (10μM) for 45 mins at 37oC. The stain was replaced with culture media and the substrates were incubated for one hour prior to imaging. The substrates were rinsed in PBS and then viewed using appropriate filters with a Zeiss Axioplan 2 fluorescence microscope (Carl Zeiss). The cell viability was also analyzed after one day of differentiation using MTT assay. The procedure described in the previous section was followed and absorbance was measured using a plate reader.

The cell morphology after 1, 4 and 7 days of differentiation was evaluated using scanning electron microscopy. The cells were fixed and dehydrated using procedure described in the previous section. They were sputter coated with 10nm of gold and imaged using a JEOL JSM 6500F at voltages ranging from 10-15kV.

In order to evaluate the neuronal phenotypic behavior, the PC12 cells were immuno-stained for neurofilament-H (NF-H) and tyrosine hydroxylase (TH) after 7 days of differentiation. Neurofilaments are the major intermediate filaments found in neurons. TH is involved in the conversion of phenylalanine to dopamine. As the rate-limiting enzyme in the synthesis of catecholamines, TH has a key role in the physiology of adrenergic neurons. It is regularly used as a marker for dopaminergic neurons. The cells were fixed with 3.7% paraformaldehyde (Sigma) for 15 mins at 37oC followed by

permeabilization with 1% Triton-X in PBS for 5 mins at room temperature. After fixing and permeabilizing, the cells were washed three times with PBS and incubated in 100 µg/ml of bovine serum albumin (BSA, Sigma) and 40 µL/mL trypan blue for 20 mins to block any non-specific interactions. Cells were then incubated in the primary antibodies (concentration 1 µg/ml), NF-H mouse monoclonal IgG and TH mouse monoclonal (Santa Cruz Biotechnologies), for 1 hr at room temp. The cells were washed three times with PBS followed by incubation in 5 µg/ml of the appropriate secondary antibody; goat anti-mouse FITC for the NF-H, and goat anti-rabbit Texas Red for the TH. The cells were then visualized using an Olympus IX81 microscope equipped with a Yokogawa CSU22 spinning disk confocal head and an EM-CCD cascade II camera (Photometrics).

3.2.5 Statistical Analysis

Each experiment was reconfirmed on three different substrates with at least three different cell populations (n = 9). All the quantitative results were analyzed using analysis of variance (ANOVA). Statistical significance was considered at $p<0.05$.

3.3 Results and Discussion

Tissue regeneration after SCI is a significant challenge in order to regain normal body function and there are no known treatments. Research for a successful therapy is ongoing and ranges from acellular tissue engineering scaffolds to direct injection of stem cells at the site of injury. All of the research shares the common goal of allowing patients to regain normal body function. One approach is to utilize the proven advantages of

nanomedicine and to couple those benefits with tissue engineering strategies. Thus, in this work I have developed a novel, solvent free nanotemplating technique to fabricate surfaces with vertically aligned nanowires from PCL that provide a favorable template for growth and maintenance of differentiated states of neuronal cells. Research on polymer-based tissue engineering scaffolds has revealed that the use of organic solvents during fabrication or bioactive molecule encapsulation may have cytotoxic effects (Jameela et al., 1997).The PCL nanowire templating technique is especially advantageous because it is solvent free technique and has the potential for incorporating active biomolecules or drugs into the scaffold without compromising their bioactivity (Jameela et al., 1997). In addition, no studies have been reported in literature where vertically aligned polymeric nanowire surfaces have been used to maintain differentiated states of neuronal cells. The results indicate that nanowire surfaces significantly enhance adhesion and differentiation of PC12 cells.

3.3.1 Fabrication of PCL Nanowire Surfaces

PCL nanowire surfaces were fabricated using the nanotemplating technique described in the methods section. Figure 3.2 shows SEM images of the nanowire surfaces at different magnifications. The surfaces are homogeneous with uniformly assembled vertical nanowires (Figure 3.2 a). At higher magnifications, the uniform surface is visible along with randomly organized regular micro-channels (Figure 3.2 b). These micro-channels formed due to the surface interactions between the nanowires

during fabrication and membrane dissolution. A closer examination of the nanowire surfaces reveals that individual nanowires are of a consistent diameter (approx. 200 nm) (Figure 3.2 d). The nanowire fabrication technique is flexible in terms of controlling different architectural parameters of the surface, thus resulting in nanowires with varying sizes and densities. The individual nanowire diameter can be varied by using membranes with different pore sizes; and the length of nanowires can be varied using thicker membranes or changing the polymer extrusion time through the membranes. Given the inherent versatility of our unique nanotemplating fabrication technique, polymeric nanowires have the potential to be used in a wide variety of tissue engineering applications including growth and maintenance of neural cells.

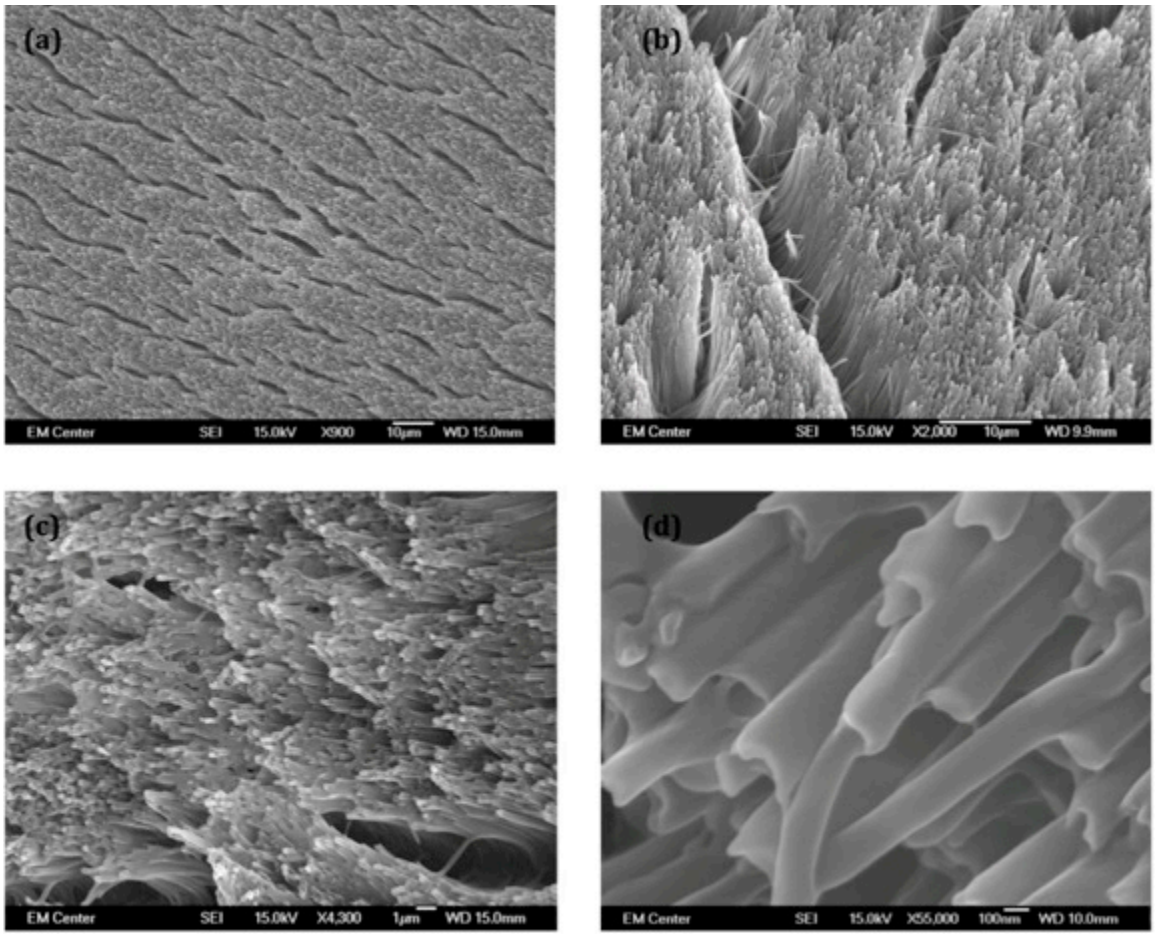

Figure 3.2: Representative high magnification SEM images of PCL nanowire surfaces at (a) 900x, (b) 2000x, (c) 4300x and (d) 55,000x.

PC12 cells were used to evaluate the ability of nanowire surfaces to maintain the growth and differentiation of cells. This cell line has been used in other neural tissue-engineering applications to evaluate and predict neuronal responses to biomaterial surfaces (Foley et al., 2005; J. Y. Lee et al., 2009; Ohnuma et al., 2009). PC12 cell interaction with nanowire and control surfaces was investigated after 1 and 4 days of initial culture. The cells were cultured on the NW, SPCL, and PS without NGF to

evaluate the cell adhesion. Typically, culture surfaces such as PS are coated with collagen to ensure appropriate PC12 cell adhesion. However, in order to investigate the effect of nanotopography on cell functionality, none of test or control surfaces evaluated here were coated with collagen.

Cell adhesion was evaluated by staining the live cells using calcein-AM stain. Fluorescence microscopy images indicate increased cell adhesion and proliferation of PC12 cells on the NW as compared to SPCL and PS (Figure 3.3). PC12cells seeded on NW displayed increased adhesion after 1 day of culture (Figure 3.3 e), and proliferation and cell-cell contact after 4 days of culture as indicated by a high degree of cell aggregation (Figure 3.3 f), a signature of natural *in vivo* behavior. Further, PC12 cells are known to aggregate and proliferate laterally in absence of NGF (Figure 33. e and f). In contrast, minimal cell adhesion and proliferation was observed on PS (Figure 3.3 a and b) and SPCL (Figure 3.3 c and d) after 1 and 4 days of culture. PS was used as a positive control to ensure efficacy of the culture conditions, and SPCL was used as a negative control, to evaluate the effect of nanowires on cell adhesion and proliferation. Our results indicate that by manipulating the surface nanoarchitecture, the cell adhesion and proliferation can be controlled. PC12 cells are known to not adhere on culture surfaces, thus culture surfaces are typically coated with collagen to improve cell adhesion. However, it is apparent from our results that providing nanotopography on the surface, the cell adhesion as well as proliferation can be enhanced without the need of collagen coating on culture surfaces.

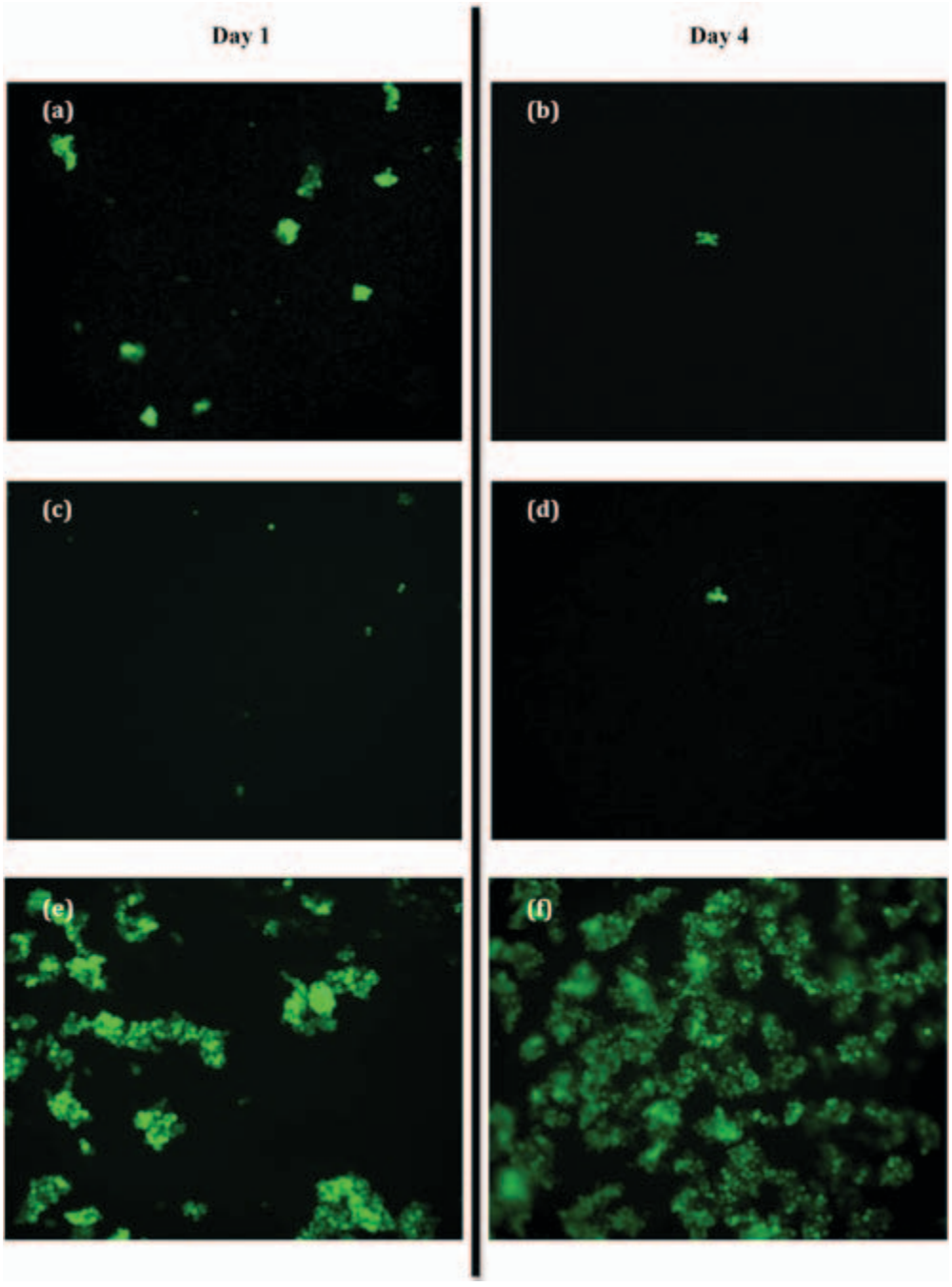

Figure 3.3: Representative fluorescence microscopy images (10X) of PC12 cells stained with calcein-AM before differentiation on (a-b) PS, (c-d) SPCL and (e-f) NW after 1 and 4 days of culture respectively.

Cell viability was measured using MTT assay (Figure 3.4). Cells cultured on NW displayed significantly higher viability than that on PS and SPCL up to 4 days of culture ($p < 0.05$). Further, cell viability after 1 and 4 days of culture on NW was significantly different ($p < 0.05$) suggesting that the cells are proliferating. These results confirm the findings from fluorescence microscopy images. Thus, NW surfaces provide a favorable template for adhesion and growth of PC12 cells.

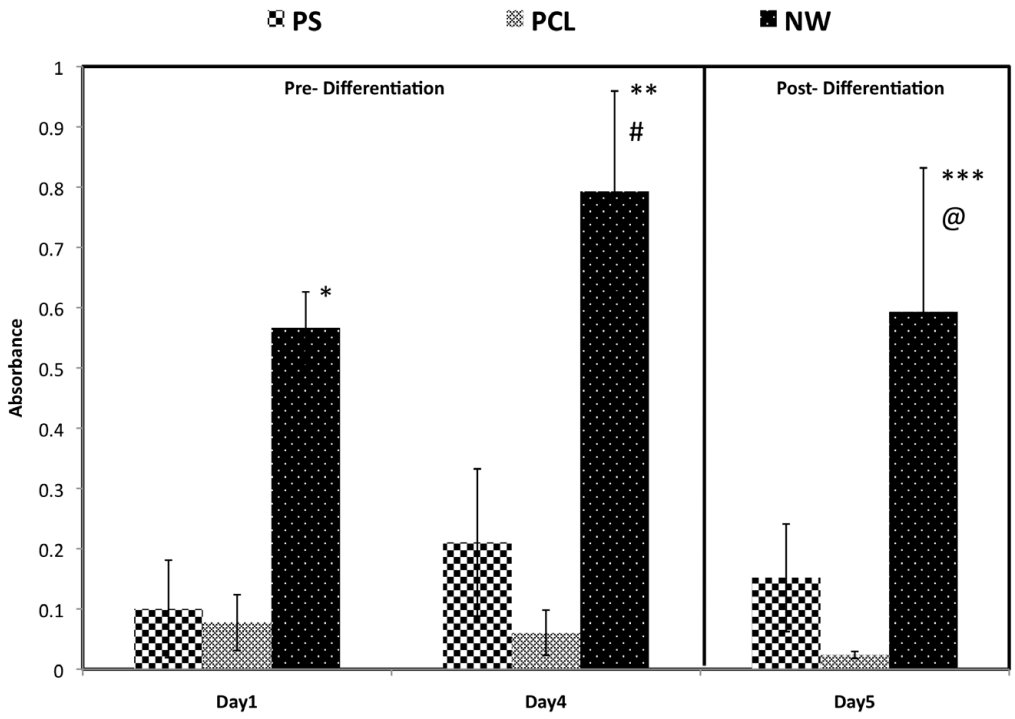

Figure 3.4: PC12 cell viability before and after differentiation measured using MTT assay; (*, **, ***) cell viability on NW statistically different ($p < 0.05$) than that on PS and SPCL for respective time points; (#) cell viability on NW statistically different ($p < 0.05$) between day 1 and 4; (@) cell viability on NW is not statistically different ($p > 0.05$) between day 1 and 5, i.e. before and after differentiation.

Cell morphology of the adhered cells on NW and SPCL was investigated using SEM imaging. Images were taken after days 1 and 4 of culture (Figure 3.5). PS surfaces were not analyzed due to the low adhesion rates as confirmed by the previous fluorescence microscopy images and MTT cell viability data. Minimal numbers of cells were visible on SPCL surfaces after 4 days of culture (Figure 3.5 a and b). This may be due to the fact that there are no physical cues available on the surface for cell attachment and subsequent growth. The cells on the NW demonstrated increased spreading (Figure 3.5 c) after 1 day of culture; followed by cell colonization and communication (Figure 3.5 d) after 4 days of culture (as shown by dotted circle in the figure). Further, after 1 day of culture, high magnification image of cells on NW showed an extensive network of cell lamellopodia and filopodia interacting with the surrounding nanowire architecture (Figure 3.5e – dotted circle). This behavior was more prominent after 4 days of culture as visible from high magnification SEM images of cells on NW (Figure 3.5 f – dotted circle). Filopodia interaction with material surface is an integrin mediated action and is extremely important for maintenance of long-term phenotypic behavior of cells on material surfaces (Hynes, 1992). Future studies are now directed towards determining the specific binding mechanism between cells and the nanowire surfaces. These results suggest that PC12 cells adhere, proliferate, and communicate more effectively on nanowire surfaces compared to control surfaces and nanowire surfaces may provide an effective template for growth and maintenance of neural cells.

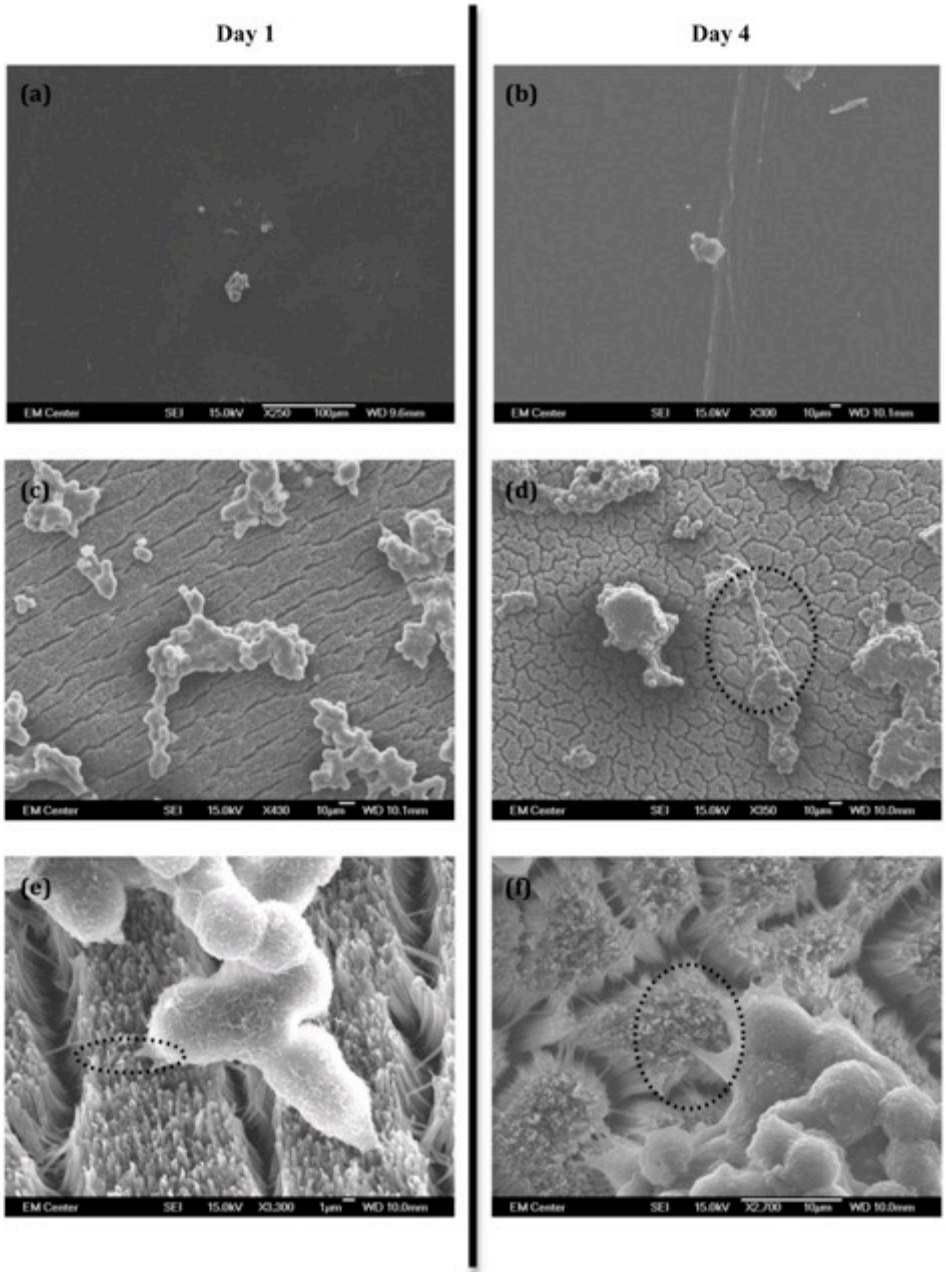

Figure 3.5: Representative SEM images of PC12 cells before differentiation on (a-b) SPCL and (c-d) NW after 1 and 4 days of culture respectively. High magnification SEM images show cells interacting with nanowire architecture after (e) 1 and (f) 4 days of culture.

The performance and potential clinical relevance of a tissue-engineering scaffold designed for SCI relies heavily on its ability to produce or accelerate the cellular production neurons and neuro-specific markers. Therefore, in addition to cell adhesion and proliferation, cell differentiation on nanowire surfaces was investigated. After 4 days of initial culture, media with NGF was provided to induce neuronal differentiation in PC12 cells (Greene & Tischler, 1976; Koike, 1983). After 4 days of culture, cells were exposed to media containing NGF to initiate differentiation. Cell viability, morphology, formation of neural networks, and expression of neuronal markers were investigated up to 7 days of culture after providing NFG supplemented media (i.e. up to 11 days of initial culture).

The effect of NGF on cell viability was investigated using MTT assay (Figure 3.4). The cell viability was measured after 1 day of providing media supplemented with NGF (i.e. after 5 days of initial culture). The viability of cells on the NW surfaces is significantly higher than that on SPCL and PS after 5 days of initial culture, indicating that the PC12 seeded on the nanowire surface are healthy ($p < 0.05$). Further, there were no statistically significant differences ($p > 0.05$) between cell viabilities pre- and post-differentiation (i.e. after 4 and 5 days of initial culture) indicating that the cells may have reached confluency and there are no cytotoxic effects of NGF.

In order to visualize neuronal network formation, the PC12 cells were stained with CMFDA after 1, 4 and 7 days of differentiation (Figure 3.6). CMFDA was chosen because of its ability to fill up the entire cell body and in turn, illuminate the cytoplasm,

cellular extensions and neurites formed from the differentiated cells. Significant numbers of cells were present on NW than that on SPCL after 7 days of differentiation (Figure 3.6). Minimal numbers of cells were present without any noticeable neurite growth on SPCL after 1, 4 and 7 days of differentiation (Figure 3.6 a, c and e). In contrast, cells on NW show a progression of neurite growth for the entire duration of culture. After 1 day of differentiation, neurite growth has initiated and the cell show better colonization (Figure 3.6 b – dotted circle). After 4 days of differentiation, the cells show noticeably longer neurites and they seem to interact with other to form a neuronal network (Figure 3.6 d – dotted circles). Further, after 7 days of differentiation, there is significant neuronal network formation that is clearly visible with CMFDA standing (Figure 3.6 f – solid circle). The advanced level of neuronal network formation on nanowire surface suggests the role of nanoarchitecture in promoting cellular phenotypic behavior.

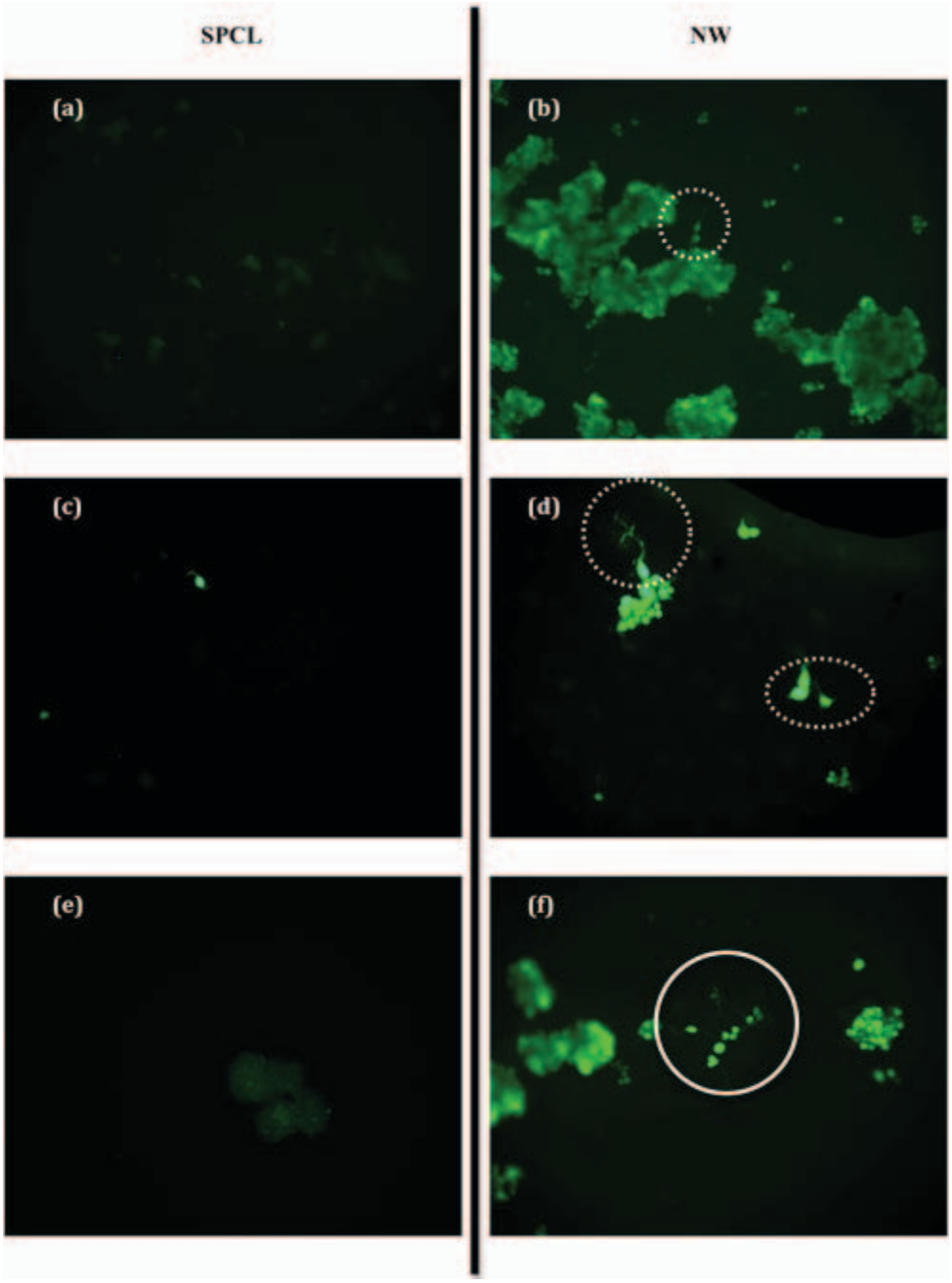

Figure 3.6: Representative fluorescence microscopy images (10X) of PC12 cells stained with CMFDA on SPCL and NW after (a-b) 1, (c-d) 4 and (e-f) 7 days of differentiation respectively

Cell morphology of differentiated cells was investigated using SEM (Figure 3.7). There are significant morphological changes in cells on NW compared to SPCL after 7 days of differentiation. Similar to fluorescence microscopy images, minimal numbers of cells were present on SPCL surface after 1, 4 and 7 days of differentiation (Figure 3.7 a, d and g). The cells have a spherical morphology and no evidence of neurite growth. In contrast, the cells on NW have a spreading morphology with individual cells interacting with each other. After 1 day of differentiation the cells seem to be communicating with each other (Figure 3.7 b). High magnification images show that the cellular extensions are interacting with the nanowire architecture (Figure 3.7 b – solid circle, Figure 3.7 c). After 4 days of differentiation, similar to fluorescence microscopy images, the SEM images show initiation of neurite growth (Figure 3.7 e). High magnification images show that the neurites are interacting with the nanowire architecture. The branching of neuritis is also visible (Figure 3.7 e – solid circle, Figure 3.7 f). Further, after 7 days of differentiation, significant neuronal network formation is visible. The cells are communicating with each other by forming neurite extensions, and eventually will form a neuronal network (Figure 3.7 h and i). These results prove that the nanowire architecture is favorable for maintaining differentiated states of PC12 cells. The lack of nanoarchitecture on SPCL did not allow the cell to attach strongly and prevented the cells from forming neuronal network.

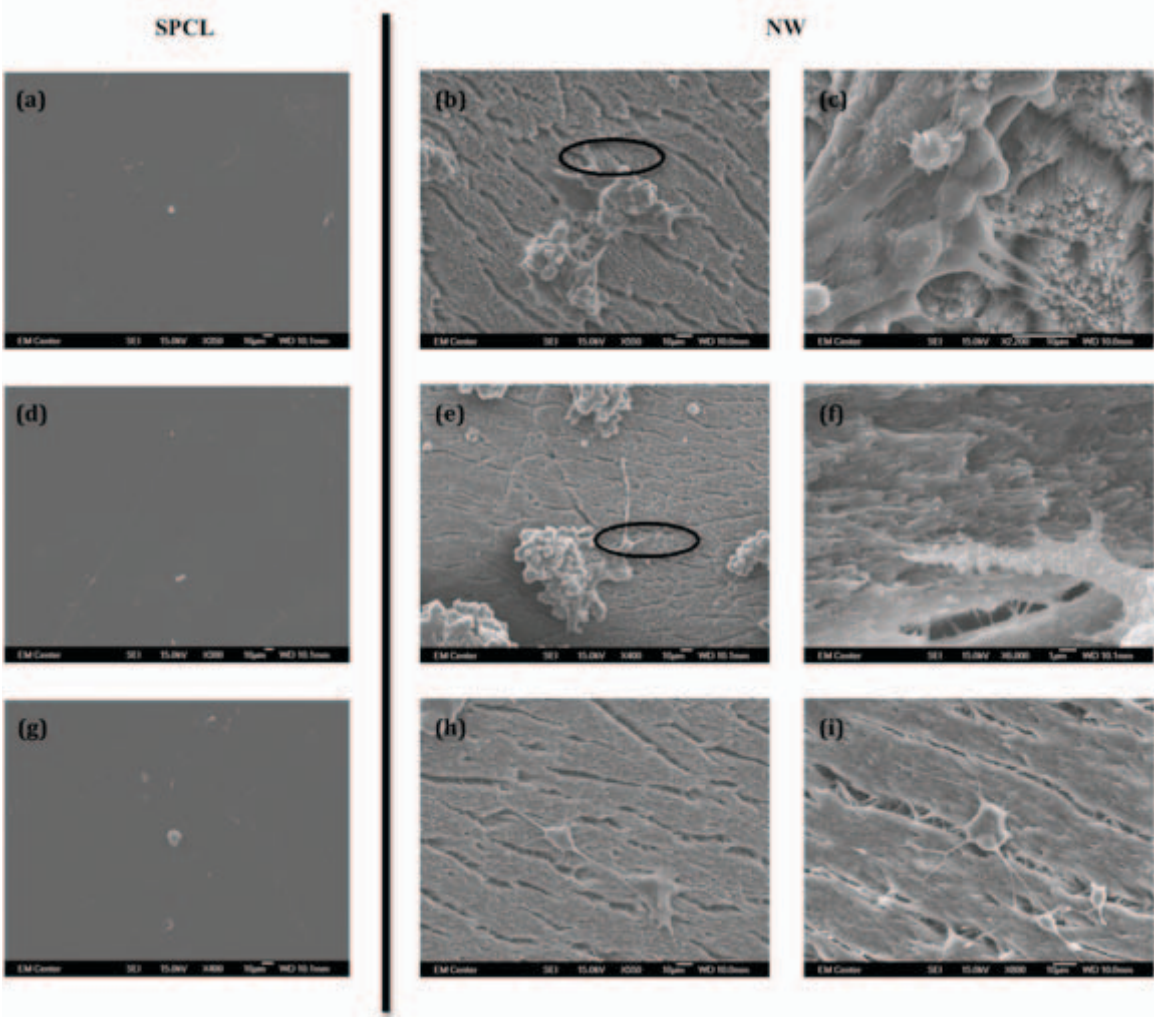

Figure 3.7: Representative SEM images of PC12 cells on SPCL and NW after (a-b-c) 1, (d-e-f) 4 and (g-h-i) 7 days of differentiation respectively

Although the CMFDA staining and SEM imaging provide reasonable evidence that the differentiated PC12 cells were expressing a neuronal phenotype, immunofluorescence studies were conducted to ensure expression of key neural markers. After 7 days of differentiation, the PC12 cells were tested for expression of two neuronal markers, NF-H and TH (Figure 3.8). As a critical player in axonal growth, neurofilaments

(including NF-H) are found primarily in growing neuronal axons (Janmey, Leterrier, & Herrmann, 2003; Julien, 1999; Matheson, Diocee, & Roots, 1980). It is evident from the expression of NF-H in immunofluorescence images that PC12 cells on NW indeed have a neuronal phenotype (Figure 3.8 a). Further, NF-H is localized to the perimeter of the cells implying axonal growth as visible from immunofluorescence images. During axonal growth, new neurofilament subunits are incorporated all along the axon in a dynamic process that involves the addition of subunits along the filament length, as well as the addition of subunits at the filament ends. TH plays an important role in neurons, as it is the enzyme that catalyzes the synthesis of DOPA, a molecular precursor to both norepinephrine and epinephrine. Norepinephrine and epinephrine are both important neurotransmitters commonly referred to as the molecules important in the “fight or flight” mechanism. Expression of TH was observed primarily in the cell body (Figure 3.8 b). The composite immunofluorescence image shows the distribution of NF-H and TH in cells on NW (Figure 3.8 c). Due to the extremely low cell coverage, immunofluorescence studies were not conducted on SPCL.

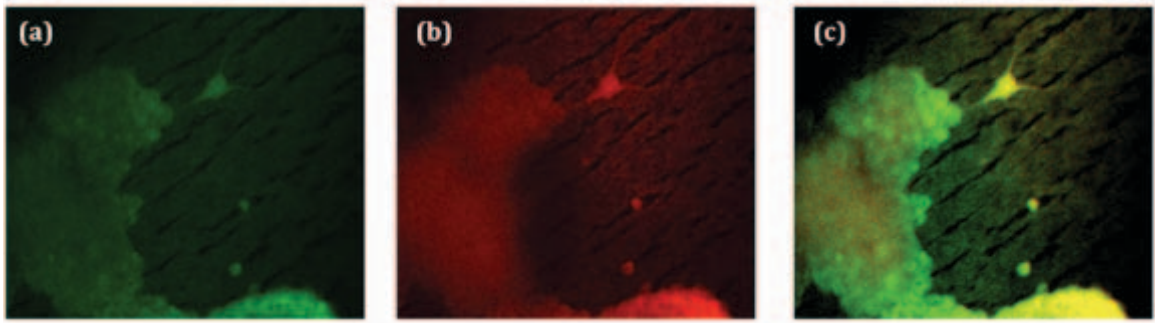

Figure 3.8: Representative immunofluorescence images showing expression of (a) NF-H and (b) TH by PC12 cells differentiated for 7 days on NW; (c) Composite overlay immunofluorescence images of NF-H and TH expressed by PC12 cells.

3.4 Conclusions

Considering the limitations of maintaining differentiated states of neuronal cells for neural tissue engineering application, the proposed nanowire surfaces hold considerable promise for future treatment regimes. In this study, we have developed a novel solvent-free nanotemplating technique for fabricating PCL templates with controlled arrays of high aspect ratio substrate-bound nanowires for the growth and maintenance of differentiated states of neuronal cells. The PCL nanowire templating technique is especially advantageous because it is solvent free and has the potential for incorporating active biomolecules or drugs into the scaffold without compromising their bioactivity. Our results indicate that our initial hypothesis is true, cell adhesion and proliferation is related to surface nano-topography, and PC12 cells will preferentially adhere and will experience enhanced proliferation on nanowire scaffolds. Our results demonstrated increased functionality of PC12 cells on nanowire surfaces in terms of adhesion, proliferation, neuronal network formation and expression of key neuronal markers. Thus,

by manipulating the nanotopography of a surface and creating unique nanoarchitectures, we can enhance neuronal cell functionality that will be beneficial for neural tissue engineering applications. Further studies are now directed towards understanding the underlying mechanisms of neuronal cell functionality on nanowire surfaces.

3.5 References

Chew, S. Y., Mi, R., Hoke, A., & Leong, K. W. (2008). The effect of the alignment of electrospun fibrous scaffolds on Schwann cell maturation. *Biomaterials*, *29*(6), 653-61. doi:10.1016/j.biomaterials.2007.10.025

Flynn, L., Dalton, P. D., & Shoichet, M. S. (2003). Fiber templating of poly(2-hydroxyethyl methacrylate) for neural tissue engineering. *Biomaterials*, *24*(23), 4265-72. Retrieved from http://www.ncbi.nlm.nih.gov/pubmed/12853258

Foley, J. D., Grunwald, E. W., Nealey, P. F., & Murphy, C. J. (2005). Cooperative modulation of neuritogenesis by PC12 cells by topography and nerve growth factor. *Biomaterials*, *26*(17), 3639-44. doi:10.1016/j.biomaterials.2004.09.048

Ghasemi-Mobarakeh, L., Prabhakaran, M. P., Morshed, M., Nasr-Esfahani, M.-H., & Ramakrishna, S. (2008). Electrospun poly(epsilon-caprolactone)/gelatin nanofibrous scaffolds for nerve tissue engineering. *Biomaterials*, *29*(34), 4532-9. doi:10.1016/j.biomaterials.2008.08.007

Greene, L. A., & Tischler, A. S. (1976). Establishment of a noradrenergic clonal line of rat adrenal pheochromocytoma cells which respond to nerve growth factor. *Proceedings of the National Academy of Sciences of the United States of America*, *73*(7), 2424-8. Retrieved from http://www.pubmedcentral.nih.gov/articlerender.fcgi?artid=430592&tool=pmcentrez&rendertype=abstract

Hile, D. D., & Pishko, M. V. (n.d.). Solvent-free protein encapsulation within biodegradable polymer foams. *Drug delivery*, *11*(5), 287-93. doi:10.1080/10717540490493961

Hynes, R. O. (1992). Integrins: versatility, modulation, and signaling in cell adhesion. *Cell*, *69*(1), 11-25. Retrieved from http://www.ncbi.nlm.nih.gov/pubmed/1555235

Jameela, S. R., Suma, N., & Jayakrishnan, A. (1997). Protein release from poly(epsilon-caprolactone) microspheres prepared by melt encapsulation and solvent evaporation techniques: a comparative study. *Journal of biomaterials science. Polymer edition*, *8*(6), 457-66. Retrieved from http://www.ncbi.nlm.nih.gov/pubmed/9151193

Janmey, P. A., Leterrier, J.-F., & Herrmann, H. (2003). Assembly and structure of neurofilaments. *Current Opinion in Colloid & Interface Science*, *8*(1), 40-47. doi:10.1016/S1359-0294(03)00010-4

Julien, J. P. (1999). Neurofilament functions in health and disease. *Current opinion in neurobiology*, *9*(5), 554-60. doi:10.1016/S0959-4388(99)00004-5

Koike, T. (1983). Nerve growth factor-induced neurite outgrowth of rat pheochromocytoma PC 12 cells: dependence on extracellular Mg2+ and Ca2+. *Brain research*, *289*(1-2), 293-303. Retrieved from http://www.ncbi.nlm.nih.gov/pubmed/6318896

Lee, J. Y., Bashur, C. A., Goldstein, A. S., & Schmidt, C. E. (2009). Polypyrrole-coated electrospun PLGA nanofibers for neural tissue applications. *Biomaterials*, *30*(26), 4325-35. doi:10.1016/j.biomaterials.2009.04.042

Lin, W. J., & Yu, C. C. (n.d.). Comparison of protein loaded poly(epsilon-caprolactone) microparticles prepared by the hot-melt technique. *Journal of microencapsulation*, *18*(5), 585-92. doi:10.1080/02652040010019569

Matheson, D. F., Diocee, M. S., & Roots, B. I. (1980). Distribution of neurofilaments in myelinated axons of the optic nerve of goldfish (Carassius auratus L.). *Journal of the neurological sciences*, *48*(2), 233-42. Retrieved from http://www.ncbi.nlm.nih.gov/pubmed/6253602

Miyai, T., Ito, A., Tamazawa, G., Matsuno, T., Sogo, Y., Nakamura, C., Yamazaki, A., et al. (2008). Antibiotic-loaded poly-epsilon-caprolactone and porous beta-tricalcium phosphate composite for treating osteomyelitis. *Biomaterials*, *29*(3), 350-8. doi:10.1016/j.biomaterials.2007.09.040

Miyoshi, Y., Date, I., Ohmoto, T., & Iwata, H. (1996). Histological analysis of microencapsulated dopamine-secreting cells in agarose/poly(styrene sulfonic acid) mixed gel xenotransplanted into the brain. *Experimental neurology*, *138*(1), 169-75. doi:10.1006/exnr.1996.0055

Mooney, D. J., Baldwin, D. F., Suh, N. P., Vacanti, J. P., & Langer, R. (1996). Novel approach to fabricate porous sponges of poly(D,L-lactic-co-glycolic acid) without the use of organic solvents. *Biomaterials*, *17*(14), 1417-22. Retrieved from http://www.ncbi.nlm.nih.gov/pubmed/8830969

Nisbet, D. R., Rodda, A. E., Horne, M. K., Forsythe, J. S., & Finkelstein, D. I. (2009). Neurite infiltration and cellular response to electrospun polycaprolactone scaffolds implanted into the brain. *Biomaterials*, *30*(27), 4573-80. doi:10.1016/j.biomaterials.2009.05.011

Oh, S. H., Park, I. K., Kim, J. M., & Lee, J. H. (2007). In vitro and in vivo characteristics of PCL scaffolds with pore size gradient fabricated by a centrifugation method. *Biomaterials*, *28*(9), 1664-71. doi:10.1016/j.biomaterials.2006.11.024

Ohnuma, K., Toyota, T., Ariizumi, T., Sugawara, T., & Asashima, M. (2009). Directional migration of neuronal PC12 cells in a ratchet wheel shaped microchamber. *Journal of bioscience and bioengineering*, *108*(1), 76-83. doi:10.1016/j.jbiosc.2009.02.020

Park, K.-H., & Yun, K. (2004). Immobilization of Arg-Gly-Asp (RGD) sequence in a thermosensitive hydrogel for cell delivery using pheochromocytoma cells (PC12). *Journal of bioscience and bioengineering*, *97*(6), 374-7. doi:10.1016/S1389-1723(04)70221-2

Porter, J. R., Henson, A., & Popat, K. C. (2009). Biodegradable poly(epsilon-caprolactone) nanowires for bone tissue engineering applications. *Biomaterials*, *30*(5), 780-8. doi:10.1016/j.biomaterials.2008.10.022

Schnell, E., Klinkhammer, K., Balzer, S., Brook, G., Klee, D., Dalton, P., & Mey, J. (2007). Guidance of glial cell migration and axonal growth on electrospun nanofibers of poly-epsilon-caprolactone and a collagen/poly-epsilon-caprolactone blend. *Biomaterials*, *28*(19), 3012-25. doi:10.1016/j.biomaterials.2007.03.009

Tiaw, K. S., Goh, S. W., Hong, M., Wang, Z., Lan, B., & Teoh, S. H. (2005). Laser surface modification of poly(epsilon-caprolactone) (PCL) membrane for tissue engineering applications. *Biomaterials*, *26*(7), 763-9. doi:10.1016/j.biomaterials.2004.03.010

Vallbacka, J. J., Nobrega, J. N., & Sefton, M. V. (2001). Tissue engineering as a platform for controlled release of therapeutic agents: implantation of microencapsulated dopamine producing cells in the brains of rats. *Journal of controlled release : official journal of the Controlled Release Society*, *72*(1-3), 93-100. Retrieved from http://www.ncbi.nlm.nih.gov/pubmed/11389988

Williamson, M. R., & Coombes, A. G. A. (2004). Gravity spinning of polycaprolactone fibres for applications in tissue engineering. *Biomaterials*, *25*(3), 459-65. Retrieved from http://www.ncbi.nlm.nih.gov/pubmed/14585694

Xie, J., Willerth, S. M., Li, X., Macewan, M. R., Rader, A., Sakiyama-Elbert, S. E., & Xia, Y. (2009). The differentiation of embryonic stem cells seeded on electrospun nanofibers into neural lineages. *Biomaterials*, *30*(3), 354-62. doi:10.1016/j.biomaterials.2008.09.046

Yoshimoto, H., Shin, Y. M., Terai, H., & Vacanti, J. P. (2003). A biodegradable nanofiber scaffold by electrospinning and its potential for bone tissue engineering. *Biomaterials*, *24*(12), 2077-82. Retrieved from http://www.ncbi.nlm.nih.gov/pubmed/12628828

Chapter 4 Varying Nanowire Diameter does not effect C17.2 Cellular Response

4.1 Introduction

In this work we fabricated and compared 2 different sizes of nanowires and their effect on neural progenitor cell line adhesion and proliferation to address specific aim 2. We hypothesized that if nanotopography is important for optimal neural stem cell growth conditions, varying the nanowire size will affect C17.2 activity. In this work we show that varying the nanowire size does not significantly effect C17.2 cellular activity.

4.2 Materials and Methods

4.2.1 Fabrication and Characterization of PCL Nanowire Scaffolds

PCL nanowire scaffolds were fabricated according to a protocol previously developed in our lab and described in detail elsewhere (Figure 4.1) (S. L. Bechara et al., 2010; J. R. Porter, Henson, et al., 2009). In brief, PCL discs were placed on the surface of a nanoporous aluminum oxide membrane (Figure 4.1 A). The nanowires were extruded through the membranes by heating the polymer in an oven at 115oC for 3 mins (Figure 4.1 B and C). After cooling, the aluminum oxide membranes were dissolved in 1M NaOH for 75 mins, thus releasing the extruded nanowires (Figure 4.1 D). Nanowire surfaces were then rinsed in DI water, dried, and stored in a desiccator until further use. Scanning electron microscopy was used to characterize the surface nanoarchitecture.

4.2.2 C17.2 Murine Neural Stem Cell Culutre on PCL Nanowire Scaffolds

C17.2 murine neural stem cells, developed by the group of Dr. Evan Y. Synder (P Lu, Jones, Snyder, & Tuszynski, 2003), were used for the studies presented here. Cells below passage 3 were used for all the studies. 20-NW, 200-NW and SPCL substrates were sterilized in 24-well plates by incubating them with 70% ethanol for 30 minutes followed by exposure to UV light for 30 mins in a biosafety cabinet. Prior to cell seeding, all the substrates were washed three times with sterile PBS. The cells were seeded at a density of 10,000 cells/well. The medium used for culturing the cells consisted of Dulbecco's Modified Eagle's Medium (DMEM) enhanced by 10% fetal bovine serum (FBS), 5% horse serum (HS), 1% 2mM L-glutamine, 1% penicillin/streptomycin (PS). The medium was changed every 2 days and the cells were maintained in an incubator at 37°C and 5% CO2 for up to 7 days of culture. Each experiment was reconfirmed on three different substrates with at least three different cell populations (nmin = 9). All the quantitative results were analyzed using analysis of variance (ANOVA). Statistical significance was considered at $p<0.05$.

4.2.3 Cell Adhesion, Proliferation, and Differentiation

Cell adhesion and proliferation was investigated using calcein-AM live cell stain after 1, 2, and 7 days of culture. The scaffolds were removed from culture media; rinsed with PBS and incubated in calcein-AM (2 µM in PBS) solution for 45 min at 37°C. The cells were images using appropriate filters using a fluorescence microscope. The calcein-

AM images were used to calculate cell coverage using ImageJ software. To investigate the cell differentiation, the cells were immunolabelled for MAP2 and Nestin. Briefly, the cells were fixed with 3.7% paraformaldehyde for 15 mins at 37oC followed by permeabilization with 1% Triton-X in PBS for 5 mins at room temperature. The cells were washed three times with PBS and incubated in 100 µg/ml of bovine serum albumin (BSA) and 40 µL/mL trypan blue for 20 mins to block any non-specific interactions. Cells were then incubated in the primary antibodies (rabbit anti-MAP2 polyclonal and goat anti-nestin polyclonal, both 1 µg/ml) for 1 hr at room temp. The cells were washed three times with PBS followed by incubation in appropriate secondary antibody (bovine anti-rabbit TR and donkey anti-goat FITC, both 5 µg/ml). The cells were images using appropriate filters using a fluorescence microscope.

4.2.4 Cell Morphology

The morphology of adhered cells was investigated after 1, 2, and 7 days of culture using SEM imaging. The cells were fixed in a solution of 3% glutaraldehyde, 0.1 M sodium cacodylate, and 0.1 M sucrose for 45 mins. The scaffolds were soaked in a buffer solution containing 0.1 M sodium cacodylate and 0.1 M surcrose for 10 mins. This was followed by dehydrating the cells by soaking the scaffolds in increasing concentrations of ethanol (35%, 50%, 70%, 95%, and 100%) for 10 minutes each. The cells were further dehydrated by soaking the scaffolds in hexamethyldisilazane (HMDS, Sigma) for 10 min. The surfaces were then dried under vacuum and stored in a desiccator until examined

with SEM. The scaffolds were sputter coated with 10 nm of gold and imaged using a SEM at voltages ranging from 10-15kV.

4.3 Results and Discussion

In this work, we have investigated NSC response to polycaprolactone (PCL) nanowire scaffolds. PCL is a biodegradable and biocompatible polymer and has been commonly used for variety of tissue engineering applications ranging from cardiovascular repair (Ashton et al., 2011; Heydarkhan-Hagvall et al., 2008; Sell, McClure, Garg, Wolfe, & Bowlin, 2009), bone tissue regeneration (Guarino et al., 2008; Ruckh, Kumar, Kipper, & Popat, 2010; Williams et al., 2005) and neural tissue engineering (Ghasemi-Mobarakeh et al., 2008; Schnell et al., 2007). The nanowire scaffolds were fabricated using a simple, solvent free nanotemplating technique (S. L. Bechara et al., 2010; J. R. Porter, Henson, et al., 2009). Commercially available ANOPORE^{TM} membranes with two different pore sizes (20 nm and 200 nm) were used as templates to extrude very fine nanowires by melting the polymer into the nanopores of the membrane. Upon completion of extrusion, the membranes were dissolved in NaOH to form substrate-bound vertically aligned high-aspect ratio nanowire scaffolds. The nanowire scaffolds were characterized in terms of their nanotopography using scanning electron microscopy (SEM). A smooth PCL surface without any nanotopography was used as a control substrate to evaluate the effects of nanotopography on NSC functionality. In the rest of this chapter, the following notations will be used for different

substrates – **SPCL**: smooth PCL surface without any nanotopography; **20-NW**: nanowire scaffolds fabricated with membranes of pore size 20 nm; and **200-NW**: nanowire scaffolds fabricated with membranes of pore size 200 nm. The results indicate that both 20-NW and 200-NW scaffolds have uniform surface architecture with high-aspect ratio, substrate bound-nanowires (**Figure 4.1, SEM images**). Occasionally, the uniformity of the scaffolds was interrupted by the presence of random micro-channels on the scaffold formed due to the surface tension interaction during membrane dissolution. Further, high magnification SEM images revealed that the 20 nm membranes resulted in scaffolds with nanowires approximately 100-150 nm in diameter; whereas the 200 nm membranes resulted in scaffolds with nanowires approximately 300-400 nm in diameter. The reason for the discrepancy between the membrane pore size and nanowire diameter is due to the thermodynamic expansion of the polymer upon cooling. During the extrusion step of the nanotemplating process, the molten PCL fills the nanopores of the membranes (**Figure 4.1, schematic, B and C**). As the polymer cools, it exerts pressure on the nanopore walls. Upon dissolving the membrane, the cooled polymer slightly expands resulting in nanowires that are larger in diameter than the nanopores.

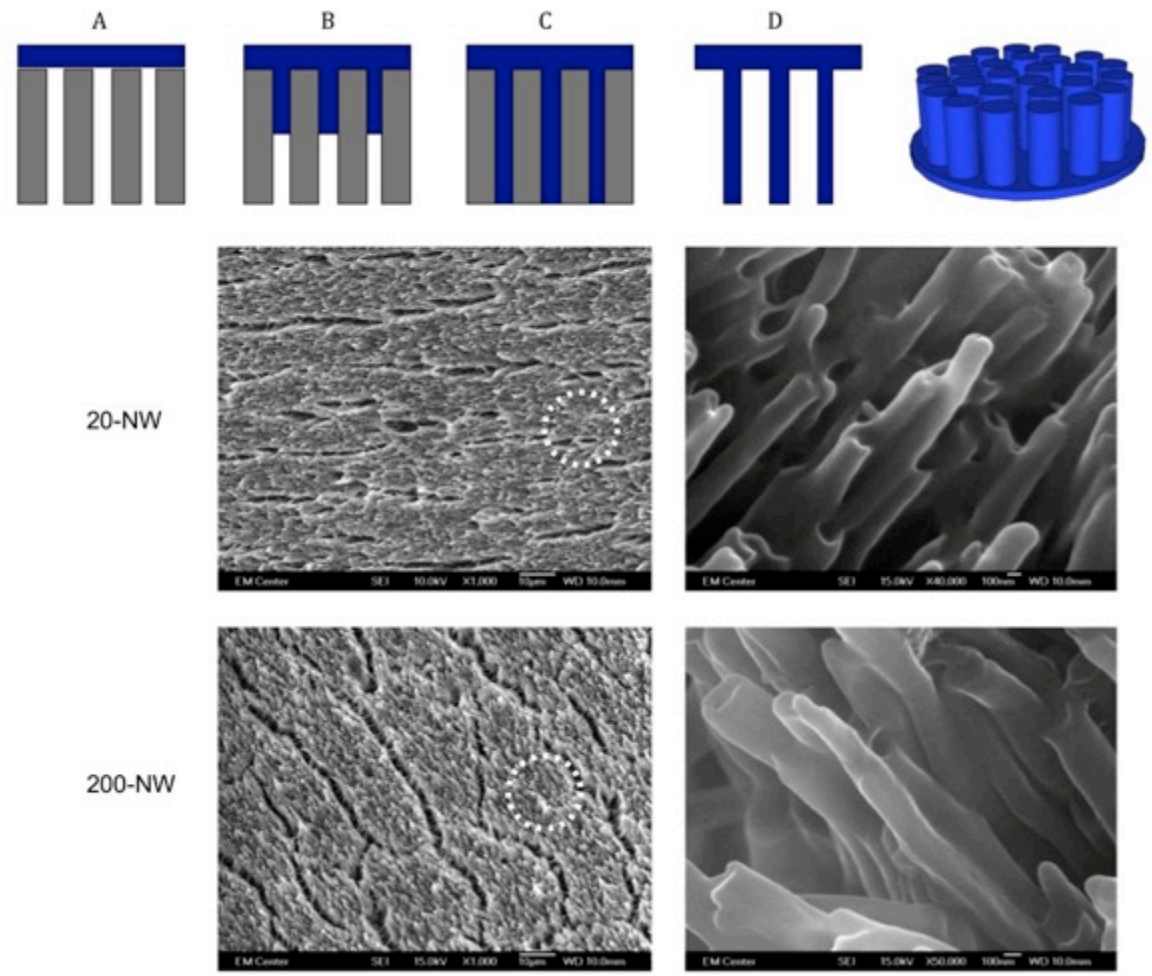

Figure 4.1: The figure shows the schematic of fabrication of PCL nanowire scaffolds using templating technique. The figure also shows representative SEM images (low and high magnification) for PCL nanowire surfaces fabricated using 20 nm and 200 nm pore size ANOPORETM membranes indicated as 20-NW and 200-NW respectively.

The neuronal potential of the nanowire scaffolds was evaluated using C17.2 murine NSCs. This multipotent neural precursor cell line was derived from the external germinal layer of a neonatal mouse cerebellum (Snyder, Yoon, Flax, & Macklis, 1997). These NSCs have the potential to differentiate into mature cells of all neural lineages including neurons, glial cells, astrocytes and oligodendrocytes (P Lu et al., 2003), and

thus were used in this study. The NSCs were cultured up to 7 days on SPCL, 20-NW and 200-NW scaffolds. The cell adhesion and proliferation was investigated using fluorescence microscopy by staining the cells with calcein-AM stain. Calcein-AM is a cell-permeant and non-fluorescent compound. It is hydrolyzed by the intracellular esterases into a strongly green fluorescent anion calcein upon cellular uptake. The fluorescent calcein is well retained in the cytoplasm in live cells and thus can be imaged using fluorescence microscopy. The viability of the adhered cells can also be assessed using this stain because the dead cells lack esterases and will not fluoresce. The results indicate increased NSC adhesion and proliferation on nanowire scaffolds as compared to SPCL. The increased adhesion on nanowire scaffolds was clearly evident after 1 day of culture (**Figure 4.2, Day 1**). After 2 days of culture, the cells on nanowire scaffolds appear to be clustering indicating cell communication (**Figure 4.2, Day 2**). By day 7, the cells on nanowire scaffolds have proliferated and have formed a "neuronal" network (**Figure 4.2, Day 7, Dotted circle shows "neuronal" network formation**). Such behavior is not supported on SPCL indicating that the nanotopography on the scaffold surface enhanced NSC adhesion and proliferation. The fluorescence microscopy images were also analyzed for cell coverage using the ImageJ software. The results indicate significant increase in NSC coverage on nanowire scaffolds as compared to SPCL (**Figure 4.2, Cell coverage**). Interestingly, the 20-NW and 200-NW scaffolds did not appear to be significantly different as indicated by the fluorescence microscopy images and calculated cell coverage (**Figure 4.2)**. This implies that the size of the nanowires up

to 400 nm did not significantly affect the NSC adhesion and proliferation; however the adhesion and proliferation was significantly enhanced by the unique nanotopography on the scaffold surface.

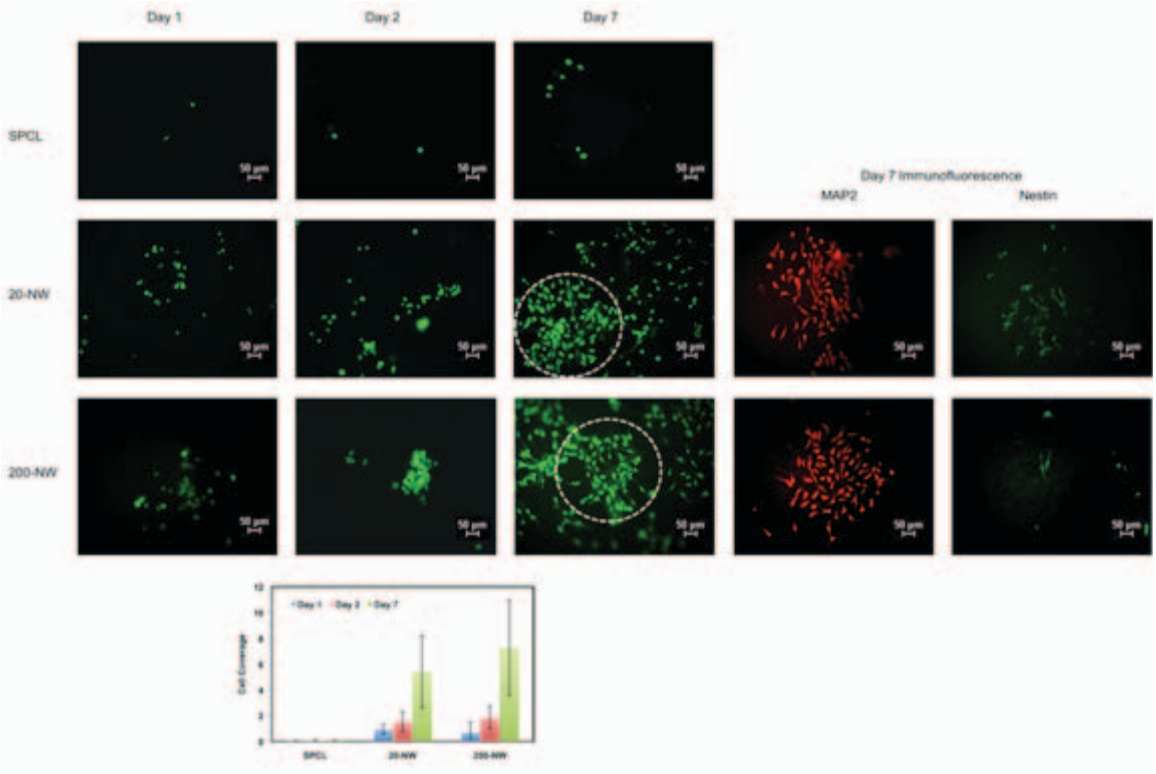

Figure 4.2: The figure shows representative fluorescence microscopy images of NSCs stained with calcein-AM after 1, 2, and 7 days culture on SPCL, 20-NW and 200-NW. The dotted circle indicates "neuronal" network formation by the cells on nanowire scaffolds. The images stained with calcein-AM were processed using ImageJ software to calculate the cell coverage, shown at the bottom of the figure. The figure also shows representative immunofluorescence images of cells expressing MAP2 and nestin after 7 days of culture indicating that the NSCs are differentiating.

In order to evaluate the ability of the nanowire scaffolds to support NSC differentiation, the adhered cells were immunolabelled for Microtubule Associated Protein 2 (MAP2) and Nestin; and expression for these markers was imaged using a

fluorescence microscope. MAP2 belongs to the microtubule-associated protein family. The proteins of this family are thought to be involved in microtubule assembly, which is an essential step in neurogenesis("MAP2 microtubule-associated protein 2 [Homo sapiens] - Gene - NCBI," n.d.). MAP2 serves to stabilize microtubules growth by crosslinking microtubules with intermediate filaments and other microtubules, and is expressed primarily in neurons. Nestin is a Class VI intermediate filament expressed in the developing central nervous system in the early embryonic neuroepithelial stem cells but not in mature central nervous system cells(Michalczyk & Ziman, 2005). Its expression is commonly associated with undifferentiated NSCs. Its transient expression is a critical step in the neural differentiation pathway and upon NSC differentiation nestin expression is downregulated. Due to the low cell coverage, immunofluorescence studies were not conducted on SPCL. The results indicate that a significant number of cells on nanowire scaffolds have expressed MAP2, suggesting that NSCs have differentiated into neurons (**Figure 4.2, MAP2**). Fewer cells expressed nestin indicating that the some NSCs are still undifferentiated and will eventually differentiate into a specific neuronal phenotype (**Figure 4.2, Nestin**). These results supports the notion that unique nanotopography on the scaffold surface augmented neuronal differentiation of NSCs.

The morphology of adhered cells and their interaction with the nanowires was evaluated using SEM imaging. Cells were fixed and images were taken after 1, 2, and 7 days of culture (**Figure 4.3**). As expected, similar to the fluorescence microscopy observations, there were very few cells adhered on SPCL (data not shown). The lack of

cells on SPCL is most likely explained by the absence of nanoscale physical cues on the scaffold surface available for cell attachment. However, the cells on the nanowire scaffolds show increased spreading and clustering just after 1 day of culture (**Figure 4.3, Day 1**). It appears that most of the cells maintained a spherical morphology and probably are in their undifferentiated state. However, after 2 days of culture, the cells are spreading with increased clustering, and morphology indicates that the cells are communicating and have started differentiating (**Figure 4.3, Day 2**). After 7 days of culture, it is clear from the SEM images that majority of the cells have neuronal morphology and the cells have formed a "neuronal" network by communicating with each other. This correlates well live cell imaging as well as immunofluorescence imaging, which indicated high degree of neuronal differentiation after 7 days of culture (**Figure 4.2, MAP2**). High magnification SEM images indicate that the cell filopodia are intimately interacting and the cells are anchoring with the nanowire architecture of the scaffolds (**Figure 4.3, high magnification images on the right are for the area indicated by dotted circle for images at Day 7**). This is contrasted by the complete lack of cellular communication or adhesion on the SPCL (data not shown).

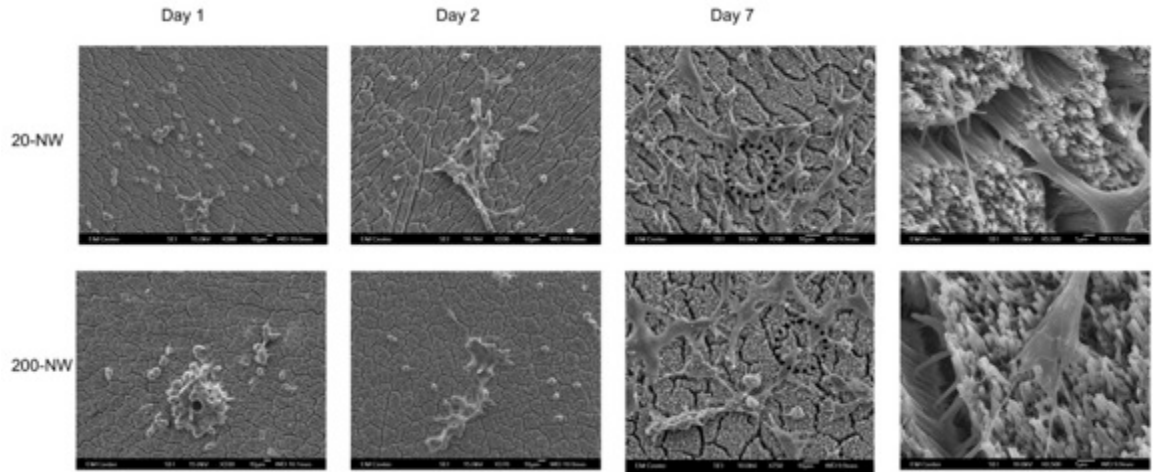

Figure 4.3: The figure shows representative SEM images of NSCs after 1, 2, and 7 days of culture on 20-NW and 200-NW. The dotted circle indicates high magnification SEM images that were taken after 7 days of culture.

4.4 Conclusion

In conclusion, the nanowire surface architecture offers a favorable template on the scaffold surface for growth and maintenance of differentiated states of NSCs. However, our hypothesis that varying nanowire diameter would have an effect on C17.2 cellular functionality remains unproven. The results reported here indicate that the nanowire scaffolds support significantly higher NSC adhesion and proliferation as compared to surfaces with no nanotopography. However, no significant differences were observed between 20-NW and 200-NW scaffolds. It is possible that varying the nanowire size below 150 nm or above 400 nm may alter the cell response. Significant NSC adhesion and proliferation is key to enhanced differentiation into neuronal lineages long-term, which is critical for the scaffolds to be functional once implanted in vivo. The PCL nanowire scaffolds were fabricated using a simple solvent-free nanotemplating technique.

The technique is versatile in terms of fabricating nanowire scaffolds with varied structural hierarchy either below 100 nm or above 400 nm. Thus, by manipulating the nanotopography of the scaffold surface, NSC functionality can be altered allowing for potential tissue engineering applications to several nervous system diseases and disorders.

4.5 References

Ashton, J. H., Mertz, J. A. M., Harper, J. L., Slepian, M. J., Mills, J. L., McGrath, D. V., & Vande Geest, J. P. (2011). Polymeric endoaortic paving: Mechanical, thermoforming, and degradation properties of polycaprolactone/polyurethane blends for cardiovascular applications. *Acta biomaterialia*, *7*(1), 287-94. doi:10.1016/j.actbio.2010.09.004

Bechara, S. L., Judson, A., & Popat, K. C. (2010). Template synthesized poly([var epsilon]-caprolactone) nanowire surfaces for neural tissue engineering. *Biomaterials*, *31*(13), 3492-3501. Retrieved from http://www.sciencedirect.com/science/article/B6TWB-4YC39RW-5/2/b9a281830087f2631912339503ac195e

Ghasemi-Mobarakeh, L., Prabhakaran, M. P., Morshed, M., Nasr-Esfahani, M.-H., & Ramakrishna, S. (2008). Electrospun poly(epsilon-caprolactone)/gelatin nanofibrous scaffolds for nerve tissue engineering. *Biomaterials*, *29*(34), 4532-9. doi:10.1016/j.biomaterials.2008.08.007

Guarino, V., Causa, F., Taddei, P., di Foggia, M., Ciapetti, G., Martini, D., Fagnano, C., et al. (2008). Polylactic acid fibre-reinforced polycaprolactone scaffolds for bone tissue engineering. *Biomaterials*, *29*(27), 3662-70. doi:10.1016/j.biomaterials.2008.05.024

Heydarkhan-Hagvall, S., Schenke-Layland, K., Dhanasopon, A. P., Rofail, F., Smith, H., Wu, B. M., Shemin, R., et al. (2008). Three-dimensional electrospun ECM-based hybrid scaffolds for cardiovascular tissue engineering. *Biomaterials, 29*(19), 2907-14. doi:10.1016/j.biomaterials.2008.03.034

Lu, P., Jones, L. L., Snyder, E. Y., & Tuszynski, M. H. (2003). Neural stem cells constitutively secrete neurotrophic factors and promote extensive host axonal growth after spinal cord injury. *Experimental neurology*, *181*(2), 115-29. Retrieved from http://www.ncbi.nlm.nih.gov/pubmed/12781986

MAP2 microtubule-associated protein 2 [Homo sapiens] - Gene - NCBI. (n.d.). Retrieved March 6, 2012, from http://www.ncbi.nlm.nih.gov/sites/entrez?Db=gene&Cmd=ShowDetailView&TermToSearch=4133

Michalczyk, K., & Ziman, M. (2005). Nestin structure and predicted function in cellular cytoskeletal organisation. *Histology and histopathology*, *20*(2), 665-71. Retrieved from http://www.ncbi.nlm.nih.gov/pubmed/15736068

Porter, J. R., Henson, A., & Popat, K. C. (2009). Biodegradable poly(epsilon-caprolactone) nanowires for bone tissue engineering applications. *Biomaterials*, *30*(5), 780-8. doi:10.1016/j.biomaterials.2008.10.022

Ruckh, T. T., Kumar, K., Kipper, M. J., & Popat, K. C. (2010). Osteogenic differentiation of bone marrow stromal cells on poly(epsilon-caprolactone) nanofiber scaffolds. *Acta biomaterialia*, *6*(8), 2949-59. doi:10.1016/j.actbio.2010.02.006

Schnell, E., Klinkhammer, K., Balzer, S., Brook, G., Klee, D., Dalton, P., & Mey, J. (2007). Guidance of glial cell migration and axonal growth on electrospun nanofibers of poly-epsilon-caprolactone and a collagen/poly-epsilon-caprolactone blend. *Biomaterials*, *28*(19), 3012-25. doi:10.1016/j.biomaterials.2007.03.009

Sell, S. A., McClure, M. J., Garg, K., Wolfe, P. S., & Bowlin, G. L. (2009). Electrospinning of collagen/biopolymers for regenerative medicine and cardiovascular tissue engineering. *Advanced drug delivery reviews*, *61*(12), 1007-19. doi:10.1016/j.addr.2009.07.012

Snyder, E. Y., Yoon, C., Flax, J. D., & Macklis, J. D. (1997). Multipotent neural precursors can differentiate toward replacement of neurons undergoing targeted apoptotic degeneration in adult mouse neocortex. *Proceedings of the National Academy of Sciences of the United States of America*, *94*(21), 11663-8. Retrieved from http://www.pubmedcentral.nih.gov/articlerender.fcgi?artid=23575&tool=pmcentrez&rendertype=abstract

Williams, J. M., Adewunmi, A., Schek, R. M., Flanagan, C. L., Krebsbach, P. H., Feinberg, S. E., Hollister, S. J., et al. (2005). Bone tissue engineering using polycaprolactone scaffolds fabricated via selective laser sintering. *Biomaterials*, *26*(23), 4817-27. doi:10.1016/j.biomaterials.2004.11.057

Chapter 5 Electro-Conductive Polymeric Nanowire Templates Facilitates Neural Stem Cell Line Adhesion, Proliferation and Differentiation

5.1 Introduction

In this work, we have developed a solvent-free nanotemplating technique for fabricating polycaprolactone (PCL) nanowire surfaces as templates for growth and differentiation of NSCs. These nanowire surfaces were then coated with PPy to provide an electrically conductive surface for cell-surface interactions in order to address specific aim 3. We hypothesized that if nervous system cells are known to react to electrical stimulation, creating an electrically conductive surfaces will enhance neural stem cell line activity. PCL was used to fabricate nanowire surfaces due to its biocompatibility and controlled biodegradability. PPy coated PCL nanowire surfaces were characterized using X-ray photoelectron spectroscopy (XPS) and scanning electron microscopy (SEM). Further, the stability of PPy coatings on PCL nanowire surfaces in physiological conditions was evaluated using SEM and XPS. C17.2 murine neural stem cells were used as model cells to study the viability, adhesion, proliferation, and differentiation on PPy coated PCL nanowire surfaces. This cell line was derived from the external germinal layer of a neonatal mouse cerebellum (Snyder et al., 1992). C17.2 cells are true NSCs in the sense that after isolation they still retain their ability to differentiate into both neurons and glial cells (Niles et al., 2004). The cell line has also been shown to express significant

levels of several neurotrophic factors including nerve growth factor, brain-derived neurotrophic factor, and glial cell line derived neurotrophic factor (P Lu et al., 2003).

5.2 Materials and Methods

5.2.1 Fabrication of PCL Nanowire Surfaces

PCL nanowire (NW) surfaces were fabricated according to a protocol previously developed in our lab (J. Porter, Henson, & Popat, 2009). Briefly, nanowire surfaces were fabricated via template synthesis from PCL using commercially available nanoporous aluminum oxide membranes with 20 nm pore size (ANOPORE^{TM}, Whatman). Polymer discs (10 mm diameter and approximately 2 mm thick) were placed on the surface of the membrane, and the nanowire were extruded through the membranes in an oven at 115^{o}C for 3 mins. The aluminum oxide membranes were dissolved in 1M NaOH for 75 mins to remove the membrane thus releasing the extruded nanowires. Nanowire surfaces were then soaked and rinsed in DI water, dried, and stored in a desiccator until further use.

5.2.2 PPy Coating on PCL Nanowire Surfaces

The as-fabricated NW surfaces were coated with PPy using a polymerization technique described elsewhere (Gomez et al., 2007; J. Y. Lee et al., 2009). Briefly, the nanowire surfaces were sonicated in a solution of 14mM pyrrole and 14mM sodium para-toluene sulfonate for 30 secs to saturate the surfaces with pyrrole. This was followed by gentle shaking and incubating the nanowire surfaces for 1 hour at 4°C. Next, 38mM

ferric chloride was added followed by gentle shaking and incubating for 24 hrs at 4°C. After removing the excess reaction solution, PPy coated PCL nanowires surfaces (PPy-NW) were sonicated for 1 min in DI water followed by drying in vacuum oven.

5.2.3 Characterization of PCL Nanowire Surfaces

NW surfaces, both coated and uncoated, were characterized using SEM, XPS and surface resistivity measurements. The stability of the coating in physiological environment was also characterized using SEM and XPS.

The surface nanoarchitecture before and after PPy coating was evaluated using SEM imaging. The surfaces were sputter coated with 10nm of gold and imaged using a JEOL JSM 6500F at voltages ranging from 10-15kV.

The polymerization of PPy from pyrrole on PCL nanowire surfaces involves the incorporation of chlorine and sodium para-toluene sulfonate, which can be detected using XPS. XPS survey spectra were collected from 0 to 1100eV with pass energy of 187.85 eV, and high-resolution spectra were collected for C1s peak with pass energy of 10eV. Data for percent elemental composition, elemental ratios and peak fit analysis were calculated using Multipack and XPSPeak 4.1 (Freeware) software.

PPy film thickness on NW surfaces was determined from the attenuation of XPS signals from the substrates. The thickness was obtained by using the standard uniform overlayer model, which is given by equation 1 (Damodaran, Fee, Ruckh, & Popat, 2010;

Petrovykh, Kimura-Suda, Tarlov, & Whitman, 2004; K. C. Popat, Leary Swan, & Desai, 2005; K. C. Popat, Mor, Grimes, & Desai, 2004; Tao, Popat, Norman, & Desai, 2008).

$$I = I_0\left(\frac{t}{E_L \sin\theta} - 1\right) \text{----- (1)}$$

where I_0: intensity of carbon peaks before surface modification

I_l: intensity of carbon peaks from after modification with PPy

t: thickness of the film

E_L: electron attenuation length for carbon peak

θ: angle at which X-ray hits the surface

In order to obtain film thickness from this equation, the electron attenuation lengths (E_L) for carbon peak needs to be calculated. E_L was calculated using equation 2 (Damodaran et al., 2010).

$$E_L = \frac{49}{E^2\rho} + 0.11\frac{\sqrt{E}}{\rho} \text{----- (2)}$$

where E: electron energy (X-ray core energy – core binding energy for carbon) = (1486 – 285) = 1201eV

ρ: density of PPy (1.1 gm/cm^3)

The surface resistivity of PPy-NW surfaces was measured using a method described elsewhere(J. Y. Lee et al., 2009). In brief, two copper contacts, 0.4 cm wide, were placed 0.5 cm apart on the surfaces and the resistance was measured using a digital multimeter (Omega). The resistivity was calculated using equation 3.

$$\rho_s = \frac{W}{L} R_s \text{----- (3)}$$

where ρ_s: resistivity

W: width of the copper contacts

L: distance between the contacts on the surfaces

R_s: resistance measured using the digital multimeter

The stability of PPy-NW surfaces was determined under physiological conditions. The surfaces were incubated in phosphate buffer solution (PBS) at 37°C for 7 days. After 7 days, the surfaces were washed with DI water and dried followed by characterization using SEM and XPS as described previously.

5.2.4 Neural Stem Cell Culture

C17.2 murine neural stem cells, developed by the group of Dr. Evan Snyder, were used for the studies presented here. This cell line is known to differentiate into all neural lineages. Cells below passage 3 were used for all the studies. The medium used for growing the C17.2 cells was Dulbecco's Modified Eagle's Medium (Invitrogen) supplemented by 10% fetal bovine serum (Sigma), 5% horse serum (Sigma), 1% 2mM L-glutamine (Sigma), 1% penicillin/streptomycin (Sigma). The medium was changed every 2-3 days, and the subculture was done at a ratio of 1:10. The cells were maintained in an incubator at 37°C and 5% CO_2 for the entire duration of culture. NW and PPy-NW surfaces were sterilized in 24-well plates by incubating them with 70% ethanol for 30 minutes followed by exposure to UV light for 30 mins in a biosafety cabinet. Prior to

cell seeding, all the substrates were washed three times with sterile PBS. C17.2 cells were seeded at a density of 10,000 cells/well. Each experiment was reconfirmed on three different substrates with at least three different cell populations (n_{min} = 9). All the quantitative results were analyzed using analysis of variance (ANOVA). Statistical significance was considered at $p<0.05$.

5.2.5 Adhesion and Proliferation of C17.2 Cells on PCL Nanowire Surfaces

Cell adhesion and proliferation was investigated using calcein-AM live cell stain after 1, 2, and 7 days of culture. The surfaces were removed from culture media; rinsed with PBS and incubated in calcein-AM (2 μM in PBS) solution for 45 min at 37°C. They were then rinsed in PBS and viewed using FITC MF101 green filter with a Zeiss Axioplan 2 fluorescence microscope. The cell coverage on different surfaces was calculated using the fluorescence images and the Image J software.

5.2.6 Morphology of C17.2 Cells on PCL Nanowire Surfaces

The morphology of adhered C17.2 cells was investigated after 1, 2, and 7 days of culture using SEM imaging. The cells on different surfaces were fixed in a solution of 3% glutaraldehyde, 0.1 M sodium cacodylate, and 0.1 M sucrose for 45 min. The surfaces were then soaked in a buffer solution containing 0.1 M sodium cacodylate and 0.1 M sucrose. This was followed by dehydrating the cells by soaking the surfaces in increasing concentrations of ethanol (35%, 50%, 70%, 95%, and 100%) for 10 minutes each. The cells were further dehydrated by soaking the surfaces in hexamethyldisilazane (HMDS)

for 10 min. The surfaces were then dried under vacuum and stored in a desiccator until examined with SEM. They were sputter coated with 10nm of gold and imaged using a JEOL JSM 6500F at voltages ranging from 10-15kV.

5.2.7 Differentiation of C17.2 Cells on PCL Nanowire Surfaces

In order to evaluate differentiation of C17.2 cells into different neuronal phenotypes, the cells were immunostained for specific marker proteins (**Table 5.1**). The cells were fixed with 3.7% paraformaldehyde for 15 mins at 37^{o}C followed by permeabilization with 1% Triton-X in PBS for 5 mins at room temperature. After fixing and permeabilizing, the cells were washed three times with PBS and incubated in 100 µg/ml of bovine serum albumin (BSA) and 40 µL/mL trypan blue for 20 mins to block any non-specific interactions. Cells were then incubated in the primary antibodies (concentration 1 µg/ml) for 1 hr at room temp. The cells were washed three times with PBS followed by incubation in 5 µg/ml of the appropriate secondary antibody. The cells were then visualized using appropriate filters with Zeiss Axioplan 2 fluorescent microscope.

Table 5.1: Description of key neuronal markers, primary antibodies and secondary antibodies, and blocking agents used for immunofluorescence identification for NSCs.

Differentiation Marker	Description	Primary Antibody	Secondary Antibody	Blocking Serum
Nestin	Type VI intermediate filament protein, expressed mostly in nerve cells where they are implicated in the radial growth of the axon; expressed by undifferentiated cells	Goat Anti-Nestin Polyclonal	Donkey Anti-Goat FITC	Normal Donkey Serum
Neurofilament-H (NF-H)	Approximately 10nm intermediate filaments found specifically in neurons	Mouse Anti-NF-H Monoclonal	Bovine Anti-Mouse FITC	Normal Bovine Serum
Glial fibrillary acidic protein (GFAP)	Intermediate filament protein specific to astrocytes	Goat Anti-GFAP Polyclonal	Donkey Anti-Goat FITC	Normal Donkey Serum
Microtubule-associated protein 2 (MAP2)	Thought to be involved in microtubule assembly, which is an essential step in neurogenesis; expressed by neurons	Rabbit Anti-MAP2 Polyclonal	Bovine Anti-Rabbit TR	Normal Bovine Serum
Adenomatous polyposis coli (APC)	Protein that plays a critical role in several cellular processes; expressed by oligodendrocytes	Rabbit Anti-APC Polyclonal	Bovine Anti-Rabbit TR	Normal Bovine Serum

5.2.8 Statistics

Each experiment was reconfirmed on three different substrates with at least three different cell populations ($n_{min} = 9$). All the quantitative results were analyzed using an analysis of variance (ANOVA). Statistical significance was considered at $p < 0.05$.

5.3 Results and discussion

Tissue regeneration aimed at myelopathic disorders is vital due to the current lack of treatment options for ailments such as SCI. It is indisputable that a material which is able to foster neural stem cells and coax them to differentiate would be beneficial to finding a cure for many nervous system disorders and diseases. As such, there has been great interest in the field of tissue engineering for solutions aimed at such disorders.

Neural progenitor cells on scaffolds with unique nanotopography have shown the most promising results for tissue engineering approaches to cure myelopathic disorders. Thus, in this work, we have developed polymeric scaffolds with nanowire surfaces that were bio-functionalized with an electro-conductive polymer capable of providing physiological levels of electrical stimulation to NSCs. The results presented here show that these nanowire surfaces enhance NSC adhesion, proliferation and differentiation for up to 7 days of culture.

NW surfaces were fabricated using the nanotemplating technique described in the methods section. PCL was chosen as the scaffold material due to its biocompatibility and controlled biodegradability. It has been used for variety of tissue engineering applications ranging from cardiovascular repair (Caragine, Halbach, Ng, & Dowd, 2002)], bone tissue regeneration (Olive et al., 2002) and neural tissue engineering (Xiaohai Wang, Arcuino, et al., 2004). Our unique nanotemplating technique used for fabrication of NW surfaces is especially advantageous because it does not use solvents and can produce scaffolds with consistent surface-bound high aspect nanowires. **Figure 5.2 (NW)** shows representative SEM images of as-fabricated NW surfaces. The images show that the NW surfaces have a uniform architecture with occasional interruption in the uniformity by the presence of random micro-channels formed due to surface charge effects. Further, high magnification SEM images reveal that the individual nanowires of the surface have a consistent diameter of around 100-150 nm (**Figure 5.2, NW)**. The reason for the discrepancy between the membrane pore size and nanowire diameter can

be accounted due to the thermodynamic expansion of the polymer upon cooling. During the extrusion step of the nanotemplating process, the molten PCL fills the nanopores of the membranes. As the polymer cools, it exerts pressure on the nanopore walls. Upon dissolving the membrane, the cooled polymer slightly expands resulting in nanowires that larger in diameter than the nanopores. However, by using different pore size membranes, surfaces with different size nanowires diameters can be fabricated using the nanotemplating technique.

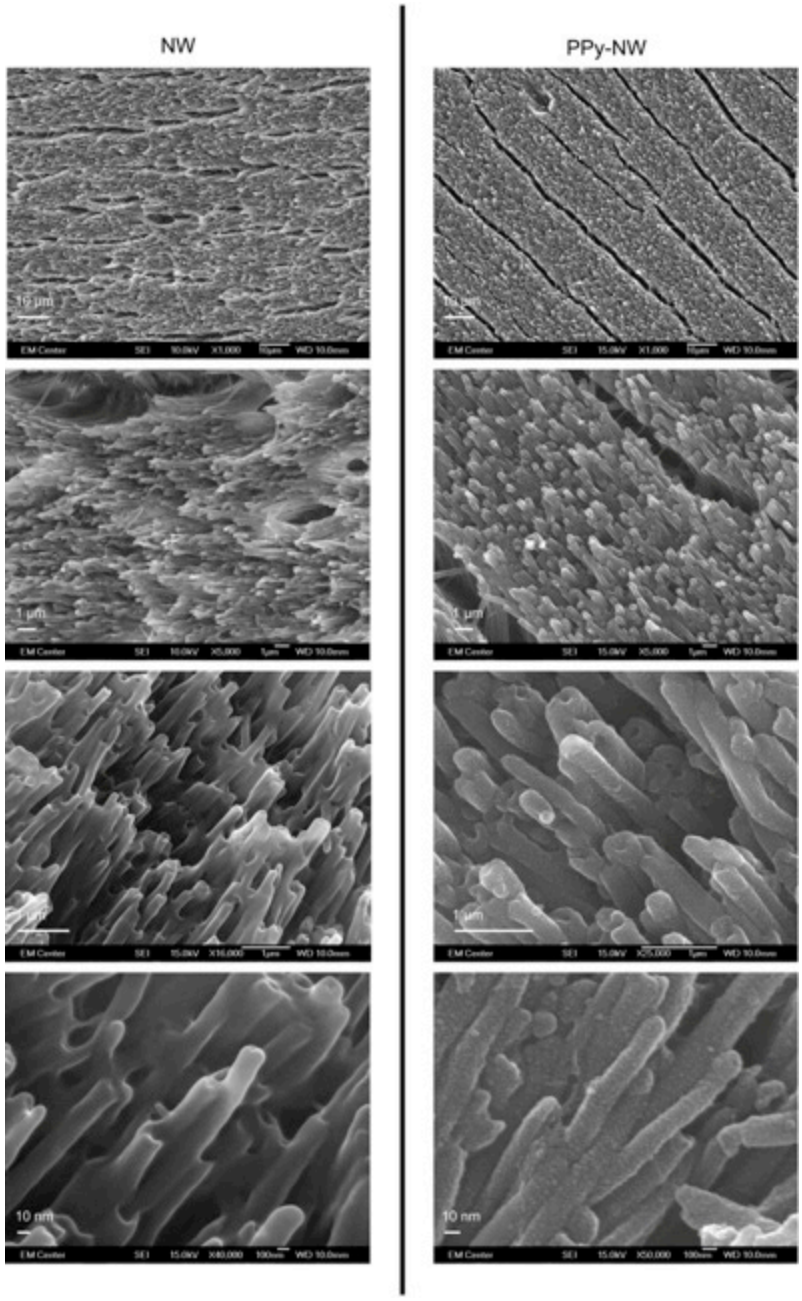

Figure 5.2: Representative SEM images of NW and PPy-NW; the high magnification SEM images show an altered and rougher surface architecture on individual nanowires that were coated with PPy.

The NW surfaces were coated with PPy using a polymerization technique as described in the methods section (Hulsebosch, 2002). The need for an electrically conductive polymer for neural tissue engineering applications arises from the fact that uncharged surfaces are less than optimal for neuronal phenotypic behavior. Additionally, the ability to deliver an electrical current to the cells via the scaffold surface may have several advantages in future tissue engineering applications. **Figure 5.2 (PPy-NW)** shows the representative SEM images of PPy-NW surfaces. The images show that the PPy-NW surfaces have a similar architecture as that of NW surfaces at lower magnifications. The nanowires on PPy coated surfaces maintain their orientation, and more importantly the individual nanowires maintain a consistent diameter. Further, high magnification SEM images reveal that the individual nanowires of PPy-NW surfaces have a slightly larger diameter as compared to those on NW surfaces. The high magnification SEM images also indicate an altered and rougher surface architecture on individual nanowires, which is consistent with literature on PPy coatings on different polymer surfaces (**Figure 5.2, PPy-NW**) (Q. Cao, 2002).

NW and PPy-NW surfaces were characterized using XPS to compare the chemical composition of each surface and in turn, determine whether successful polymerization took place on the NW surfaces or not. The surface elemental composition for NW and PPy-NW surfaces was determined using XPS survey scans. **Table 5.2** shows the elemental composition of NW and PPy-NW surfaces. High-resolution C1s and N1s scans were also taken to determine the precise changes in the amounts of carbon and

nitrogen on the surface (**Figure 5.3**). The results indicate higher amounts of carbon on the surface after modification with PPy. Further, the PPy molecule consists of two amine groups that were detected both in survey as well as high-resolution N1s scans on PPy-NW surfaces. No nitrogen was detected on NW surfaces (**Table 5.2, Figure 5.3**). The survey scans also detected small amounts of sulfur and chlorine on PPy-NW surfaces. This further confirms the polymerization of PPy from pyrrole on nanowire surface since the reaction involves incorporation of chlorine and sodium para-toluene sulfonate. Thus, the XPS results indicate successful modification of NW surfaces with PPy. Further, a standard overlayer model was used to determine the PPy film thickness on nanowire surfaces (Bakshi et al., 2004; Harley et al., 2004; Kataoka et al., 2001; Maquet et al., 2001). As expected, the polymerization process deposited a thin layer of PPy on nanowire surfaces. The results from standard overlayer model indicate that the thickness of PPy on nanowire surfaces is approximately 4.162 nm.

Table 5.2: Surface elemental composition (%) measured using XPS survey scans for NW and PPy-NW surfaces

	C	O	N	S	Cl
NW	73.5	26.5	0	0	0
PPy-NW	74.7	15.6	8.4	1.1	0.2

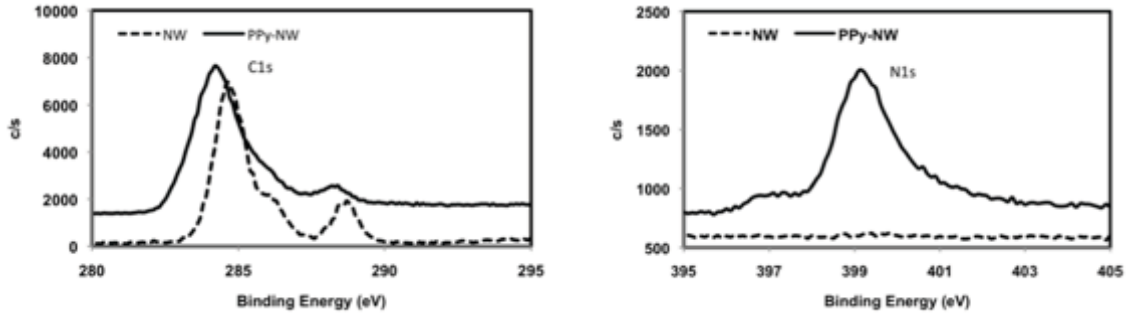

Figure 5.3: High-resolution C1s and N1s scan for NW and PPy-NW surfaces indicating precise changes in surface carbon and nitrogen concentrations after coating the surfaces with PPy.

The electrical properties of the PPy-NW were analyzed by measuring the surface resistivity (R_s). The PPy-NW surfaces had an average R_s = 3.68 ± 1.44 kΩ/square. For comparison, NW surfaces registered greater than 40 MΩ/square. The PPy coating results in a dramatic decrease in surface resistivity, on the order of 13,000× less than NW surfaces. This decrease in resistivity will allow electrical current to conduct through the surface easily where it otherwise would be unable. Such a decrease in electrical resistivity and increase in conductivity may have several advantages for growth and maintenance of NSCs. Studies have shown enhanced cell adhesion on surfaces with lower resistivity *in vitro* (Karimi-Abdolrezaee et al., 2006). Furthermore, studies have shown enhanced

functionality of neurons when exposed to electrical fields *in vivo* (Hofstetter et al., 2005). Thus, PPy-NW surfaces fabricated in this study have a two-fold advantage, a unique nanotopography and decreased surface electrical resistivity, which can attribute to enhanced NSC response.

The stability of PPy-NW surfaces was monitored for up to 7 days in PBS at 37°C under physiological conditions. High magnification SEM imaging was to determine whether there were changes to the rougher surface architecture of the individual nanowires. The results indicate similar surface morphology of PPy-NW surfaces after 7 days as that of as-coated NW surfaces implying that these coatings are robust and did not rapidly degrade under physiological conditions (**Figure 5.4 and Figure 5.2 PPy-NW**). Further XPS was used to determine the changes in surface composition as well as thickness of PPy coating on NW surfaces. The surface elemental composition for PPy-NW surfaces after 7 days in physiological conditions was determined using XPS survey scans. **Table 5.3** shows the elemental composition of PPy-NW surfaces. The results indicate negligible decrease in carbon, nitrogen, sulfur and chlorine concentrations after 7 days in physiological conditions as compared to as-coated PPy-NW surfaces. Further, the thickness of PPy coating was calculated using standard overlayer model. After 7 days in physiological conditions, the thickness of PPy coating was approximately 3.987 nm as compared to 4.162 nm for as-coated PPy-NW surfaces indicating about 4% decrease in thickness. The surface resistivity was also measured to be approximately R_s = 3.45 ± 1.44 kΩ/square after 7 days in physiological conditions as compared to R_s = 3.68 ± 1.44

kΩ/square for as-coated PPy-NW surfaces. These results indicate that PPy coating on stable and will be able to withstand physiological environment with minimal degradation.

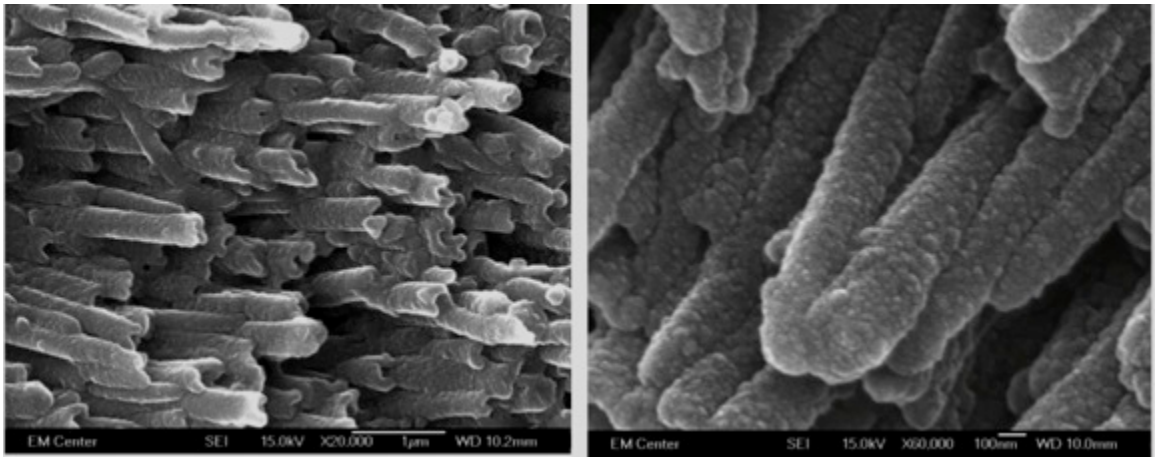

Figure 5.4: Similar surface morphology of nanowires after 7 days in physiological environment as that of as-coated surfaces (Figure 5.2, PPy-NW) indicating that the coatings are robust and will not rapidly degrade.

Table 5.3: Surface elemental composition (%) measured using XPS survey scans as-coated PPy-NW surfaces and PPy-NW surfaces under physiological conditions for 7 days.

	C	O	N	S	Cl
Day 0	74.7	15.6	8.4	1.1	0.2
Day 7	73.5	17.5	7.9	0.9	0.2

In order to evaluate the ability of electro-conductive PPy coated nanowire surfaces to maintain growth and differentiated states of neuronal cells, C17.2 murine NSCs were cultured on NW and and PPy-NW surfaces. Our previous work has demonstrated significantly enhanced functionality of PC12 cells on NW surfaces compared to smooth surfaces in terms of adhesion, proliferation, neuronal network

formation and expression of key neuronal markers (S. L. Bechara et al., 2010). Although PC12 cells are typically used to analyze neural cell response to tissue engineering scaffolds (Silva, 2006), the C17.2 NSC cell line was used for this study due to the ability of these cells to differentiate into all lineages of nervous system including neurons and glial cells (Moxon et al., 2004). Thus in this study, we have evaluated the cellular functionality on NW and PPy-NW surfaces.

NSC adhesion and proliferation was evaluated after 1, 2, and 7 days of culture by staining the adhered cells with calcein-AM and imaging the surfaces using fluorescence microscopy. Calcein-AM is commonly referred to as a "live" cell stain because it is readily transported into the cell and fluoresces upon interaction with esterases. Because dead cells lack the esterases to cause calcein-AM to fluoresce, only live cells appear green. The results indicate that PPy-NW surfaces supported significantly higher cell adhesion as compared NW surfaces after 1 day of culture (**Figure 5.5, Day 1**). The cells also seem to have a spreading morphology on PPy-NW surfaces (as indicated by dotted circle). After 2 days of culture, the cells on PPy-NW surfaces have proliferated and appear to be communicating (as indicated by dotted circle) with each other (**Figure 5.5, Day 2**). In contrast, while the cells are proliferating on NW surfaces, there appears to be little to no communication or aggregation. After 7 days of culture, there are significantly higher numbers of viable cells on PPy-NW surfaces as compared to NW surfaces (**Figure 5.5, Day 7**). The cells appear to be forming a "neuronal network" on PPy-NW surfaces. The fluorescence microscopy images were also analyzed for cell coverage using open-

source Image J software. The results of the cell coverage calculations confirm the visual inspection and quantitatively indicate an increase of more than 2× in cell coverage on PPy-NW surfaces as compared to NW surfaces after 7 days of culture (**Figure 5.5, cell coverage**). Thus, the results indicate that surface nanotopography enhances cell adhesion and proliferation. However, it is apparent from our results that providing nanotopography with electro-conductive surface significantly enhances cell adhesion and proliferation, thus providing an optimal template for maintaining differentiated states of NSCs.

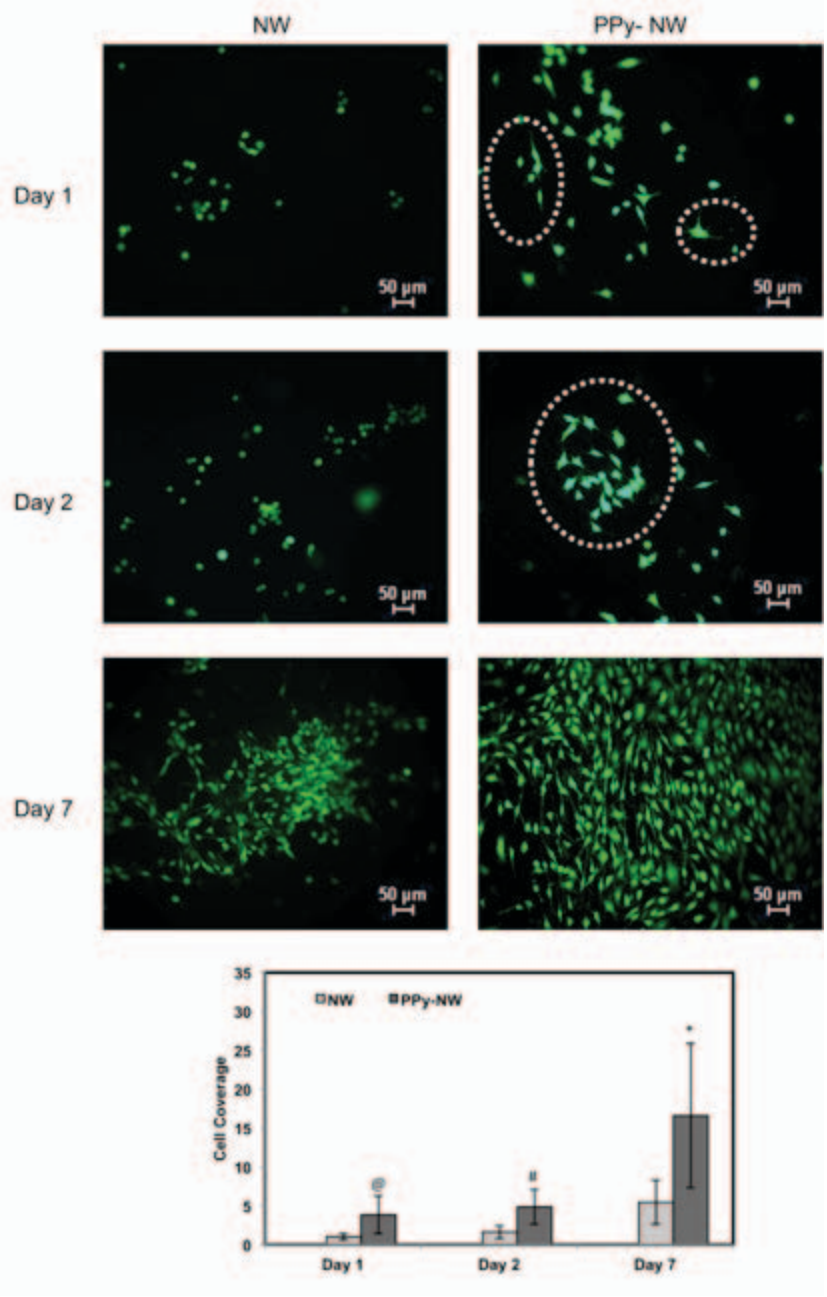

Figure 5.5: Representative fluorescence microscopy images of NSCs stained with calcien-AM on NW and PPy-NW surfaces after 1, 2, and 7 days of culture; the dotted circle represents cell spreading and communication, and “neuronal network” formation. The figure at the bottom shows cell coverage on NW and PPy-NW surfaces calculated using ImageJ software.

NSC morphology on NW and PPy-NW surfaces was investigated after 1, 2 and 7 days of culture using SEM imaging. As expected from the fluorescence microscopy images, the cells on PPy-NW surfaces exhibit a more spread out morphology when compared to those on NW surfaces after 1 day of culture (**Figure 5.6, Day 1**). After 2 days of culture, the cells on PPy-NW surfaces show a significantly higher degree of spreading and appear to be communicating when compared to cells on NW surfaces (**Figure 5.6, Day 2**). High-resolution SEM images for cells on PPy-NW surfaces show that the cellular extensions are relatively shorter and are interacting with the nanowire architecture (**Figure 5.6, Day 2, PPy-NW, image on the right is high magnification for the dotted circle**). After 7 days of culture, the cells have formed what appears to be a complex "neuronal network" on PPy-NW surfaces as compared to the cells on NW surfaces (**Figure 5.6, Day 7**). Further, high-resolution SEM images for cells on PPy-NW surfaces show that the cells have longer extensions that are interacting with the nanowire architecture (**Figure 5.6, Day 2, PPy-NW, image on the right is high magnification for the dotted circle**). Such interaction with material nanoarchitecture is an integrin mediated action and is extremely important for maintenance of differentiated phenotypes of NSCs on material surfaces. Further studies are being conducted to understand the mechanisms of cellular interaction with nanowire architecture.

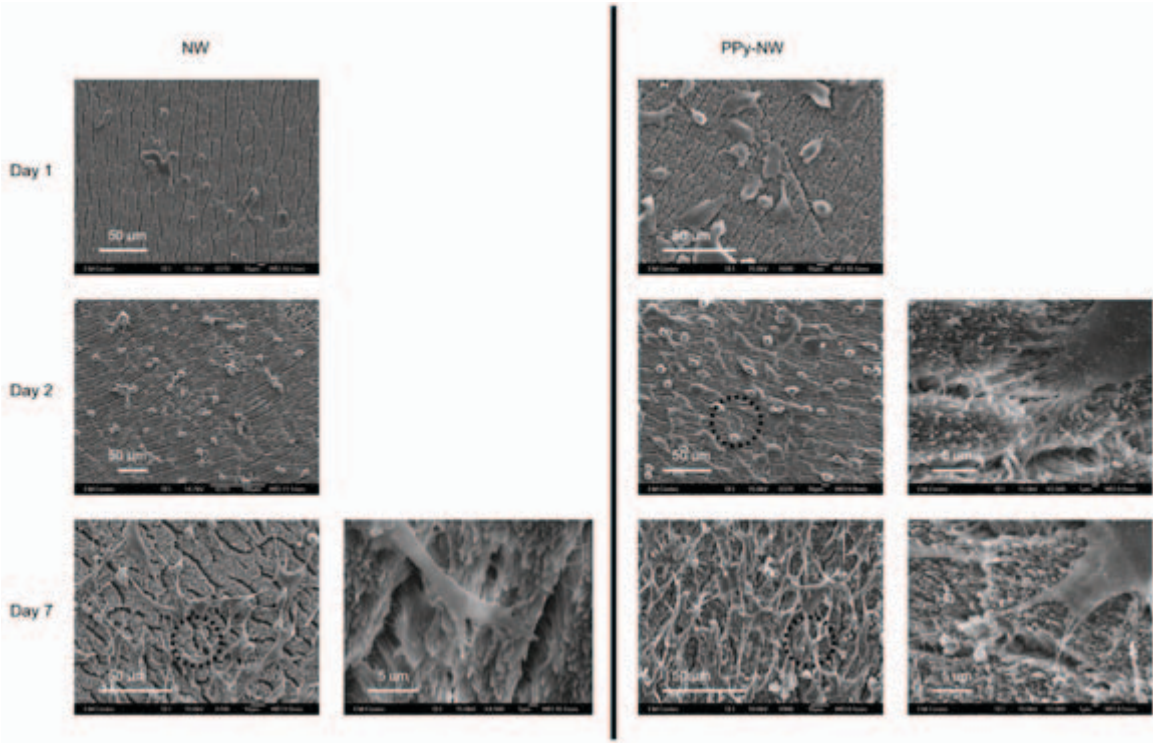

Figure 5.6: Representative SEM images NSCs on NW and PPy-NW surfaces after 1, 2 and 7 days of culture. Significanly higher "neuronal network" formation is observed on PPy-NW surfaces. The high magnification images (for the dotted circle) confirm that the cells interacting the nanowire architecture.

In order to evaluate the efficacy of PPy-NW surfaces for neural tissue engineering applications, it is important to evaluate the ability of these surfaces to maintain the differentiated states of NSCs. Thus, immunofluorescence imaging was used to ensure expression of key neuronal markers in the differentiated states of NSCs on PPy-NW surfaces after 7 days of culture (**Table 5.2**). Immunofluorescence imaging was not performed on NW surfaces due to lack of extensive "neuronal network" formation. The C17.2 murine NSCs are known to differentiate in all neural lineages including neurons, astrocytes and oligodendrocytes. First, the adhered cells were immunostained for Nestin.

Nestin is a type VI intermediate filament protein that is expressed mostly in stem cells from the central nervous systems but not in mature central nervous system cells (Fan et al., 2002). Its expression is commonly used as a marker for undifferentiated NSCs. Its transient expression is a critical step in the neural differentiation pathway, meaning that its expression indicates that the cells will eventually differentiate into one of the neural lineages. The results indicate that fewer cells expressed nestin suggesting that majority of the cells on PPy-NW surfaces have differentiated into neural lineages, and these undifferentiated NSCs are on the path of neuronal differentiation (**Figure 5.7, Nestin**). Further, the cells were immunostained for neurofilament-H (NH-F) and microtubule-associated protein 2 (MAP2), both of which are expressed by neurons (Kam et al., 2001; Koh et al., 2008; Matsuzawa et al., 1996; Silva et al., 2004). Neurons are electrically excitable cells that processes and transmit information by electrical and chemical signaling. The cytoskeleton of neurons consists of three types of cytosolic fibers; actin microfilaments, intermediate filaments and microtubules. Neurofilaments are the major intermediate filaments found in neurons. They are critical for radial axon growth and determine axon caliber, whereas microtubules are involved in axon elongation. MAP2 is thought to be involved in microtubule assembly, which is an essential step in neurogenesis. The results indicate that NSCs are expressing both NF-H and MAP2 on PPy-NW surfaces suggesting that the cells have differentiated into neurons (**Figure 5.7, NF-H and MAP2**). The cells were also immunostained for glial fibrillary acidic protein (GFAP), which is primarily expressed by astrocytes. GFAP is thought to help in

maintaining astrocyte mechanical strength, as well as the shape of cells (Yang et al., 2004). The results indicate that the cells on PPy-NW surfaces are expressing GFAP suggesting that some populations of NSCs have differentiated into astrocytes (**Figure 5.7, GFAP**). Astrocytes are important cells, especially in a nervous system disorder application. The principal role of astrocytes is in the repair and scarring process of the brain and spinal cord following traumatic injuries. Further, astrocytes also provide biochemical support to endothelial cells that form the blood-brain barrier, they provide nutrients to the nervous tissue, and they maintain extracellular ionic balance. Finally, the cells were immunostained for adenomatous polyposis coli (APC), which is primarily expressed by oligodendrocytes. The results indicate that the cells on PPy-NW surfaces are expressing APC, have differentiated, and have morphology unique to oligodendrocytes. The main function of oligodendrocytes is the insulation of axons (the long projection of nerve cells) in the central nervous system. Like all other glial cells, they provide a supporting role for neurons. The expression of APC by oligodendrocytes is known to direct cholinergic synapse assembly between the neurons (Oh et al., 2007; J. R. Porter, Henson, et al., 2009; Tiaw et al., 2005; Williamson & Coombes, 2004; Yoshimoto et al., 2003). Thus, the results presented here substantiate the efficacy of PPy-NW surfaces in maintaining the differentiated states of NSCs into major neuronal phenotypes.

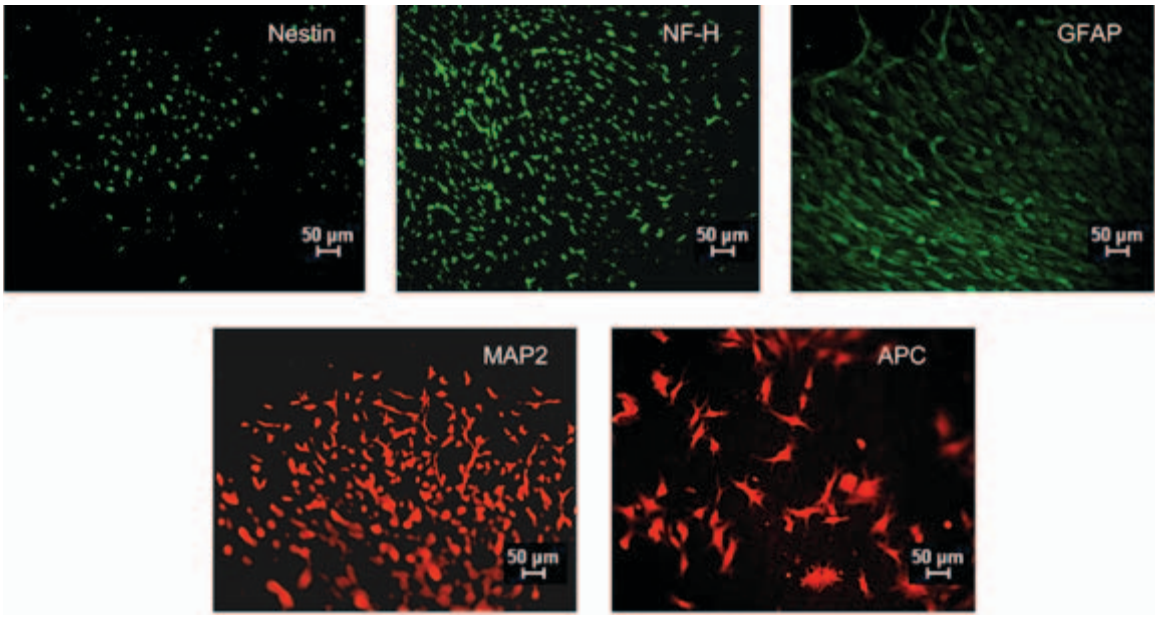

Figure 5.7: Representative immunofluorescence images showing expression of Nestin, NF-H, GFAP, MAP2, and APC on PPy-NW surfaces confirming that the NSCs have differentiated into all neural lineages.

5.4 Conclusions

In this work, we have developed a simple nanotemplating technique to fabricate PCL nanowire surfaces. These surfaces were further coated with PPy to provide a physiologically relevant template for growth and maintenance of NSCs. The results presented here confirm that PPy coating reduces the electrical resistivity of the PCL nanowires to a functional level where electrical stimulation may be applied to control the growth of neurons. Furthermore, the results indicate that decreasing the electrical resistivity of the surface increases the functionality of C17.2 neural stem cells in terms of their adhesion, proliferation, and differentiation. Finally, our hypothesis was shown to be true, an electically conductive coating does enhance C17.2 cellular activity. Thus, by

controlling the surface nanotopography and providing a physiologically relevant surface charge, neuronal cell functionality can be altered for potential applications in neural tissue engineering.

5.5 References

Bakshi, A., Fisher, O., Dagci, T., Himes, B. T., Fischer, I., & Lowman, A. (2004). Mechanically engineered hydrogel scaffolds for axonal growth and angiogenesis after transplantation in spinal cord injury. *Journal of neurosurgery. Spine*, *1*(3), 322-9. doi:10.3171/spi.2004.1.3.0322

Bechara, S. L., Judson, A., & Popat, K. C. (2010). Template synthesized poly([var epsilon]-caprolactone) nanowire surfaces for neural tissue engineering. *Biomaterials*, *31*(13), 3492-3501. Retrieved from http://www.sciencedirect.com/science/article/B6TWB-4YC39RW-5/2/b9a281830087f2631912339503ac195e

Cao, Q. (2002). Differentiation of Engrafted Neuronal-Restricted Precursor Cells Is Inhibited in the Traumatically Injured Spinal Cord. *Experimental Neurology*, *177*(2), 349-359. doi:10.1006/exnr.2002.7981

Caragine, L. P., Halbach, V. V., Ng, P. P., & Dowd, C. F. (2002). Vascular myelopathies-vascular malformations of the spinal cord: presentation and endovascular surgical management. *Seminars in neurology*, *22*(2), 123-32. doi:10.1055/s-2002-36535

Damodaran, V. B., Fee, C. J., Ruckh, T., & Popat, K. C. (2010). Conformational studies of covalently grafted poly(ethylene glycol) on modified solid matrices using X-ray photoelectron spectroscopy. *Langmuir : the ACS journal of surfaces and colloids*, *26*(10), 7299-306. American Chemical Society. doi:10.1021/la9041502

Fan, Y. W., Cui, F. Z., Hou, S. P., Xu, Q. Y., Chen, L. N., & Lee, I.-S. (2002). Culture of neural cells on silicon wafers with nano-scale surface topograph. *Journal of neuroscience methods*, *120*(1), 17-23. Retrieved from http://www.ncbi.nlm.nih.gov/pubmed/12351203

Gomez, N., Lee, J. Y., Nickels, J. D., & Schmidt, C. E. (2007). Micropatterned Polypyrrole: A Combination of Electrical and Topographical Characteristics for the Stimulation of Cells. *Advanced functional materials*, *17*(10), 1645-1653. doi:10.1002/adfm.200600669

Harley, B. A., Spilker, M. H., Wu, J. W., Asano, K., Hsu, H.-P., Spector, M., & Yannas, I. V. (2004). Optimal degradation rate for collagen chambers used for regeneration of peripheral nerves over long gaps. *Cells, tissues, organs*, *176*(1-3), 153-65. doi:10.1159/000075035

Hofstetter, C. P., Holmström, N. A. V., Lilja, J. A., Schweinhardt, P., Hao, J., Spenger, C., Wiesenfeld-Hallin, Z., et al. (2005). Allodynia limits the usefulness of intraspinal neural stem cell grafts; directed differentiation improves outcome. *Nature neuroscience*, *8*(3), 346-53. doi:10.1038/nn1405

Hulsebosch, C. E. (2002). RECENT ADVANCES IN PATHOPHYSIOLOGY AND TREATMENT OF SPINAL CORD INJURY. *Advan Physiol Educ*, *26*(4), 238-255. Retrieved from http://advan.physiology.org/cgi/content/abstract/26/4/238

Kam, L., Shain, W., Turner, J. N., & Bizios, R. (2001). Axonal outgrowth of hippocampal neurons on micro-scale networks of polylysine-conjugated laminin. *Biomaterials*, *22*(10), 1049-54. Retrieved from http://www.ncbi.nlm.nih.gov/pubmed/11352086

Karimi-Abdolrezaee, S., Eftekharpour, E., Wang, J., Morshead, C. M., & Fehlings, M. G. (2006). Delayed transplantation of adult neural precursor cells promotes remyelination and functional neurological recovery after spinal cord injury. *The Journal of neuroscience : the official journal of the Society for Neuroscience*, *26*(13), 3377-89. doi:10.1523/JNEUROSCI.4184-05.2006

Kataoka, K., Suzuki, Y., Kitada, M., Ohnishi, K., Suzuki, K., Tanihara, M., Ide, C., et al. (2001). Alginate, a bioresorbable material derived from brown seaweed, enhances elongation of amputated axons of spinal cord in infant rats. *Journal of biomedical materials research*, *54*(3), 373-84. Retrieved from http://www.ncbi.nlm.nih.gov/pubmed/11189043

Koh, H. S., Yong, T., Chan, C. K., & Ramakrishna, S. (2008). Enhancement of neurite outgrowth using nano-structured scaffolds coupled with laminin. *Biomaterials*, *29*(26), 3574-82. doi:10.1016/j.biomaterials.2008.05.014

Lee, J. Y., Bashur, C. A., Goldstein, A. S., & Schmidt, C. E. (2009). Polypyrrole-coated electrospun PLGA nanofibers for neural tissue applications. *Biomaterials*, *30*(26), 4325-35. doi:10.1016/j.biomaterials.2009.04.042

Lu, P., Jones, L. L., Snyder, E. Y., & Tuszynski, M. H. (2003). Neural stem cells constitutively secrete neurotrophic factors and promote extensive host axonal growth after spinal cord injury. *Experimental neurology*, *181*(2), 115-29. Retrieved from http://www.ncbi.nlm.nih.gov/pubmed/12781986

Maquet, V., Martin, D., Scholtes, F., Franzen, R., Schoenen, J., Moonen, G., & Jér me, R. (2001). Poly(D,L-lactide) foams modified by poly(ethylene oxide)-block-poly(D,L-

lactide) copolymers and a-FGF: in vitro and in vivo evaluation for spinal cord regeneration. *Biomaterials*, *22*(10), 1137-46. Retrieved from http://www.ncbi.nlm.nih.gov/pubmed/11352093

Matsuzawa, M., Weight, F. F., Potember, R. S., & Liesi, P. (1996). Directional neurite outgrowth and axonal differentiation of embryonic hippocampal neurons are promoted by a neurite outgrowth domain of the B2-chain of laminin. *International journal of developmental neuroscience : the official journal of the International Society for Developmental Neuroscience*, *14*(3), 283-95. Retrieved from http://www.ncbi.nlm.nih.gov/pubmed/8842805

Moxon, K. A., Kalkhoran, N. M., Markert, M., Sambito, M. A., McKenzie, J. L., & Webster, J. T. (2004). Nanostructured surface modification of ceramic-based microelectrodes to enhance biocompatibility for a direct brain-machine interface. *IEEE transactions on bio-medical engineering*, *51*(6), 881-9. doi:10.1109/TBME.2004.827465

Niles, L. P., Armstrong, K. J., Rincón Castro, L. M., Dao, C. V., Sharma, R., McMillan, C. R., Doering, L. C., et al. (2004). Neural stem cells express melatonin receptors and neurotrophic factors: colocalization of the MT1 receptor with neuronal and glial markers. *BMC neuroscience*, *5*, 41. doi:10.1186/1471-2202-5-41

Olive, J. L., McCully, K. K., & Dudley, G. A. (2002). Blood flow response in individuals with incomplete spinal cord injuries. *Spinal cord*, *40*(12), 639-45. Nature Publishing Group. doi:10.1038/sj.sc.3101379

Petrovykh, D. Y., Kimura-Suda, H., Tarlov, M. J., & Whitman, L. J. (2004). Quantitative characterization of DNA films by X-ray photoelectron spectroscopy. *Langmuir : the ACS journal of surfaces and colloids*, *20*(2), 429-40. Retrieved from http://www.ncbi.nlm.nih.gov/pubmed/15743088

Popat, K. C., Leary Swan, E. E., & Desai, T. A. (2005). Modeling of RGDC film parameters using X-ray photoelectron spectroscopy. *Langmuir : the ACS journal of surfaces and colloids*, *21*(16), 7061-5. doi:10.1021/la047749y

Popat, K. C., Mor, G., Grimes, C. A., & Desai, T. A. (2004). Surface modification of nanoporous alumina surfaces with poly(ethylene glycol). *Langmuir : the ACS journal of surfaces and colloids*, *20*(19), 8035-41. doi:10.1021/la049075x

Porter, J., Henson, A., & Popat, K. (2009). Biodegradable poly(ε-Caprolactone) nanowires for bone tissue engineering applications. *Biomaterials*, *30*(5), 780-788.

Silva, G. A. (2006). Neuroscience nanotechnology: progress, opportunities and challenges. *Nature reviews. Neuroscience*, *7*(1), 65-74. doi:10.1038/nrn1827

Silva, G. A., Czeisler, C., Niece, K. L., Beniash, E., Harrington, D. A., Kessler, J. A., & Stupp, S. I. (2004). Selective differentiation of neural progenitor cells by high-epitope density nanofibers. *Science (New York, N.Y.)*, *303*(5662), 1352-5. doi:10.1126/science.1093783

Snyder, E. Y., Deitcher, D. L., Walsh, C., Arnold-Aldea, S., Hartwieg, E. A., & Cepko, C. L. (1992). Multipotent neural cell lines can engraft and participate in development of mouse cerebellum. *Cell*, *68*(1), 33-51. Retrieved from http://www.ncbi.nlm.nih.gov/pubmed/1732063

Tao, S. L., Popat, K. C., Norman, J. J., & Desai, T. A. (2008). Surface modification of SU-8 for enhanced biofunctionality and nonfouling properties. *Langmuir : the ACS journal of surfaces and colloids*, *24*(6), 2631-6. doi:10.1021/la703066z

Wang, X., Arcuino, G., Takano, T., Lin, J., Peng, W. G., Wan, P., Li, P., et al. (2004). P2X7 receptor inhibition improves recovery after spinal cord injury. *Nature medicine*, *10*(8), 821-7. doi:10.1038/nm1082

Chapter 6 Nerve growth factor conjugated multifunctional nanowires enhance C17.2 cellular function

6.1 Introduction

Due to the promise NGF has shown in multiple paradigms, we have formulated a novel technique to attach NGF onto multifunctional substrates previously developed by our lab. This research aim adresses specific aim 4. Previous research has indicated that these multifunctional polymeric substrates have both a beneficial nanotopography (S. L. Bechara et al., 2010) and surface conductivity (S. Bechara, Wadman, & Popat, 2011) that promotes enhanced neural stem cell functionality. The specific nanotopography consists of protruding vertically aligned nanowires (NW) made from the FDA approved biomaterial polycaprolactone (PCL). The aforementioned surface conductivity arises from a polypyrrole (PPy) coating. We hypothesized that if neural stem cells react to biochemical cues, by introducing the biomolecule NGF to the substrate surface, we can enhance the functionality of neural progenitor cells. In this study, NGF was confirmed to conjugate onto multifunctional polypyrrole coated nanowire surfaces (NGF-PPy-NW) and in turn, promoted favorable neural stem cell response.

6.2 Materials and Methods

6.2.1 Nanowire fabrication and polypyrrole coating

Nanowires were fabricated by a method developed in our laboratory and published elsewhere (S. L. Bechara et al., 2010). Briefly, a flat PCL disc is laid on top of a nanoporous alumina membrane (20nm pore size) and extruded for 3mins at 115C. Next, the membrane was dissolved by incubating in 1M NaOH for 75mins to release substrate bound nanowires. The surfaces were rinsed with DI water prior to further modification. The polypyrrole coating procedure is also published elsewhere (S. Bechara et al., 2011). Briefly, the nanowire surfaces were incubated in a mixture of 14mM pyrrole and 14mM para-toluene sulfonate solution for 1hr at 4oC. This was followed by incubation in 38mM ferric chloride solution for 24hrs at 4oC to conjugating polypyrrole on the surfaces. The coated nanowire surfaces were thoroughly rinsed in DI water and stored in a desiccator until further use.

6.2.2 Chemical Conjugation of NGF

NGF was conjugated to the surfaces via a simple 3-step technique. First, the substrates are incubated in a 5% (v/v) aqueous solution of polyallyamine while simultaneously exposing it to ultraviolet radiation for 25min. After rinsing with DI water, the surfaces were incubated on a shaker plate in a solution containing N,N-dimethylformamide (3.3ml) and N-succinimidyl-3-maleimidoproprionate (25mg) for 1 hour. The surfaces were rinsed with DI water and incubated on a shaker plate in a

solution of NGF or NGF-FITC for 2 hours. After rinsing with surfaces with DI water and drying, they were immediately characterized or cultured with cells.

6.2.3 Characterization of NGF conjugated surfaces

NGF conjugation was characterized by XPS, ELISA and fluorescence microscopy. To visualize the coating, NGF was conjugated to the fluorescent molecule FITC and then to the substrates and finally imaged using an Axio Imager A2 microscope. XPS analysis was done after each step of modification. Survey spectra were collected from 0 to 1100eV with pass energy of 187.85 eV, and high-resolution spectra were collected for N1s peak with pass energy of 10eV. Data for percent elemental composition, elemental ratios and peak fit analysis were calculated using Multipack and XPSPeak 4.1 (Freeware) software.

An ELISA was used to characterize the stability of NGF and whether it was releasing from the surface. NGF-PPy-NW surfaces were incubated in PBS (500µL) for 8 hours, 1, 2, 5, and 10 days at 37°C and 5% CO2. At each time point, the amount of NGF in the PBS was measured following manufacturer provided instructions for the ELISA kit.

6.2.4 Cell Culture

C17.2 murine neural stem cells developed by the group of Dr. Evan Snyder were used for the studies presented here. Cells were cultured using standard protocol. Cells below passage 3 were used for all of the studies. The surfaces were ethanol and uv

sterilized prior to culturing the cells. The cells were seeded at a density of 10000 cells/cm2 for 5 days. Cell medium was not replaced for the entire duration of the study.

6.2.5 Cellular response to NGF conjugated surfaces

C17.2 cell adhesion was investigated by staining the cells with CMFDA, rhodamine-phalloidin and DAPI. After 5 days of culture, the surfaces were incubated with a solution of CMFDA (25μM) in PBS 30mins at 37°C. Next, the CMFDA solution was aspirated, the substrates were washed with PBS, and fresh cell culture media was added followed by further incubation for 30mins at 37°C. The surfaces were then fixed by incubating in an aqueous formaldehyde solution (3.7% v/v) for 15mins at room temperature followed permeabilizing in aqueous Triton-X solution (1% v/v) for 3mins at room temperature. The surfaces were then incubated in a solution of rhodamine-phalloidin (5μL/ml) in PBS for 30 minutes. During the last 5 minutes of incubation, DAPI was added (300nM). The surfaces were rinsed with DI water and imaged immediately with a fluorescence microscope.

6.2.6 Differentiation of C17.2 Cells on NGF conjugated surfaces

After 5 days of culture, the cells were simultaneously immunostained for nestin (for undifferentiated cells), neuron specific class III β-tubulin (TUJ1, for neurons), and glial fibrillary acidic protein (GFAP, for glial cells). The cells were fixed and permeabilized as indicated above. Non-specific binding was blocked by incubating the surfaces in 10% normal goat serum in PBS for 20mins. The surfaces were incubated in a

solution of primary anti-bodies for 60 minutes followed by rinsing with PBS and further incubation in a solution of secondary antibodies (Table 6.1). The surfaces were rinsed with DI water and imaged immediately with a fluorescence microscope.

Table 6.1: Description of key neuronal markers, primary antibodies and secondary antibodies, and blocking agents used for immunofluorescence identification for NSCs

	Undifferentiated	**Neurons**	**Glial**
Marker	Nestin	TUJ1	GFAP
Primary antibody and dilution	Mouse Protien G Purified IgG2A 1:100	Chicken Affinity Purified IgG 1:100	Rabbit Polyclonal IgG 1:50
Secondary antibody and dilution	Goat Anti-Mouse DyLight 350 1:200	Goat Anti-Chicken TR 1:100	Goat Anti-Rabbit FITC 1:100
Blocking agent	Normal goat serum		

6.2.7 Image Processing

All fluorescence microscopy images were taken with a Carl Zeiss Axiocam ERc5s camera attached to a Carl Zeiss Axio Imager A2 microscope. All images were processed and pseudo colored using Carl Zeiss AxioVision version 4.8.2 software. The only image manipulation performed was linear and was for contrast and brightness enhancement. Similar image manipulation was preformed on both controls and samples. Image manipulation that would obscure data was avoided. Each experiment was preformed on at least 3 different surfaces, with 3 different cell populations (nmin = 9).

6.3 Results and Discussion

The specific chemical conjugation technique used in this study can be utilized with any material that has functionalized amine groups on the surface. In this study, NGF was conjugated on flat polycaprolactone surfaces (PCL) and polypyrrole coated flat polycaprolactone surfaces (PPy-PCL) (both used as controls); and polypyrrole coated polycaprolactone nanowire surfaces (PPy-NW). The surface conjugation chemistry involves a simple 3-step procedure (Figure 6.1, left). First, the surfaces are incubated in a polyallylamine solution while simultaneous exposing to uv radiation to covalently conjugate amine groups on the surface. Next, the surfaces are incubated in a solution of N-succinimidyl-3-maleimidoproprionate in N,N-dimethylformamide (DMF). In this step, the N-succinimidyl terminal of the N-succinimidyl-3-maleimidoproprionate reacts with the amine groups on the surface forming stable amide linkages. This reaction is favored by the use of polar DMF. The DMF acts as a nucleophillic activator thereby speeding up the reaction. This step results in the incorporation of maleimides, which are excellent reagents for thiol-selective modifications and produces N-hydroxysuccinimide (NHS) as a byproduct. In the final step, the substrates are incubated in a solution containing NGF. In this step, the maleimide terminals from the modified surface reacts with free thiol groups present in the NGF (Angeletti & Bradshaw, 1971) resulting in stable thioesters, which effectively grafts NGF to the substrates via strong covalent bonds.

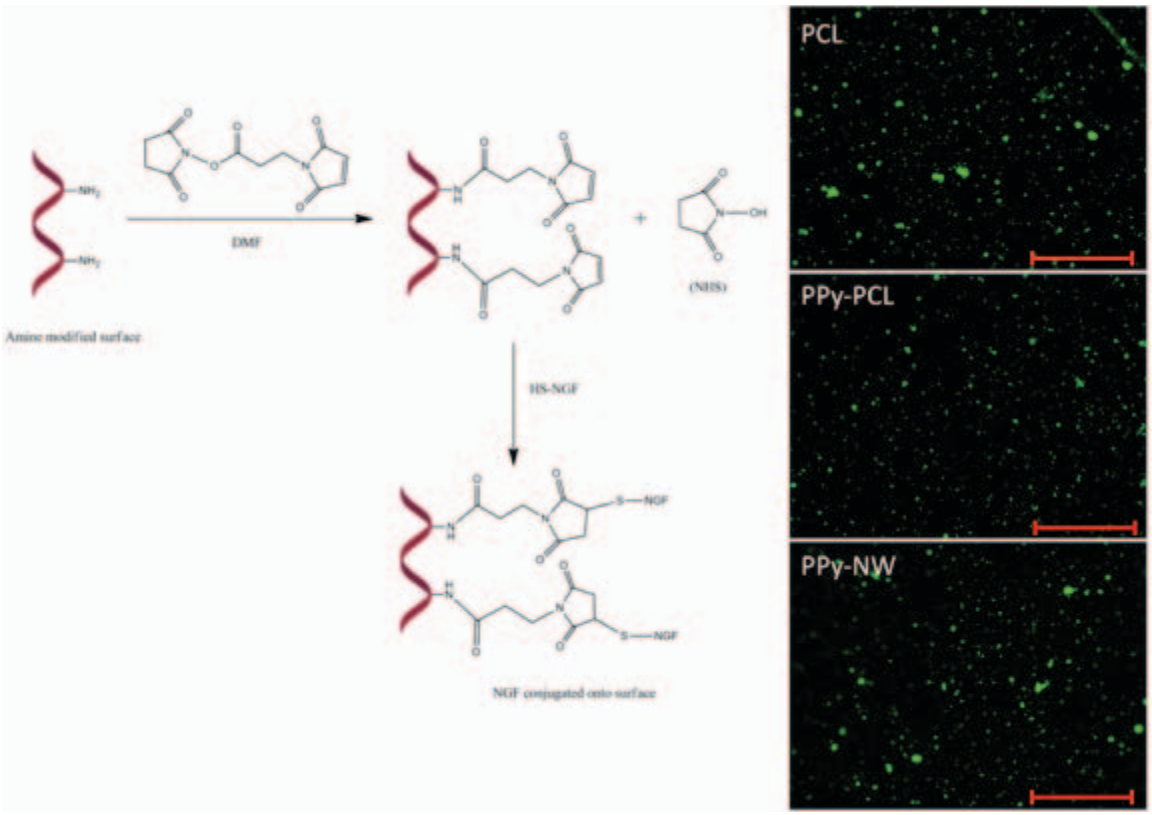

Figure 6.1: (Left) Schematic representation of NGF conjugation to polymeric surfaces. First, materials are modified to contain free amine groups. Next, maleimides are incorporated onto the amine groups. Finally, the NGF is attached to the maleimides via thiol groups present on the NGF. (Right) Representative fluorescence microscopy images of NGF-FITC conjugated on PCL, PPy-PCL and PPy-NW surfaces. (Scale bar: 50μm)

NGF conjugation was verified using a previously developed fluorescence imaging technique (Gomez & Schmidt, 2007). The method involves chemically conjugating the fluorescent molecule fluorescein (FITC) to NGF and imaging the resulting NGF-FITC conjugated surfaces using a fluorescence microscope. As indicated by the images (Figure 6.1, right), it is apparent that the NGF is uniformly distributed on all the surfaces indicating that the surface conjugation was successful.

NGF conjugation was further characterized using X-ray photoelectron spectroscopy (XPS). XPS was used before and after modification of PPy-NW surfaces with amine groups and NGF. The surface elemental composition for all the surfaces was determined using XPS survey scans. Table 6.2 shows the elemental composition of all the surfaces determined using XPS suvey scans. The survey scans also detected small amounts of sulfur and chlorine on PPy-NW surfaces. This is because the polymerization reaction involves incorporation of chlorine and sodium para-toluene sulfonate. After amine modification, the amount of carbon, sulfur and chlorine was slightly decreased whereas the amount of nitrogen increased indicating successful incorporation of amine groups on the surface. Following NGF conjugation, the amount of carbon, nitrogen and sulfur increased whereas no chlorine was detected on the surfaces. Since XPS is a depth sensitive technique, the observed relative changes in the surface elemental composition indicates successful conjugation of NGF. Further, high-resolution N1s scans were also taken and the results indicate an increase in the amounts of nitrogen on the surface (Figure 6.2).

Table 6.2: Surface elemental composition (%) measured using XPS survey scans.

	C	**N**	**O**	**S**	**Cl**
PPy-NW	75.0	8.3	15.0	1.0	0.7
NH_2-PPy-NW	74.5	10.2	14.4	0.5	0.4
NGF-PPy-NW	75.6	11.1	12.2	1.1	0

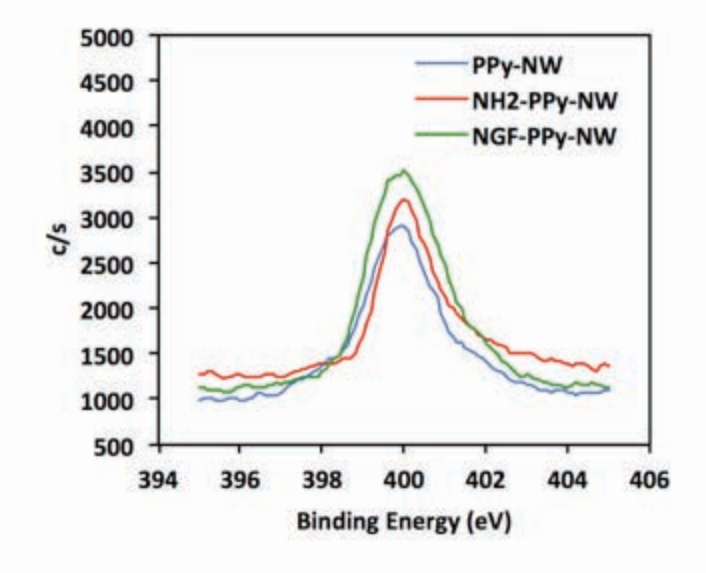

Figure 6.2: High resolution XPS scans of nitrogen showing the different peaks after three distinct steps in the conjugation process.

This further confirms the polymerization of PPy from pyrrole on nanowire surfaces since the reaction involves incorporation of chlorine and sodium para-toluene sulfonate. Thus, the XPS results indicate successful modification of NW surfaces with PPy.

Further, an ELISA was used to characterize the stability of NGF conjugation and to determine whether it was releasing from the surface. The results (not shown here) indicate that no measureable amount of NGF was released from the surface for up to 10 days of incubation in a physiological environment.

To investigate the effect of the NGF conjugation on cell functionality, C17.2 murine neural stem cells were cultured NGF conjugated surfaces (NGF-PPy-NW). PPy-NW surfaces were used as controls. Our previous research has indicated that PPy-NW surfaces provides a favorable template for enhanced neural stem cell functionality and

hence other surfaces were not used for cell studies (S. Bechara et al., 2011). After 5 days of culture, the cells were labeled with the 5-Chloromethylfluorescein Diacetate (CMFDA), a stain that identifies live cells. The cytoskeleton protein actin and the cell nucleus were also stained with rhodamine-phalloidin and 4',6-diamidino-2-phenylindole (DAPI) respectively. The results indicate that there were significantly higher numbers of live cells on NGF-PPy-NW surfaces as compared to PPY-NW surface (Figure 6.3). Furthermore, the cells on NGF-PPy-NW surfaces have altered morphologies and appear to be differentiating into the distinctive neural phenotypes as indicated by the actin stain (Figure 6.3). The cells on NGF-PPy-NW surfaces have different morphologies including neuron-like (Figure 6.4) to glial-like (Figure 6.5) morphologies. This is contrasted by the spherical morphologies of on the PPy-NW surfaces, which indicates that the cells are still undifferentiated state (Figure 6.6).

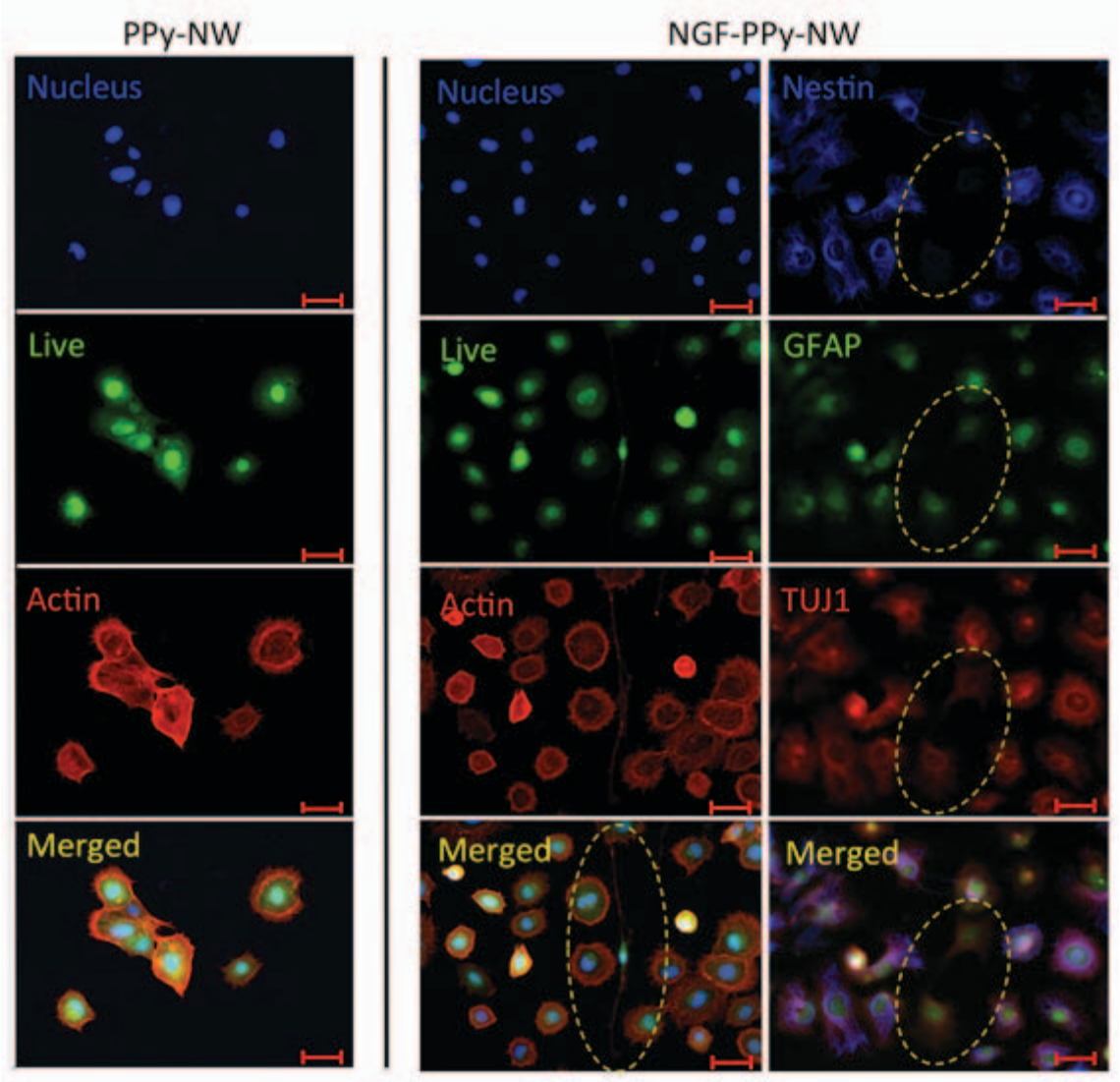

Figure 6.3: Representative fluorescence microscopy images of C17.2 cells on PPy-NW and NGF-PPy-NW substrates after 5 days of culture. Higher number of cells observed on the NGF-PPy-NW surfaces compared to PPy-NW surface. It appears that the cells on NGF-PPy-NW have taken on complex morphologies (dotted circle) as opposed to spherical morphology on PPy-NW surface. Furthermoe, immunofluorescence images indicate that the cells have started differentiating into neuronal phenotypes (dotted circle). Markers used: Nestin – undifferentiated cells, GFAP – glial cells, TUJ1 – neurons. (Scale bar: 50µm)

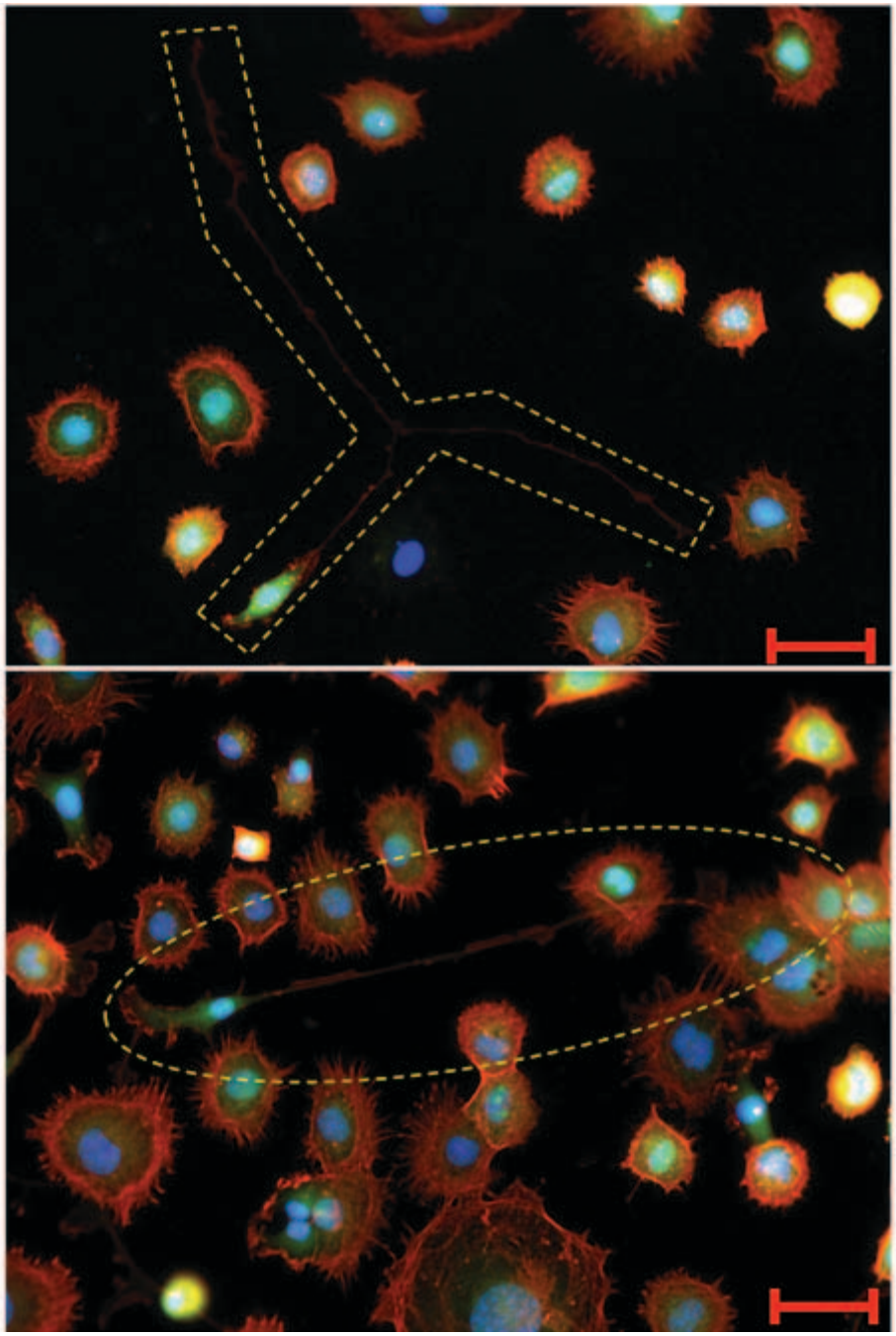

Figure 6.4: Representative fluorescence microscopy image for CMFDA/rhodamine-phalloidin/DAPI stained surfaces illustrating the altered morphologies of C17.2 cells on NGF-PPy-NW surfaces after 5 days of culture. Many cells have morphologies that could be classified as neuron-like (see cells enclosing dotted areas). (Scale bar: 50μm)

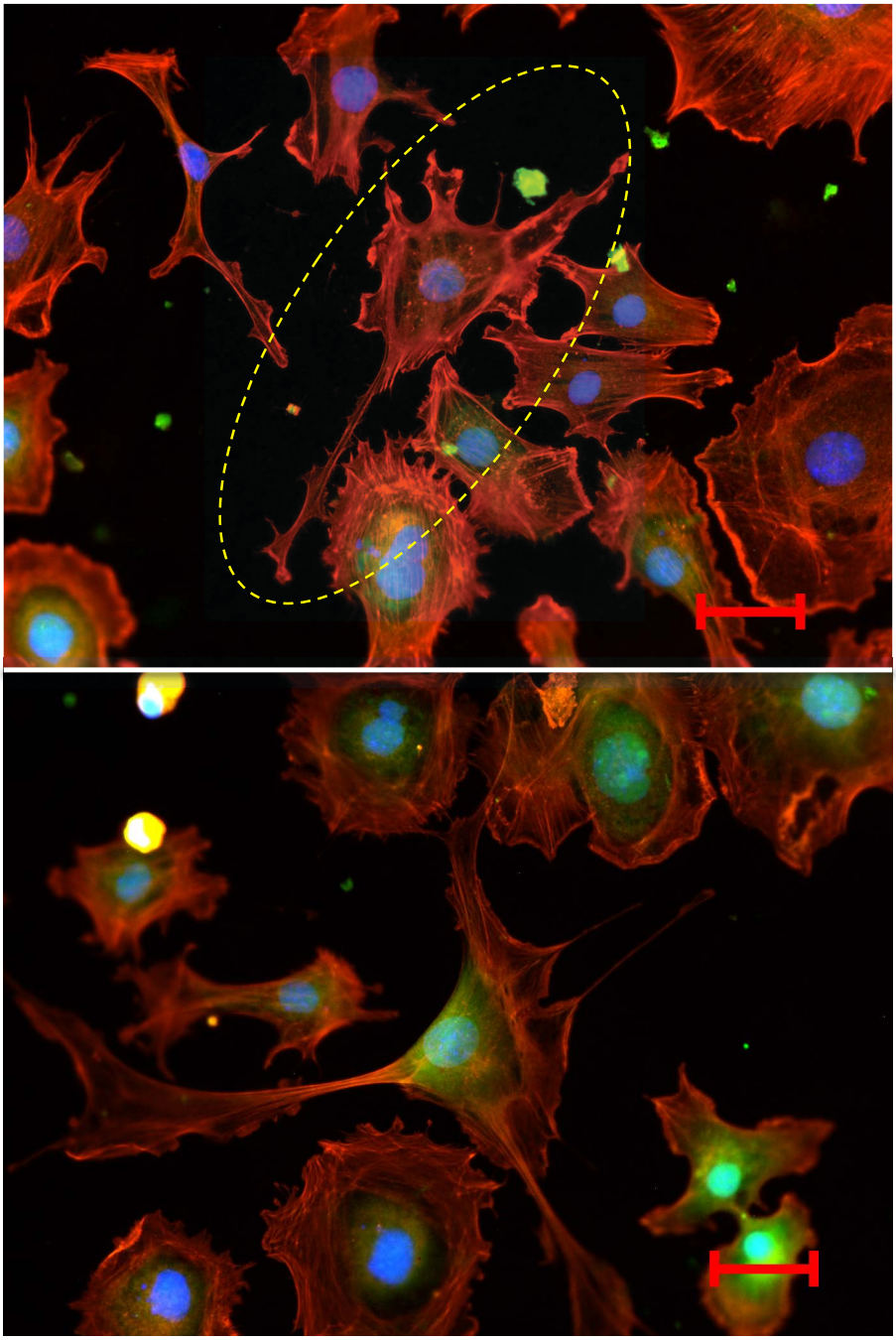

Figure 6.5: Representative fluorescence microscopy image for CMFDA/rhodamine-phalloidin/DAPI stained surfaces illustrating the altered morphologies of C17.2 cells on NGF-PPy-NW surfaces after 5 days of culture. Many cells have morphologies that could be classified as glial cell-like (see cells enclosing dotted areas). (Scale bar: 50μm)

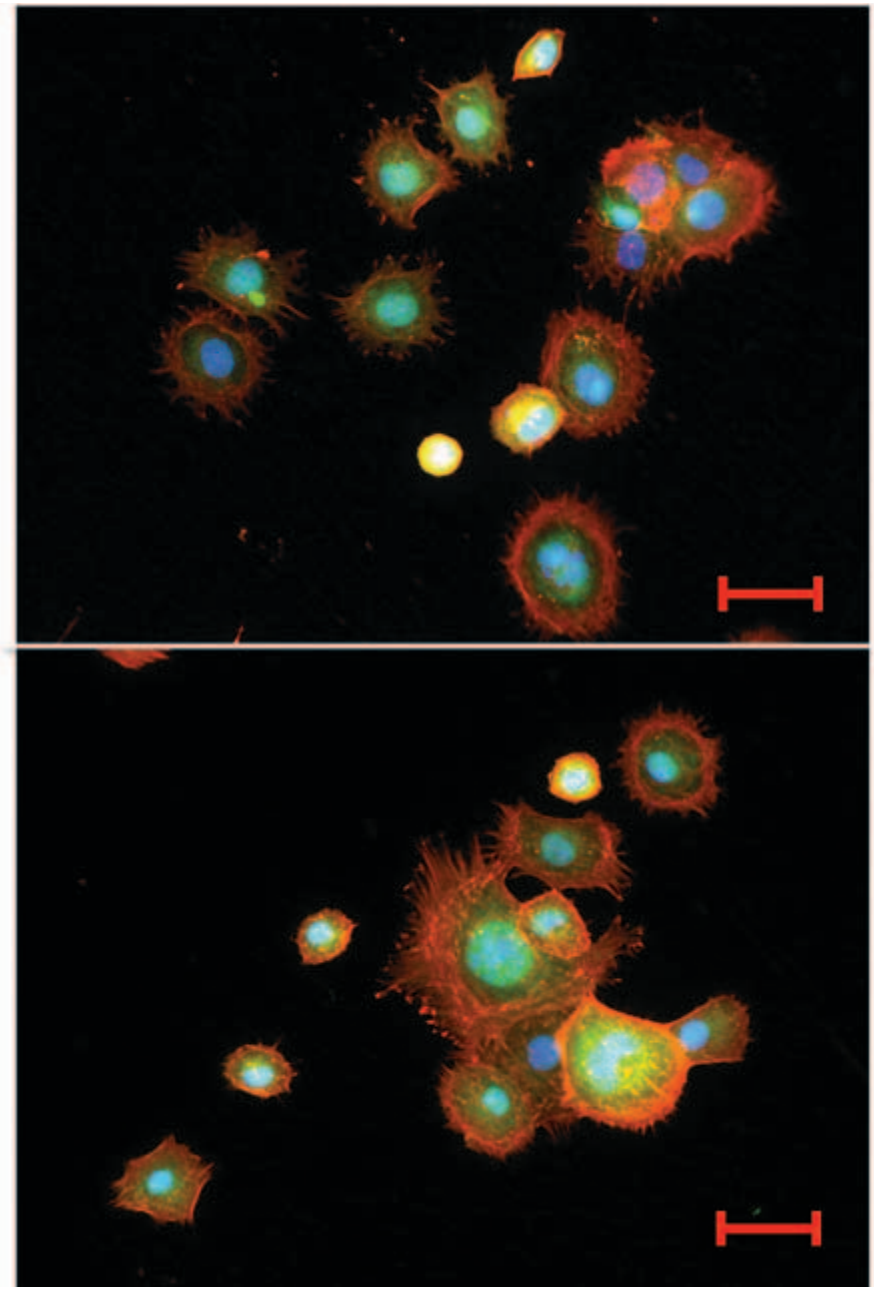

Figure 6.6: Representative fluorescence microscopy image for CMFDA/rhodamine-phalloidin/DAPI stained surfaces illustrating the spherical morphologies of C17.2 cells on PPy-NW surfaces after 5 days of culture indicating that the cells have not differentiated. (Scale bar: 50μm)

In order to characterize the differentiation potential of NGF-PPy-NW surfaces, the cells were immunostained for nestin, neuron specific class III beta-tubulin (TUJ1), and glial fibrillary acidic protein (GFAP) that stains undifferentiated stem cells, neurons, and glial cells respectively (Table 6.3). The results indicate that majority of cells on NGF-PPy-NW surfaces are expressing both nestin and GFAP (Figure 6.3, right). Cells expressing both nestin and GFAP have been suggested to perform an important role in the repair of central nervous system ("Nestin-containing cells express glial fibrillary acidic protein in the proliferative regions of central nervous system of postnatal developing and adult mice 10.1016/S0165-3806(02)00509-6 : Developmental Brain Research | ScienceDirect.com," n.d.). Further, the images also indicate that some cells expressed TUJ1 suggesting that they are differentiating into neurons (Figure 6.7, red dotted circles).

Table 6.3: Description of key neuronal markers, primary antibodies and secondary antibodies, and blocking agents used for immunofluorescence identification for NSCs.

	Undifferentiated	**Neurons**	**Glial**
Marker	Nestin	TUJ1	GFAP
Primary antibody and dilution	Mouse Protien G Purified IgG2A 1:100	Chicken Affinity Purified IgG 1:100	Rabbit Polyclonal IgG 1:50
Secondary antibody and dilution	Goat Anti-Mouse DyLight 350 1:200	Goat Anti-Chicken TR 1:100	Goat Anti-Rabbit FITC 1:100
Blocking agent	Normal goat serum		

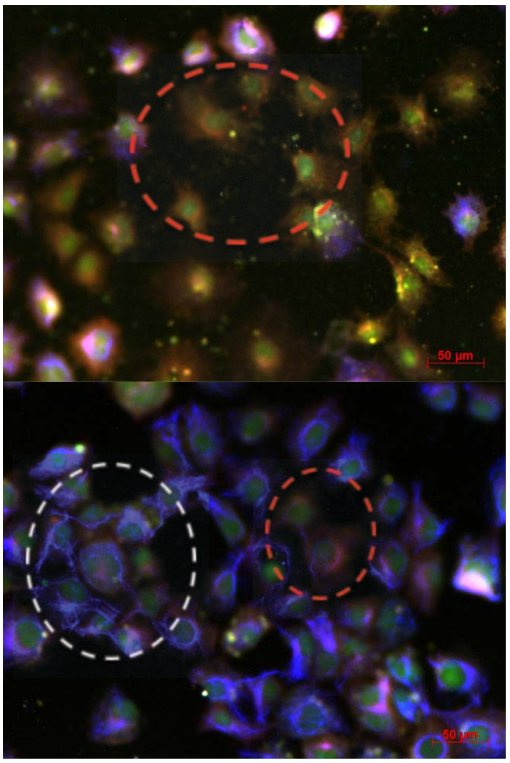

Figure 6.7: Immunofluorescence images indicate that the cells have started differentiating into neuronal phenotypes. Markers used: Nestin (blue) – undifferentiated cells, GFAP (green) – glial cells, TUJ1 (red) – neurons. (Scale bar: 50µm)

6.4 Conclusion

In conclusion, we have developed a novel method to conjugate NGF to polypyrrole coated polycaprolactone nanowire surfaces. The method is simple, easy to reproduce, and has the potential to be used on any number of different materials with functionalized amine groups. The results indicate that our hypothesis is true, that NGF conjugation onto PPy-NW surfaces promotes C17.2 cell functionality. A surface with unique nanoarchitecture such as nanowires that coated with a conductive polymer polypyrrole

and conjugated with NGF can have potential developing multifunctional scaffolds for neural tissue engineering applications.

6.5 References

Angeletti, R. H., & Bradshaw, R. a. (1971). Nerve growth factor from mouse submaxillary gland: amino acid sequence. *Proceedings of the National Academy of Sciences of the United States of America*, *68*(10), 2417-20. Retrieved from http://www.pubmedcentral.nih.gov/articlerender.fcgi?artid=389434&tool=pmcentrez&rendertype=abstract

Bechara, S. L., Judson, A., & Popat, K. C. (2010). Template synthesized poly([var epsilon]-caprolactone) nanowire surfaces for neural tissue engineering. *Biomaterials*, *31*(13), 3492-3501. Retrieved from http://www.sciencedirect.com/science/article/B6TWB-4YC39RW-5/2/b9a281830087f2631912339503ac195e

Bechara, S., Wadman, L., & Popat, K. C. (2011). Electroconductive polymeric nanowire templates facilitates in vitro C17.2 neural stem cell line adhesion, proliferation and differentiation. *Acta biomaterialia*, *7*(7), 2892-901. doi:10.1016/j.actbio.2011.04.009

Gomez, N., & Schmidt, C. E. (2007). Nerve growth factor-immobilized polypyrrole: bioactive electrically conducting polymer for enhanced neurite extension. *Journal of biomedical materials research. Part A*, *81*(1), 135-49. doi:10.1002/jbm.a.31047

Nestin-containing cells express glial fibrillary acidic protein in the proliferative regions of central nervous system of postnatal developing and adult mice 10.1016/S0165-3806(02)00509-6 : Developmental Brain Research | ScienceDirect.com. (n.d.). Retrieved January 24, 2012, from http://www.sciencedirect.com/science/article/pii/S0165380602005096

Chapter 7 Micro-patterned nanowire surfaces and their effect on C17.2 neural progenitor cell line adhesion and proliferation

7.1 Introduction

In this study, a simple technique for micro-patterning poly(ε-caprolactone) nanowire surfaces (μ-NW) was developed to adresses specific aim 6. Poly(ε-caprolactone) is a biodegradable and biocompatible polymer and has been widely investigated for use in neural tissue engineering appilcations (X. Kang et al., 2007; Nisbet et al., 2009; Runge et al., 2010). The μ-NW surfaces consist of lineally aligned regions of nanowires, bordered by flat PCL regions lacking a nanotopography (Figure 7.1). C17.2 murine NPCs were used as model cells to study the ability of μ-NW surfaces to mitigate cellular growth along an axis as would be required in a peripheral nerve injury model. This cell line has been extensively used as a model system for investigating NPC reaction to different tissue engineering scaffolds (Ghasemi-Mobarakeh et al., 2008; He et al., 2009; B. Li, Ma, Wang, & Moran, 2005). C17.2 cells are an immortalized mouse NPC line and in addition to expressing key neural progenitor markers, are capable of differentiating in vitro (Niles et al., 2004; Snyder et al., 1992). We hypothesized that if neural stem cells have been shown to adhere and proliferate with increased activity on nanowire surfaces, we can direct cellular growth by patterning surfaces with regions of nanowires bordered by regions lacking a nanotopography. The results presented here shows that the μ-NW surfaces allow murine NPCs to correctly migrate, adhere, and

proliferate according to physical guidance cues alone when compared to non-patterned nanowire (NW) and flat poly(ε-caprolactone) surfaces (PCL). Thus, μ-NW surfaces may be a suitable template for future peripheral nerve conduits and may have to guide axon regeneration in a way to transect a damaged nerve.

7.2 Materials and Methods

7.2.1 Fabrication of nanowire surfaces

NW surfaces were fabricated using a previously developed protocol and is published elsewhere (S. L. Bechara et al., 2010). Briefly, they were fabricated via template synthesis from poly(ε-caprolactone) discs and 20nm pore size ANOPORE^{TM} aluminum oxide membranes. Polymer discs, 10mm in diameter, were placed on the surface of the membrane, and the nanowires were extruded through the membranes in an oven at 115°C for 3mins. The membranes were then dissolved in 1M NaOH for 75mins to release the extruded nanowires creating the NW surface. NW surfaces were then incubated and rinsed in DI water, dried, and stored in a desiccator until further micro-patterning or for use in cell culture experiments.

7.2.2 Micro-patterning of NW surfaces

The as-fabricated NW surfaces were micro-patterned with regions lacking a nano-topography by utilizing a simple micro-patterning tool. The tool was created by several metal pieces, 60μm thick, 400μm apart so that it was approximately 10mm in width (the

same width as the NW surfaces). The tool was then drawn across the top of the surface in a linear fashion; effectively destroying the nano-architecture where the metal pieces contacted the surface thus creating linearly aligned approximately 400μm wide regions of NW topography bordered by approximately 60μm wide regions lacking nano-topography (Figure 7.1). The surface architecture was confirmed using scanning electron microscopy. Samples were sputter coated with 10 nm of gold and imaged using a JEOL JSM 6500F at voltages ranging from 10 to 15 kV.

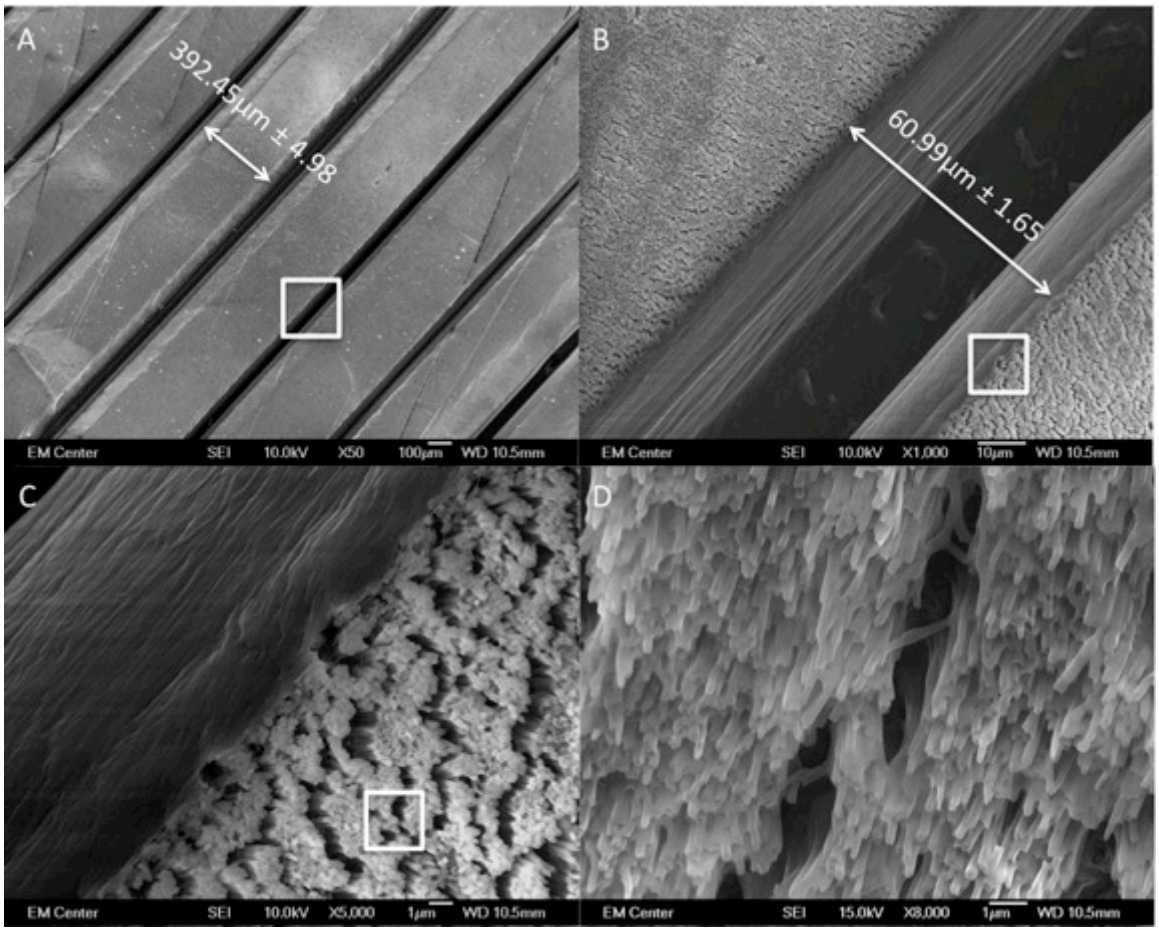

Figure 7.1: Representative SEM images showing of µ-NW surfaces. The boxes indicate that high magnification image of that area is included in the next image. A: 50x image showing consistent patterned surface with nanowire regions approximately 400µm wide. B: 1000x image showing the flat regions created by the micro-patterning tool that is approximately 60µm wide. C: 5000x image showing the boundary with flat and nanowire regions. D: 8000x image showing the nanowire architecture.

7.2.3 C17.2 Cell Culture

The C17.2 murine NPC line was developed and kindly donated by the group of Dr. Evan Snyder for use in this study. Cells under passage 3 were used. Growth medium for the C17.2 cells consisted of Dulbecco's Modified Eagle's Medium supplemented by

10% fetal bovine serum, 5% horse serum, 1% 2mM L-glutamine, and 1% penicillin/streptomycin. The medium was changed once a week and subculture was preformed at a ratio of 1:10. The cells were maintained in a 37°C and 5% CO2 incubator for the entire duration of culture. Before seeding, all surfaces were sterilized in 24 well plates by incubating them in 70% ethanol for 30 minutes followed by 30 minutes of UV exposure in a biosafety cabinet. The surfaces were then washed 3 times with sterile PBS to remove any remaining ethanol. C17.2 cells were seeded at a density of 10,000 cells/well. Each experiment was preformed on at least three different substrates with at least three different cell populations (nmin=9). Non-patterned nanowire (NW) and flat poly(ε-caprolactone) surfaces (PCL) were used as controls.

7.2.4 Adhesion and Proliferation of C17.2 Cells on μ-NW

Cell adhesion and proliferation was investigated after 2 and 5 days of culture by using the 5-Chloromethylfluorescein Diacetate (CMFDA) live stain, rhodamine-phalloidin actin stain, and 4',6-diamidino-2-phenylindole (DAPI) nucleus stain. At each time point the surfaces were removed from the culture media, and incubated in the CMFDA stain at a concentration of 10μM for 30min in a 37°C and 5% CO2 incubator. The surfaces were then allowed to incubate for another 30mins at 37°C and 5% CO2 in culture medium. The cells were then fixed by adding 3.7% formaldehyde for 15mins at room temperature. This was followed by incubating the surfaces in 1% Triton-X 100 for 3mins to permeabilize the cells. The surfaces were then incubated in rhodamine-

phalloidin at a concentration of 5μL/mL for 30 min. DAPI was added at a concentration of 1μL/mL after 25mins. All the surfaces were then rinsed and stored in PBS until visualized using a Zeiss Axioplan 2 fluorescence microscope with appropriate filters.

7.2.5 Cell shape factor approximation

NPCs adhered onto μ-NW and control surfaces after 2 days of culture with clearly defined borders were analyzed using open ImageJ software to obtain shape factor approximations similar to a previously developed method(Berger, Popat, & Prasad, 2012). Two populations of cells were analyzed: the cells that clearly touched the edge where nanowire region ends and flat surface starts on μ-NW surfaces; and the cells that resided only on the nanowire region. Cells were only analyzed on μ-NW surfaces. The cell shape factor was approximated by the ratio of cellular length to cellular width. The cellular length was defined by the diameter of the smallest circle that encompassed the entire cell; and the cellular width was defined as the diameter of the largest circle that would fit entirely within the cell.

7.2.6 Cell aggregate travel factor approximation

In order to quantify the way NPCs proliferate on μ-NW surfaces, an aggregate travel factor was calculated for all cell aggregates using ImageJ. A cell aggregate was defined as a minimum of 10 cells (determined by DAPI staining) that are in cell-cell contact (determined by rhodamine-phalloidin staining). Because the aggregates often extended beyond the field of view for the microscope, images of aggregates were stitched

together by taking multiple images of the entire aggregate and using a stitching plugin for ImageJ. The stitched cell aggregate images were then analyzed by measuring two dimensions; the maximum distance travelled in the Y and the maximum distance travelled in the X plane. The longest distance travelled by the cell aggregate was taken as the Y plane, and the X plane was measured perpendicular to the Y plane. More information is included in results and discussion section.

7.2.7 Differentiation of C17.2 cells

After 5 days of culture, the cells were simultaneously immunostained for nestin (for undifferentiated cells), neuron specific class III β-tubulin (TUJ1, for neurons), and glial fibrillary acidic protein (GFAP, for glial cells). The cells were fixed and permeabilized as indicated above. Non-specific binding was blocked by incubating the surfaces in 10% normal goat serum in PBS for 20mins. The surfaces were incubated in a solution of primary anti-bodies for 60 minutes followed by rinsing with PBS and further incubation in a solution of secondary antibodies. Optimal concentrations of primary and secondary anti-bodies were used. The surfaces were rinsed with DI water and imaged immediately with a fluorescence microscope.

7.2.8 Contact angle measurements

Surface hydrophilicity on was characterized by measuring the water contact angle using a FTA1000 B Class goniometer. A droplet of DI water, approximately 100 μL in volume, was formed on the tip of the syringe and the stage was moved upward so that the

droplet contacted and detached onto the substrate. The water droplet image on the surface was captured within 5secs after the contact by a camera leveled with the surface. Images were then analyzed with the accompanying Fta32 software to measure the contact angles. Each experiment was preformed on three different locations and on at least three different substrates of each PCL and NW surfaces (nmin = 9).

7.2.9 Nanoindentation

Nanoindentation was preformed using a XPTM, MTS Systems Corporation nanoindenter equipped with a Berkovich diamond tip. Each surface was analyzed at 8 different locations. Before running, the machine was calibrated using a silica sample with a known elastic modulus and hardness. Each experiment was preformed on at least three different substrates of each PCL and NW surfaces ($n_{min} = 24$).

7.2.10 Statistics

All the quantitative results were analyzed using an analysis of variance (ANOVA) or two way T-test where applicable. Statistical significance was considered at $p < 0.05$.

7.3 Results and Discussion

Tissue regeneration following a peripheral nerve injury is not a simple task and as such, the current treatment methodology has not advanced significantly in the past 45 years (Millesi, 1967). It is therefore necessary to continue to explore new scaffolding technologies capable of regenerating the nervous tissue. Previous work has indicated that

polymeric nanowire surfaces enhance neural cell activity when compared to flat polymer surfaces (S. L. Bechara et al., 2010). Therefore, we hypothesize that NPCs would preferentially adhere to NW regions if presented on a surface containing regions with both nanowires and flat morphology.

Prior to micro-patterning, NW surfaces were fabricated using a simple nano-templating technique. The technique used to fabricate these surfaces is advantageous because in addition to consistently creating surface-bound high aspect ratio nanowires, it is also devoid of solvents, which can cause cytotoxic aftereffects. The as-fabricated NW surfaces were then micro-patterned using a micro-patterning tool as described in materials and method section. The tool was drawn across the substrate surface linearly and with sufficient force to destroy the nanowire architecture and create flat regions with a consistent width that lacked nanotopography (Figure 7.1A). This resulted in a surface that consists of uninterrupted nanowires for 392.45 ± 4.98μm width, bordered by regions lacking nanotopography for 60.99 ± 1.65μm width (Figure 7.1A and B). The transition from nanowire to flat regions is smooth and uniform (Figure 7.1C). Further, nanowire regions show that the nanoarchitecture is uniform across the width (Figure 7.1D).

In order to evaluate the ability of μ-NW surfaces to direct cellular growth, C17.2 NPCs were cultured on μ-NW, NW, and PCL surfaces. NPCs were allowed to preferentially adhere to the substrate surfaces for 2 days before they were analyzed by staining the adhered cells with 5-Chloromethylfluorescein Diacetate (CMFDA), rhodamine-phalloidin, and DAPI. CMFDA can be referred to as a live cytoplasm stain

due to the fact that it readily transports into the cell where it is metabolized into a fluorescent molecule and unable to cross the cell membrane. If the cell is not alive, it will not metabolize and the molecule will not fluoresce. Rhodamine-phalloidin was used to visualize the cytoskeleton protein actin, and DAPI was used to label the cell nuclei. The results indicate that majority of cells preferentially adhere to the NW regions on the μ-NW substrates and avoid the flat regions (Figure 7.2). It should be noted that the cells could fit in the regions lacking nano-topography but instead preferentially adhere to the nanowire regions. Similar cell adhesion was observed on both nanowire regions of μ-NW surfaces and NW surfaces (Figure 7.2B and C), contrasted by significant lower cell adhesion on PCL surfaces (Figure 7.2A). This leads credence to the hypothesis that cells would preferentially adhere to nanowire surfaces if given a choice between nanowires and flat PCL surfaces. High magnification images also indicate that the cells on the μ-NW surfaces appear to be taking on stretched morphologies when they contact a boundary region between the nanowire and the flat regions (Figure 7.2D). The images indicate that the actin filaments are aligning themselves along the boundary region.

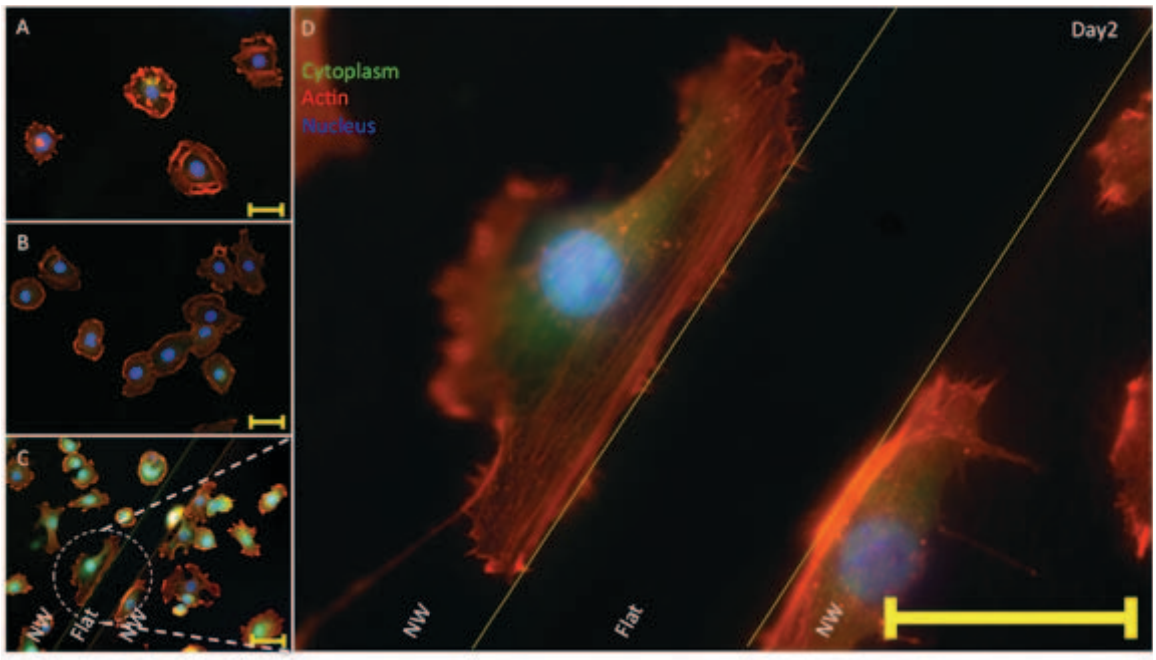

Figure 7.2: Representative fluorescence microscopy images of C17.2 cells after 2 days of culture on A: PCL surfaces, B: NW surfaces, and C: μ-NW surfaces. There are adhered cells on the PCL substrates as compared to the NW and μ-NW surfaces. D: Elongated Cells at the boundary region. Stretched actin fibers are clearly visible. Scale bars: 50μm.

Due to the fact that the cells on the boundary regions on μ-NW surfaces appear to have a stretched morphology, a cell shape factor was calculated using ImageJ software. Two populations were analyzed: cells clearly touching the boundary region, and the cells that were not touching a boundary region i.e. away from the boundary region on nanowire region. Briefly, the smallest possible circle was fitted to the outside of the cell of interest. The diameter of this circle was tabulated and labeled as the cellular length. Next, the largest possible circle was fitted within the cell and its diameter was tabulated as the cellular width. An example of such fitted circles is shown in Figure 7.3. The ratio of cellular length to cellular width was referred to as the shape factor, a dimensionless

number. A shape factor that is significantly larger than 1 indicates that the cell was not spherical and instead had a stretched morphology.

$$Shape\ Factor = \frac{Cellular\ Length\ (\mu m)}{Cellular\ Width\ (\mu m)}$$

The results show that cells that touch the boundary region have an average length of 65.58 ± 5.19μm, an average width of 23.86 ± 1.64μm, and subsequently a shape factor of 2.821 ± 0.19 (Figure 7.3). This implies that cells that touched a boundary region were on average approximately 3 times longer then they were wide. This is beneficial because cell-surface interactions have been shown to have major effects upon cell phenotypic features such as gene regulation, cytoskeletal structure, and differentiation potential (Frisch & Francis, 1994). Furthermore, studies have shown that cell spreading is critical for cells to progress through the post-mitotic phase of growth into the DNA synthesis phase of the cell-division cycle (Hansen, Mooney, Vacanti, & Ingber, 1994). Interestingly, the cells that did not touch a boundary region had a shape factor of 1.851 ± 0.091μm implying that they were still stretched in one dimension, but not as significantly stretched as the cells touching a boundary region (Figure 7.3). This also indicates that the increased cell proliferation on NW surfaces as compared to PCL surfaces may be due to the fact that the cells are interacting with the nanoscale features on the surface.

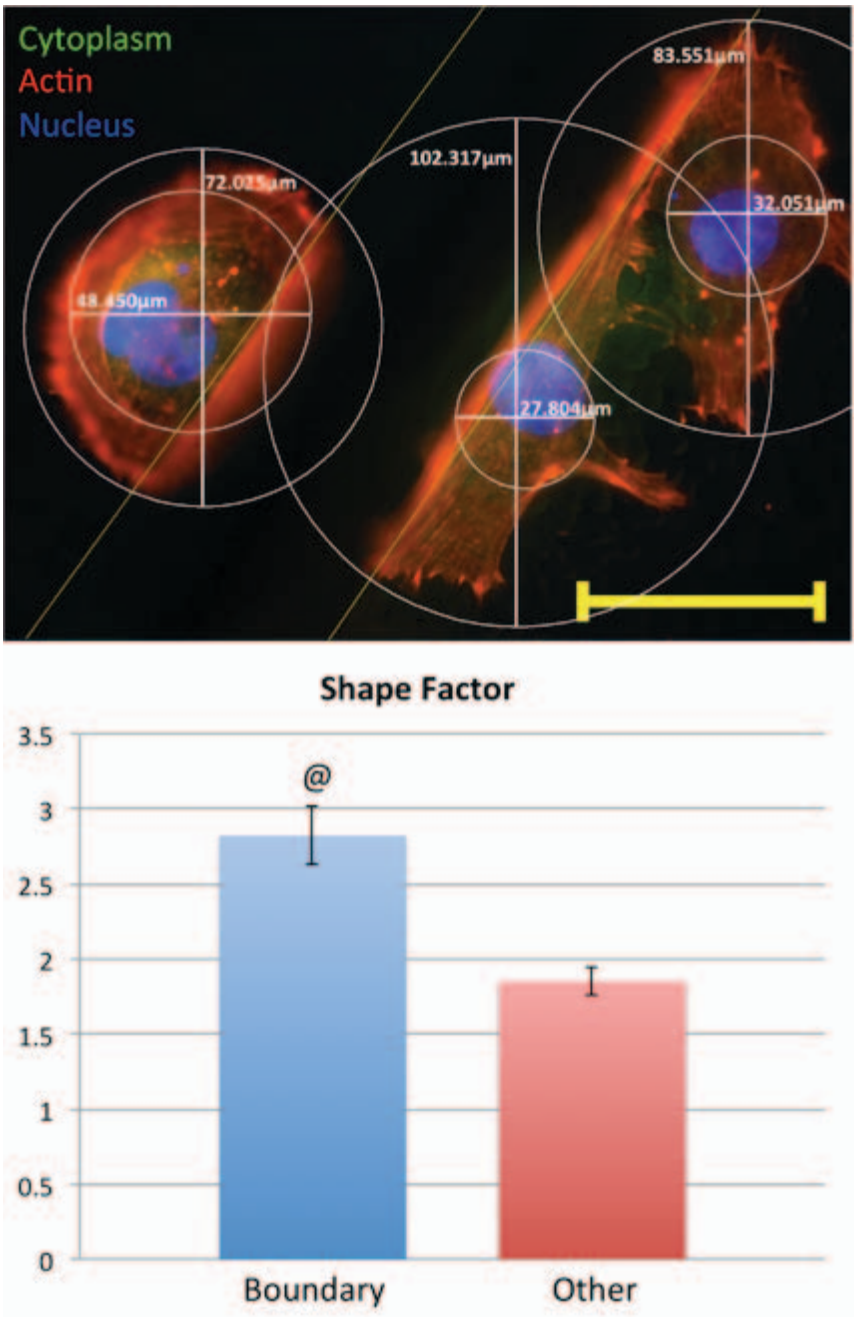

Figure 7.3: A: Representative fluorescence microscopy image showing shape factor calculation. Scale bar: 50□m. B: Calculated shape factor for cells contacting a boundary region and cells not contacting the boundary. (@ □ $p < 0.05$)

In order to investigate NPC proliferation on μ-NW surfaces, the cells were allowed to proliferate for up to 5 days in culture and stained with CMFDA, rhodamine-phalloidin, and DAPI. The results indicate similar cell proliferation on both μ-NW and on NW surfaces, and formation of cell aggregate colonies (Figure 7.4). The cell proliferation on PCL surfaces significantly lower than that on μ-NW and NW surfaces (data not shown). Further, it appears that the cell aggregate colonies on the μ-NW surfaces proliferate in a directional manner when compared to that on the NW surfaces. In order to quantify this behavior, an aggregate shape factor was calculated in a similar manner to the cellular shape factor. In brief, aggregate colony with 10 cells or was analyzed for the maximum distance travelled in the Y and X direction. The Y direction was the longest distance from edge to edge of an aggregate. The X direction was simply the longest traversed distance of the cell aggregate colony taken at a 90° angle from the Y direction. An example of the image analysis undertaken for maximum travelled distance calculations is provided in Figure 7.5. An aggregate travel factor was calculated by dividing the maximum cell aggregate colony travel in the Y direction by the X direction, a dimensionless number. An aggregate travel factor over 1 implies that the cells are proliferating in the Y direction.

$$Aggregate\ Travel\ Factor = \frac{Maximum\ Travel\ Y(\mu m)}{Maximum\ Travel\ X\ (\mu m)}$$

The results indicate that the cells on the μ-NW surfaces have an aggregate travel factor of 2.944 ± 0.23 after 5 days of culture (Figure 7.5). This is contrasted by the lack

of directional growth observed on the NW substrates. Cell aggregate colonies on NW had an aggregate travel factor of 1.21 ± 0.28 after 5 days of culture (Figure 7.5). This is also apparent from Figure 7.4 where the cell aggregate colonies clearly seem to be proliferating more in the Y direction on the μ-NW surfaces when compared to those on the NW surfaces.

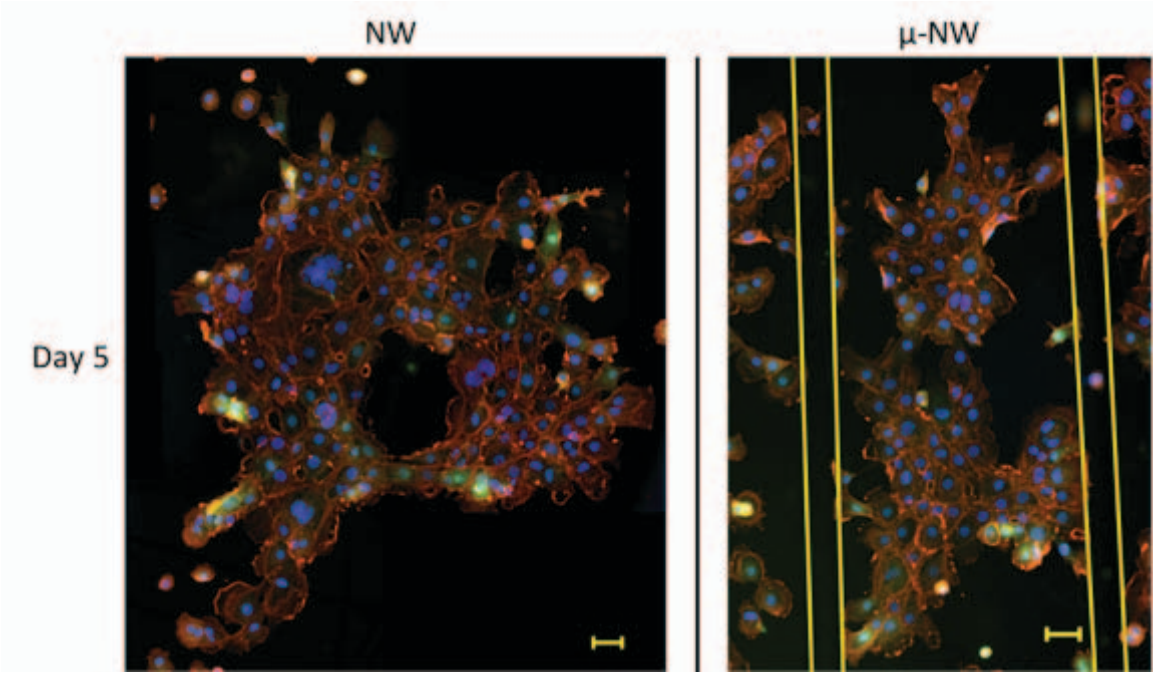

Figure 7.4: Representative fluorescence microscopy images of cell aggregate colonies on NW and μ-NW surfaces after 5 days of culture. The green channel is the cytoplasm stained by CMFDA, the red channel is actin stained by rhodamine-phalloidin, and the blue channel is the cell nuclei stained by DAPI. The cells are proliferating radially on NW surfaces, whereas the cells are proliferating in longitudinal direction on μ-NW surfaces. The images shown are the result of stitching multiple images using ImageJ. The line indicates the boundary between the nanowire and flat regions on μ-NW surface. Scale bars: 50μm.

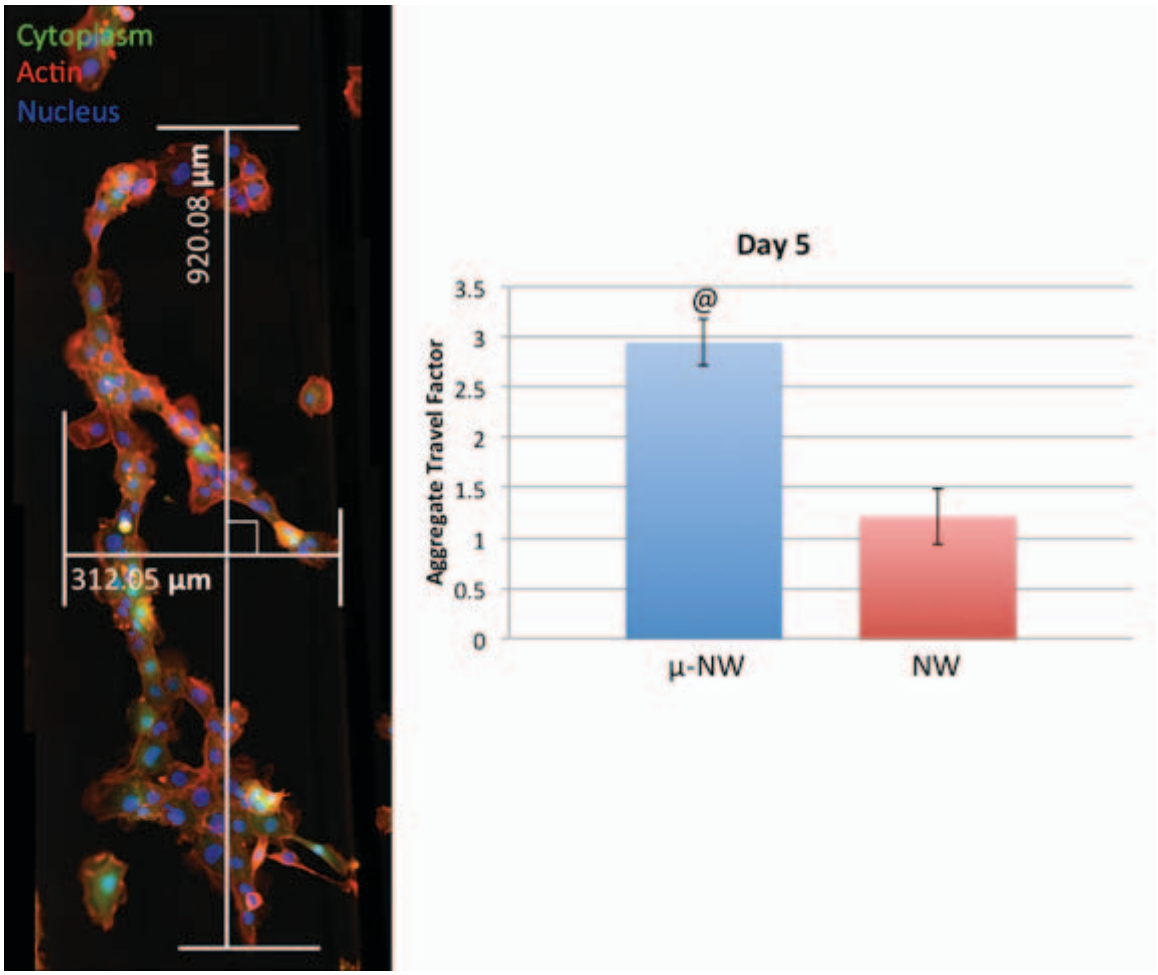

Figure 7.5: A: Representative fluorescence microscopy image showing aggregate travel factor calculation. Scale bar: 50µm. B: Calculated aggregate shape factor for cells on NW and µ-NW surface. (@ □ $p < 0.05$)

To further investigate the differentiation of NPCs µ-NW surfaces, the cells were immunolabled for β-tubulin III (Tuj1), glial fibrillary acidic protein (GFAP), and nestin. Both GFAP and nestin belong to the intermediate filament family of proteins and are typically associated with astrocytes and undifferentiated NPCs respectively. Tuj1 is a microtubule marker that is normally exclusively found in neurons. The results indicate

that after 2 and 5 days of culture, the cells appear to be expressing all of the markers (Figure 7.6). However, the results indicate that the cells are expressing higher amounts of GFAP, followed by nestin and Tuj1. Further, the results also indicate that the cells are beginning to down-regulate nestin expression by as early as day 2, indicating that they may be differentiating. After 5 days of culture, the cells appear to be expressing almost exclusively GFAP and nestin while not expressing Tuj1, indicating that all of the cells may have differentiated into astrocytes. Studies have shown that pre-differentiating NPCs into astrocytes enhances spinal cord injury outcomes over precursor cell transplantation indicating that astrocytes may be highly effective in repairing damaged neural tissue(J. E. Davies et al., 2006).

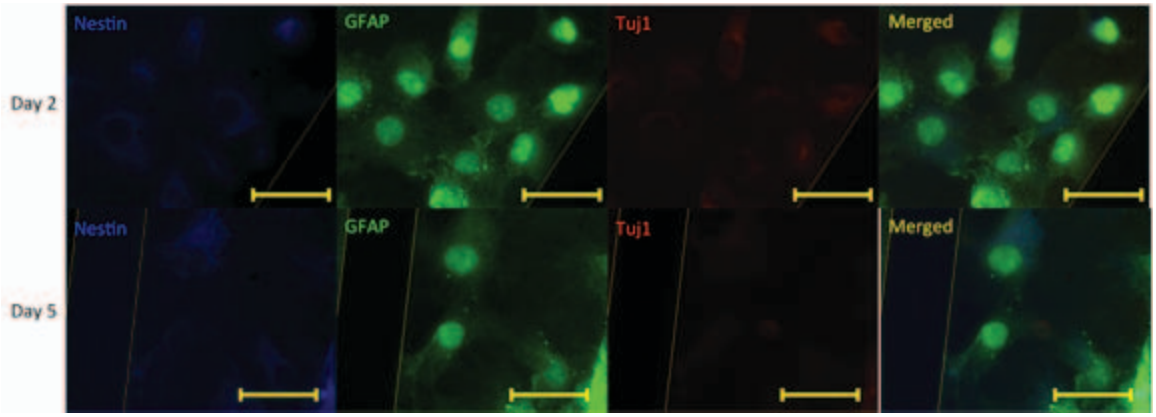

Figure 7.6: Representative immunofluorescence images showing expression of Nestin, GFAP, and Tuj1 at day 2 and day 5.

To understand why the cells preferentially adhere on nanowire regions when presented with both nanowires and flat regions on the same surface, contact angle measurements and nanoindentation was performed. μ-NW surfaces were not analyzed.

Instead it was assumed that the NW regions of the μ-NW surfaces are similar to NW surfaces and the flat regions are similar to PCL surfaces. Surface hydrophilicity was measured using a water droplet contact angle measurement. It is well known that hydrophilic substrates have higher surface energy, thus adsorbs extracellular matrix proteins and promote cellular adhesion whereas hydrophobic substrates have lower surface energy and do no promote cellular adhesion (Schakenraad, Busscher, Wildevuur, & Arends, n.d.). The water contact angle for NW surfaces was 53.93 ± 3.2° as compared to 77.81 ± 0.89° on the PCL surfaces (Figure 7.7). The results indicate that the NW substrates are significantly more hydrophilic then flat surfaces and may promote in higher cellular adhesion (Figure 7.7). Even though the NW and PCL surfaces are chemically the same polymer, the altered nanoarchitecture of the NW surfaces increases the surface energy thus spreading the water droplet (Figure 7.7A).

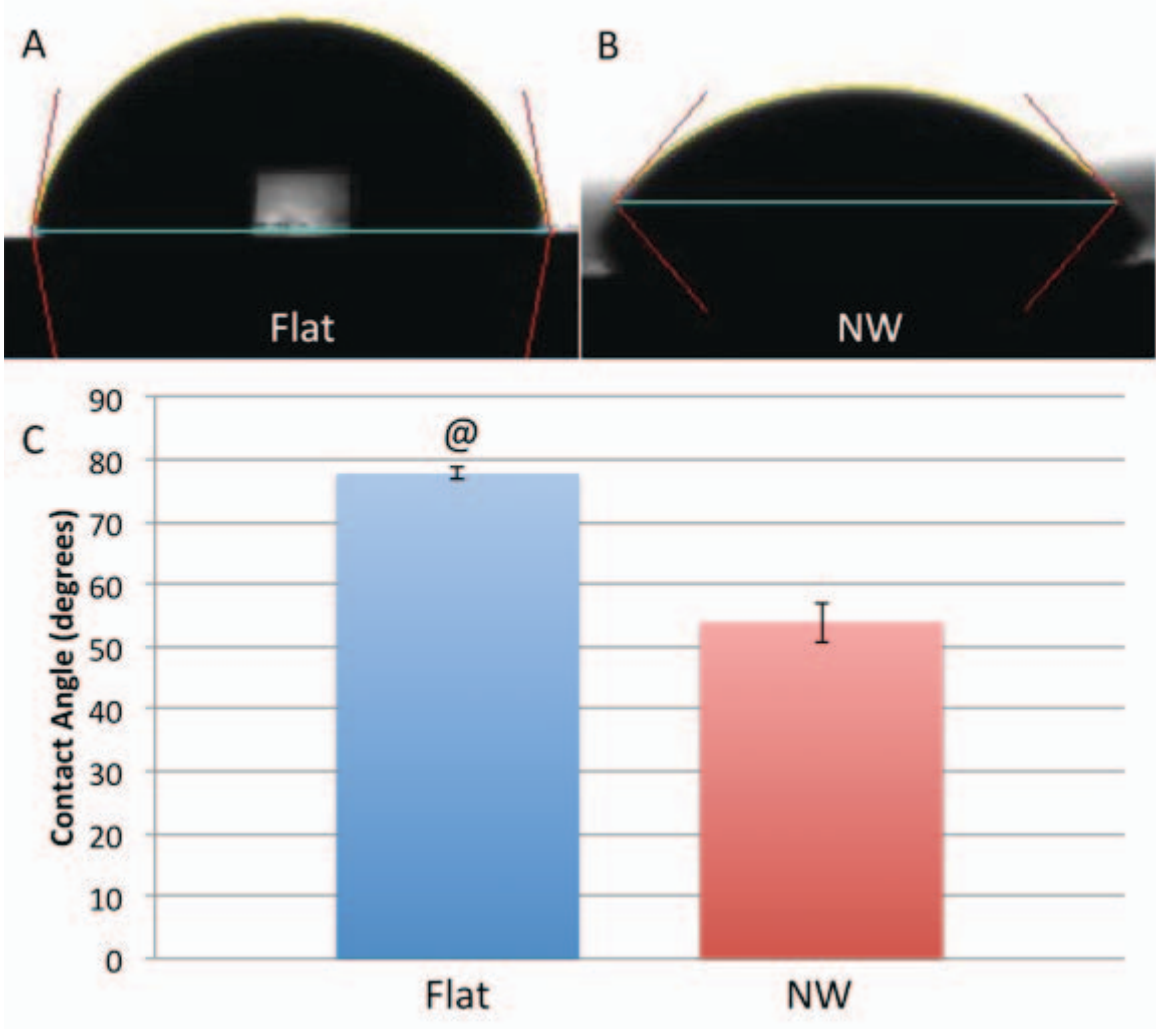

Figure 7.7: Water contact angle measured on NW and □-NW surfaces. (@ □ $p < 0.05$)

Nanoindentation was performed to evaluate the surface mechanical properties. It is well known that cells can sense and react to their localized mechanical microenvironment. For example, on alginates with RGD ligands, the rate and growth of skeletal myoblasts was higher on stiffer substrates (Rowley & Mooney, 2002). It has also

been shown that mechanical stiffness is inversely correlated to neurite extension of dorsal root ganglion cells on agarose hydrogels (Balgude, 2001). Unlike the surface energy, where hydrophilic surfaces typically promote adhesion, the relationship between the surface mechanical properties and cell adhesion is not that straightforward. Due to the variable nature of natural tissue, the most advantageous surface mechanical properties for cell adhesion are most likely the Young's modulus and hardness. The nanoindentation results indicate that architecture on the NW surfaces results in a significantly softer material with a hardness of 4.65 ± 1.03 MPa as compared to 80 ± 2.89 MPa for PCL surfaces (Figure 7.8). The NW surfaces also were less stiff with an elastic modulus of 392 ± 22 MPa as compared to 633 ± 19 MPa for PCL surfaces due to and respectively (Figure 7.8). Although the aceullular nerve tissue is significantly less stiffer than NW surfaces (Borschel, Kia, Kuzon Jr, & Dennis, 2003), the enhanced cellular functionality on NW surfaces may be due to a combination effect: the unique nanotopography, higher surface energy, and softer and less stiffer surface.

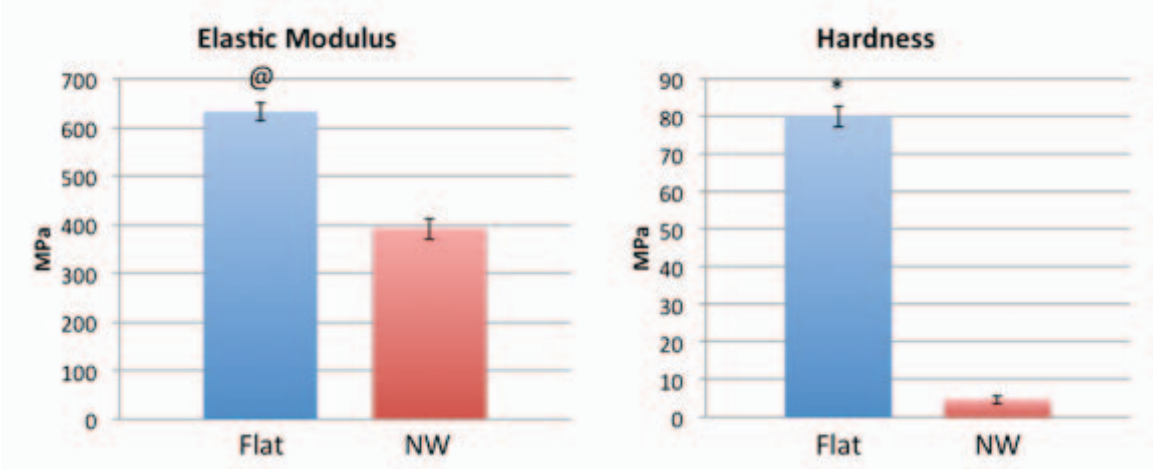

Figure 7.8: A: Young's modulus and B: Harness measured using nanoindentation. (★,@ ➔ $p < 0.05$)

7.4 Conclusion

In this work, we have developed a simple technique for micro-patterning poly(ε-caprolactone) nanowire surfaces (μ-NW) that are capable of directing NPC adhesion and proliferation. The results indicate that these μ-NW surfaces also promote stretched morphology that may further aid in stem cell differentiation. Furthermore, the results presented here show that aggregate colonies of over 10 cells proliferate in the longitudinal direction on μ-NW surfaces compare to transverse direction on non-patterned surfaces. Further, it is known that mechanical properties, such as Young's modulus and hardness; and surface properties such as surface energy play a fundamental role in directing cellular adhesion and subsequent proliferation and differentiation of NPCs. The results indicate that the nanowire surfaces have beneficial surface and mechanical properties for cell adherence and proliferation and prove our hypothesis true.

Thus, patterning NW surface, may have multifold advantages and can be used a template for growth and maintenance of neural stem cells for further development of scaffolds for neural tissue engineering.

7.5 References

Balgude, A. (2001). Agarose gel stiffness determines rate of DRG neurite extension in 3D cultures. *Biomaterials*, *22*(10), 1077-1084. doi:10.1016/S0142-9612(00)00350-1

Bechara, S. L., Judson, A., & Popat, K. C. (2010). Template synthesized poly([var epsilon]-caprolactone) nanowire surfaces for neural tissue engineering. *Biomaterials*, *31*(13), 3492-3501. Retrieved from http://www.sciencedirect.com/science/article/B6TWB-4YC39RW-5/2/b9a281830087f2631912339503ac195e

Berger, D. R., Popat, K., & Prasad, A. (2012). Nanotopography Driven Mesenchymal Stem Cell Differentiation and Proliferation. *Biophysical Journal*, *102*(3, Supplement 1), 705a-706a. Retrieved from http://www.sciencedirect.com/science/article/pii/S0006349511051782

Borschel, G. H., Kia, K. F., Kuzon Jr, W. M., & Dennis, R. G. (2003). Mechanical properties of acellular peripheral nerve. *Journal of Surgical Research*, *114*(2), 133-139. Retrieved from http://www.sciencedirect.com/science/article/pii/S0022480403002555

Davies, J. E., Huang, C., Proschel, C., Noble, M., Mayer-Proschel, M., & Davies, S. J. A. (2006). Astrocytes derived from glial-restricted precursors promote spinal cord repair. *Journal of biology*, *5*(3), 7. doi:10.1186/jbiol35

Frisch, S. M., & Francis, H. (1994). Disruption of epithelial cell-matrix interactions induces apoptosis. *The Journal of cell biology*, *124*(4), 619-26. Retrieved from http://www.pubmedcentral.nih.gov/articlerender.fcgi?artid=2119917&tool=pmcentrez&rendertype=abstract

Ghasemi-Mobarakeh, L., Prabhakaran, M. P., Morshed, M., Nasr-Esfahani, M.-H., & Ramakrishna, S. (2008). Electrospun poly(epsilon-caprolactone)/gelatin nanofibrous scaffolds for nerve tissue engineering. *Biomaterials*, *29*(34), 4532-9. doi:10.1016/j.biomaterials.2008.08.007

Hansen, L. K., Mooney, D. J., Vacanti, J. P., & Ingber, D. E. (1994). Integrin binding and cell spreading on extracellular matrix act at different points in the cell cycle to promote hepatocyte growth. *Molecular biology of the cell*, *5*(9), 967-75. Retrieved from

http://www.pubmedcentral.nih.gov/articlerender.fcgi?artid=301120&tool=pmcentrez&rendertype=abstract

He, L., Liao, S., Quan, D., Ngiam, M., Chan, C. K., Ramakrishna, S., & Lu, J. (2009). The influence of laminin-derived peptides conjugated to Lys-capped PLLA on neonatal mouse cerebellum C17.2 stem cells. *Biomaterials*, *30*(8), 1578-86. doi:10.1016/j.biomaterials.2008.12.020

Kang, X., Xie, Y., Powell, H. M., James Lee, L., Belury, M. A., Lannutti, J. J., & Kniss, D. A. (2007). Adipogenesis of murine embryonic stem cells in a three-dimensional culture system using electrospun polymer scaffolds. *Biomaterials*, *28*(3), 450-8. doi:10.1016/j.biomaterials.2006.08.052

Li, B., Ma, Y., Wang, S., & Moran, P. M. (2005). Influence of carboxyl group density on neuron cell attachment and differentiation behavior: gradient-guided neurite outgrowth. *Biomaterials*, *26*(24), 4956-63. doi:10.1016/j.biomaterials.2005.01.018

Millesi, H. (1967). [Nerve transplantation for reconstruction of peripheral nerves injured by the use of the microsurgical technic]. *Minerva chirurgica*, *22*(17), 950-1. Retrieved from http://www.ncbi.nlm.nih.gov/pubmed/6055379

Niles, L. P., Armstrong, K. J., Rincón Castro, L. M., Dao, C. V., Sharma, R., McMillan, C. R., Doering, L. C., et al. (2004). Neural stem cells express melatonin receptors and neurotrophic factors: colocalization of the MT1 receptor with neuronal and glial markers. *BMC neuroscience*, *5*, 41. doi:10.1186/1471-2202-5-41

Nisbet, D. R., Rodda, A. E., Horne, M. K., Forsythe, J. S., & Finkelstein, D. I. (2009). Neurite infiltration and cellular response to electrospun polycaprolactone scaffolds implanted into the brain. *Biomaterials*, *30*(27), 4573-80. doi:10.1016/j.biomaterials.2009.05.011

Rowley, J. A., & Mooney, D. J. (2002). Alginate type and RGD density control myoblast phenotype. *Journal of biomedical materials research*, *60*(2), 217-23. Retrieved from http://www.ncbi.nlm.nih.gov/pubmed/11857427

Runge, M. B., Dadsetan, M., Baltrusaitis, J., Knight, A. M., Ruesink, T., Lazcano, E. A., Lu, L., et al. (2010). The development of electrically conductive polycaprolactone fumarate-polypyrrole composite materials for nerve regeneration. *Biomaterials*, *31*(23), 5916-26. doi:10.1016/j.biomaterials.2010.04.012

Schakenraad, J. M., Busscher, H. J., Wildevuur, C. R., & Arends, J. (n.d.). The influence of substratum surface free energy on growth and spreading of human fibroblasts in the presence and absence of serum proteins. *Journal of biomedical materials research*, *20*(6), 773-84. doi:10.1002/jbm.820200609

Snyder, E. Y., Deitcher, D. L., Walsh, C., Arnold-Aldea, S., Hartwieg, E. A., & Cepko, C. L. (1992). Multipotent neural cell lines can engraft and participate in development of mouse cerebellum. *Cell*, *68*(1), 33-51. Retrieved from http://www.ncbi.nlm.nih.gov/pubmed/1732063

Chapter 8 Future Work

From this work it was shown the PCL nanowire scaffolds and subsequent modifications have improved neural stem cell functionality. The substrates have shown great promise as a neural tissue-engineering scaffold with the potential capability of healing damaged nervous tissue *in vivo*. However, before *in vivo* studies are pursued, several issues must first be addressed.

First and foremost, the scaffolds must be investigated using primary cells instead of cell lines. Cell lines do not display a normal physiological phenotype. In the case of PC12 cells they are derived from a pheochromocytoma and as such may contain cancerous genetic variations. C17.2 murine neural progenitor cells are better because they were derived from a mouse cerebellum. However, for ease of culture they have been immortalized and do not represent a true neural stem cell. Thus, before *in vivo* studies are preformed, future work must be directed at investigating primary neural stem cell response to the various nanowire scaffolds.

Although the scaffolds presented in this work have shown great promise, they have yet to be rolled into a conduit style graft capable of being sutured into a damaged tissue region. However, progress has been made towards getting thin films of PCL through which to extrude the nanowires through. This would provide more flexibility and allow the PCL film to be rolled into a conduit for *in vivo* repair studies. Furthermore, for a conduit-based therapy, the scaffolds need to be porous. Porosity is necessary for

vascularization and waste management and at the current time, our substrate bound nanowires do not have pores.

The electrically conductive coating of polypyrrole was shown to enhance neural stem cell functionality. However, no electrical current was run through the surface or measured from the cells. Studies have shown that electrical stimulation may be beneficial in a spinal cord injury model. Therefore, future studies should be directed at investigating neural stem cell reaction to an electrical current run through the polypyrrole coating.

Finally, micro-patterning was shown to guide neural stem cell adhesion and proliferation along an axis. Further work should be directed towards patterning both the polypyrrole coating and NGF. By being able to manipulate the coating of polypyrrole and NGF, the scaffold may be able to better guide adhesion and proliferation of neural stem cells.

After the aforementioned work has been completed, the next step would be *in vivo* studies and investigating whether a conduit constructed of inward facing nanowires (with modifications as appropriate pending primary stem cell interaction studies) has the ability to heal sciatic nerve defects greater than approved therapies.

Chapter 9 Ethical considerations

Due to the exploratory nature of the research presented in this thesis and the fact that future work has proposed *in vivo* animal models, the purpose of this section will be to investigate the ethics associated with this project, to justify the research from a moral standpoint, and to ensure that adequate precaution is taken to minimize animal use and suffering in the future.

The majority of the work in this study has investigated the reaction of a neural stem cell line to various modifications and enhancements to a polymeric biomaterial proposed for regenerating nervous system tissue. Neural stem cell lines differ from primary neural stem cells, which come directly from an animal. A neural stem cell line is simply neural stem cells that have been immortalized by introducing genes that prevent cell apoptosis. This bestows neural stem cells with several beneficial properties for *in vitro* research. For example, neural stem cell lines are able to undergo more divisions in culture when compared to primary cells while secreting similar neurotrophic factors (Lu, Jones, Snyder, & Tuszynski, 2003). However, from a scientific perspective, neural stem cell lines such as the C17.2 cell line are inferior to primary cells in understanding the true physiological response to a material for several reasons. The most pertinent however is the fact that neural stem cell lines such as C17.2 cells may secrete different growth factors and may express markers differently from the cells they were derived from (Mi et al., 2005).

Although neural stem cell isolation from neonatal and adult animals is well defined, relatively inexpensive, and would arguably have made for a more physiologically relevant model, C17.2 cells were utilized in this study to minimize animal use. The novelty in this research lies in the fact that the nanowire nanotopography has never been investigated as a potential scaffold for neural tissue engineering applications. As an exploratory and uncertain research investigation, I felt it would be immoral to sacrifice an animal and harvest its cells to use to investigate an unproven biomaterial. This is especially troubling considering that multiple animals would have to be used while neural stem cell lines are available and serve as a reasonable model.

In this work, it was shown that nanowire surfaces could promote favorable activity from a neural stem cell line. The future work section outlines the next steps of this regarding material porosity, conduit formation, and electrical stimulation. It is my opinion that those studies should be conducted using the C17.2 stem cell line for the same aforementioned reasons. Assuming that porosity is incorporated and that conduit formation is successful in directing C17.2 cell adhesion and proliferation, the next step would be to investigate *in vitro* primary cell interaction with the conduit. In order to minimize animal use, I would insist omitting control surfaces to the conduit considering the amount of research that has been conducted showing favorable neural stem cell line interaction over appropriate control surfaces. Again supposing that the primary neural stem cell interaction with the conduit is favorable, the next step would be an *in vivo* study utilizing the sciatic nerve injury model and investigating if the nanowire conduit can

encourage healing. However, unlike other studies, I would also insist that as a control, FDA approved conduits are used as opposed to leaving the animal to heal naturally. This is due to the overwhelming amount of research that has showed the limited ability of the nervous system to regenerate this tissue. It is my opinion that cutting an animal sciatic nerve and observing its inability to regenerate is immoral given the current level of scientific expertise regarding such an injury. In addition to allowing the animals to heal, using FDA approved conduits as controls has the added benefit of being a more relevant comparison for nanowire conduits.

If future research suggests that nanowire conduits are successful scaffolds for regenerating nervous tissue, the potential benefits to medicine are far ranging. However, it is of upmost importance that this research is conducted in an ethical manner due to an obligation to uphold societal ethics regarding animal pain and suffering. It is also critical if researchers wish to continue their research without further bureaucratic regulation. Bernard Rollin stated this importance eloquently when he wrote " if professionals such as physicians, veterinarians, or researchers wish to keep their autonomy and steer their own ships, they must be closely attuned in an anticipatory way to changes and tendencies in social ethics and adjust their behavior to them, else they can be shackled by unnecessarily draconian restriction." (Rollin, 2006)

9.1 References

Lu, P., Jones, L. L., Snyder, E. Y., & Tuszynski, M. H. (2003). Neural stem cells constitutively secrete neurotrophic factors and promote extensive host axonal growth after spinal cord injury. *Experimental neurology*, *181*(2), 115-29. Retrieved from http://www.ncbi.nlm.nih.gov/pubmed/12781986

Mi, R., Luo, Y., Cai, J., Limke, T. L., Rao, M. S., & Höke, A. (2005). Immortalized neural stem cells differ from nonimmortalized cortical neurospheres and cerebellar granule cell progenitors. *Experimental neurology*, *194*(2), 301-19. doi:10.1016/j.expneurol.2004.07.011

Rollin, B. (2006). *Science and Ethics*. Cambridge University Press.